SIMULATION OF MIXING CONDITIONS IN STEEL MAKING

by
SOHINI PAL

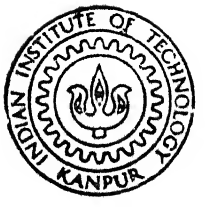

DEPARTMENT OF METALLURGICAL ENGINEERING
INDIAN INSTITUTE OF TECHNOLOGY, KANPUR

JANUARY, 1989

CERTIFICATE

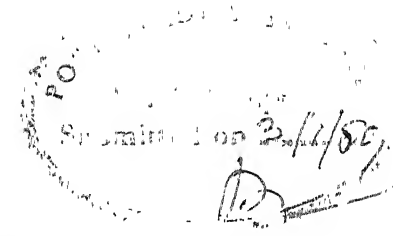

Certified that the work presented in this thesis on 'SIMULATION OF MIXING CONDITIONS IN STEELMAKING' has been carried out by Miss Sohini Pal under my supervision and that the work has not been submitted elsewhere for a degree.

January, 1989.

(Dr. S.C. Koria)
Assistant Professor
Department of Metallurgical Engg.
Indian Institute of Technology
Kanpur-208016

ACKNOWLEDGEMENTS

As author, I record at the onset, my great indebtedness and deep sense of gratitude to my respected guide Dr.S.C.Koria for his astute guidance, invaluable suggestion and freedom to work, keeping a watchful eye on the progress.

I also extend my indebtedness and respectful gratitude to Dr. A. Ghosh for his useful advice and for permitting me to use instruments of Process Metallurgy Lab.

I sincerely acknowledge the help rendered to me by the staff of Metallurgical Engg. Workshop, Mr. Sharma of Chemical Metallurgy Lab., Mr. Mukherjee of Materials Science Lab. and Mr. Mongole of Thermodynamics Lab.

It is not possible for me to give adequate, explicit credit to all those individuals who have directly or indirectly given aid to perform this project. I, am, however grateful to all of them for their kind help.

-Sohini Pal

CONTENTS

LIST OF TABLES

LIST OF FIGURES

LIST OF SYMBOLS

A	Interfacial area
C_e	equilibrium concentration
C_o	initial concentration
C_t	concentration of time t
d_b	diameter of bath
d_n	diameter of each nozzle
g	acceleration due to gravity
h_b	height of bath
k	rate constant
k_c	rate constant for combined blowing
k_m	mean value of rate constant
k_{min}	minimum value of rate constant
k_t	rate constant for top blowing
M	molecular weight
$\dot{M}$	dimensionless momentum flow rate
$\dot{m}$	momentum flow rate
$\dot{m}_b$	mass flux of benzoic acid
N	exponent
n	number of nozzles
Q	gas flow rate
q_m	dynamic pressure
$\dot{Q}_b$	bottom gas flow rate
$\dot{Q}_t$	gas flow rate for top injection
$\dot{Q}_c$	gas flow rate for top and bottom injection
$\dot{Q}_j$	jetting flow rate
$r_{1/2}$	half maximum velocity radius
t	time

T_g	temperature of gas
T_l	temperature of liquid
V_l	volume of liquid
V_w	volume of water
X	lance distance
β	mass transfer coefficient
ρ_g	density of gas
ρ_l	density of liquid
α	cone angle formed by jet boundary
$\dot{\varepsilon}_b$	mixing energy for bottom blowing
$\dot{\varepsilon}_c$	mixing energy for combined blowing
$\dot{\varepsilon}_t$	mixing energy for top blowing.

ABSTRACT

In the present investigation the intensity of stirring induced by gas injection in a steel making bath has been studied by a cold model simulation. Transfer of benzoic acid from water to paraffin oil due to gas injection has been selected as a criterion of stirring intensity.

In the main experiments, the change in concentration of benzoic acid in water with time has been measured as a function of gas injection parameters which are as follows: top gas injectio rate (or upstream pressure) ranging from 25.8 NL/min to 41.4 NL/mi (pressure from 160 KPa to 250 KPa), bottom gas injection rate rang from 1.08mNL/min to 6.2 NL/min and top lance distance ranging from 7 cm to 18 cm. From the concentration vs. time plots the rate constant (k) has been evaluated.

It has been observed that when gas is injected from top lance only, increase in upstream pressure or decrease in lance distance increases k_t. In the 'hard' blow region, gas injection parameters are not so effective to control k_t as compared to their effectiveness in 'soft' blow region. Bottom gas injection, in case of combined blowing, improves further the mixing condition in the bath. Following correlations have been developed between mixing energy and rate constant: (1) $k_t = 2.90 \times 10^{-4} \dot{\varepsilon}_t^{1.06}$ for top injection, (2) $k_c = 2.88 \times 10^{-3} \dot{\varepsilon}_c^{1.05}$ for simultaneous top and bottom injection. The exponents in the expressions being same suggests that the mechanism of mass

transfer in both the cases is same and it is dispersion formatic between slag and metal.

In this thesis all the details and results of the present investigation have been presented in subsequent chapters.

CHAPTER - 1

INTRODUCTION

1.1 GENERAL

In top blown and simultaneously top and bottom blown steelmaking processes, oxygen is supplied from top through a nozzle (single hole or multi-hole) by varying the distance above the bath surface, in the form of a "free gas jet". A free gas jet carries with it momentum flow rate which on hitting the bath surface transfers its oxygen for refining purpose and at the same time induces favourable conditions for rapid heat and mass transfer rates. Among the favourable conditions (droplet production, formation of slag/metal dispersion etc.) which are conducive for rapid heat and mass transfer rates, intensity of stirring produced by gas jet in the bath and its influence on mass transfer reactions is the most important governing the progress of the blow[1-2]. Such a knowledge has relevance further in relation to combined blown steelmaking in which additional amount of inert or inert and oxidising gas is injected through the bottom of the vessel. Here the sole purpose of gas injection through bottom in addition to the top is to enhance further the intensity of stirring produced by the top blowing of oxygen.

1.2 LITERATURE SURVEY

As in many other high temperature systems the difficulty of making precise measurements under actual operating conditions has led to the use of cold models for the simulation of intensity of stirring induced by gas jet during steelmaking.

In the literature many studies are available in which intensity of stirring induced by gas jet in steelmaking bath had been simulated by single phase liquid mixing[3-8]. In these experiments time elapsed between the addition of a tracer to the bath and the moment when its concentration reached a present fraction of the final concentration was measured[3-8]. This measured time, commonly known as "mixing time" signifies the time required to homogeneize a single phase. In relation to steel making where mass transfer is important (During steel-making, impurities such as silicon, manganese, phosphorus and sulphur are oxidized and transferred from metal to slag. Removal of carbon occurs directly by gas/liquid reaction. The total reactions for removal of impurities always involve the diffusion steps and change transfer reactions at the slag/metal interface) simulation of intensity of stirring by single phase liquid mixing is not inadequate, inspite of the fact that the homogeneization of a liquid by mixing and acceleration of mass transfer reactions are interrelated and both are dependent on the amount of gas stirring energy introduced. The experimental results of Sakane and coworkers[9], and Qu Ying et.al.[10] support the above statement. Both the investigators have studied

mixing of a single phase by measuring mixing time and mass transfer between the phases by injecting gas through the bottom of the vessel. According to Sak ne et.al. mixing time starts to level-off at much lower value of gas injection rate whereas mass transfer rate continues to increase. According to Qu Ying etal. mixing-time does not decrease with increase in agitation energy beyond 100 W/t. But the rate constant for mass transfer continues to increase beyond 100 W/t of agitation energy and starts to level off only beyond 200 W/t agitation energy.

Some investigators have simulated intensity of gas induced stirring by measuring mass transfer between the two immiscible phases. Nakanishi et.al. have investigated the intensity of stirring induced by top gas jet and bottom gas jet in a cold model[5] . The aspect ratio of the model bath was kept similar to industrial scale top blown converters. They measured concentration change of napthal in water extracted from liquid paraffin by injecting gas from top alone and bottom alone. The amount of paraffin was also varied during the experiments. According to them the mass transfer capacity coefficient between slag and metal designated by the product of mass transfer coefficient (β) and the interfacial area (A) is given by[5]

$$(\beta \times A)_B = 3.49 \times 10^{-5} \; Q^3 \; cm^3/min \qquad (1.2.1)$$

where gas is being injected through the bottom. For top injection of gas[5]

$$(\beta x\ A)_T = 1.53x10^{-5}\ Q^3\ cm^3/min \qquad (1.2.$$

The ratio $\phi = (\beta x\ A)_B/(\beta x\ A)_T = 2.28$, compares the mixing condition in the bath produced by different modes of gas injection, i.e. bottom and top. Paul and co-workers have studied mass transfer rates between slag and metal in a cold model simulation of top blown steelmaking. They measured concentratic change of iodine in water extracted from liquid benzene. According to them the product (βx A) has the following relationship[11].

For bottom blowing

$$(\beta x\ A)_B = 18.2\ Q^{0.5}\ cm^3/min \qquad (1.2.3$$

For top blowing

$$(\beta x\ A)_T = 9.4\ Q^{0.5}\ cm^3/min \qquad (1.2.4$$

The ratio, $\phi = (\beta x\ A)_B / (\beta x\ A)_T = 2.$

It is interesting to note that the exponent of Q is independent of type of blowing in the individual experimental results of Nakanishi and coworkers and Paul and coworkers. However the exponent Q is different for both the investigators. The value of pre-exponents in

both equations proposed by Nakanishi et.al. is different from that proposed by Paul et.al. However, it is interesting to note that the ratio of (βx A) between bottom and top is approximately same for both investigators. The results indicate that bottom blowing is approximately two times more effective than top blowing.

A direct comparison between (βx A) of Nakanishi with that of Paul cannot be made because the proposed equations show the trend in the variation of the product (βxA) with gas injection rate for the individual experimental conditions.

1.3 OBJECTIVE OF PRESENT INVESTIGATION

In the present investigation the intensity of stirring induced by gas jet during steelmaking has been simulated in terms of mass transfer between two immiscible liquids in a cold model. In this cold model transfer of benzoic acid from water to oil phase is studied by injecting gas from top and simultaneously from top and bottom.

In the experimental programme both photographic as well as quantitative studies have been done to illustrate the influence of gas injection parameters on the rate of mass transfer. Detailed measurement have been made on the transfer of solute from aqueous phase to oil phase over a wide range of top and bottom injection parameters. The results of the investigation are presented in the subsequent chapters.

CHAPTER - 2

SIMULATION CRITERIA

In the present investigation the intensity of stirring induced by gas jet in a bath during steel making has been studied by a cold model simulation. For this purpose transfer of benzoic acid from water to paraffin oil due to gas injection has been selected as a criterion of stirring intensity.

This cold model is a mass transfer system which consists of distribution of a species between two immiscible liquid phases. Phase I is water and phase II is 1:1 mixture of heavy paraffin oil and toluene solution; Benzoic acid is the transferring species from phase I to phase II. In this model system the impinging air jet does not induce any gas producing reaction in the bath which implies that fluid flow and mixing of the phases in the model are caused by the intensity of gas injection. The model bath height has been selected from the consideration of aspect ratio. From the industrial data it has been observed that the aspect ratio (h_b/d_b), for BOF and combined blown steel making lies in the range of 0.25 to 4[12]. In the present investigation the bath diameter is 0.2 m and bath height is 0.075 m, so that the aspect ratio is 0.375.

In BOF and combined blown steel making practice, multi supersonic nozzles are employed to deliver the necessary

amount of oxygen[12,13]. Multi nozzles are designed so as to produce non-coalescing jets[13]. Free gas jets produced by the nozzle are, although supersonic but within the limits of lance distances employed in the practice the jet hits the bath either at subsonic or sonic velocity[12,13]. Following the above, a three hole model nozzle has been employed in this study, the inclination angle of each nozzle is 15°. Free gas jet of varying intensity in the model is produced by varying the upstream driving pressure (gas injection rate) within the range subsonic to an under expanded supersonic gas jet.

The most important variables in controlling the concentration of force (or the momentum flux) during an impinging jet steel making cycle are the nozzle distance and upstream driving pressure. Upstream driving pressure is normally kept constant during the blow[12,13]. Therefore for a given upstream pressure the nozzle distance is the most important dynamic parameters. From the literature correlation between starting nozzle distance and bath diameter for different capacity converters is available[13].

$$X_i = 0.541\ (d_b)^{1.04} \qquad (2.1)$$

This distance (X_i) is for constant specific blow rate and aspect ratio of the bath. From equation (2.1) at d_b = 0.2m the nozzle height is 10.8 cm. Accordingly height has been varied from 7 cm to 18 cm, in the present investigation.

The upstream pressure and nozzle distance in the model are combined in such a way so that the modified Froude number similarity is maintained with the industrial scale converters. The modified Froude number is calculated from[14],

$$Fr = \frac{\rho_g \, u_m^2}{\rho_l \, g \, h} = \frac{2 \, q_m}{\rho_l \, g \, h} \qquad (2.2)$$

The dynamic pressure q_m is given by, the following equation[15]

$$q_m = \frac{2\dot{m}}{9.062(r_{1/2})^2} \qquad (2.3)$$

where $\dot{m}$ is momentum flow rate within the gas jet and is given by the equation[12-15]

$$\dot{m} = 0.7854 \times 10^5 \, d_n^2 \, P_a \, (1.27 \, P_o/P_a - 1) \qquad (2.4)$$

and $r_{1/2}$ is the half maximum velocity radius which is a measure of the spreading characteristic of the gas jet. This radius is calculated from the effective angle of jet spread by the equation

$$r_{1/2} = X \tan \alpha/2 \qquad (2.5)$$

where $\alpha/2$ is half angle of the cone formed by the jet boundary. According to Lee and coworkers[1] this angle is

7.5^{o} when the jets from multi-nozzles behave as an individual jet[16]. With help of the equations (2.3), (2.4), (2.5) and modified Froude No. has been calculated using equation (2.2) for this present investigation conditions. The calculations are presented in Table - 2. The model upstream pressures and lance distance similarity with the industrial scale converters are further ensured by calculating the dimensionless momentum flow rate No. (M) which is defined as[13],

$$\dot{M} = \frac{\dot{m}}{\rho_l \, g \, X^3} \qquad (2.6)$$

This number compares the action of momentum flow rate on impingin the bath at different nozzle distances with the action of gravity on the same bath.

In Table-1 the different range of dimensionless numbers for industrial scale converter has been compared with that of cold model experiment. The similarity between the two is self evident.

The amount of bottom gas for simultaneous top and bottom injection in the model is determined from the ratio of bottom gas injection rate/top gas rate employed in industrial scale combined blown processes. According to the references the ratio $\dot{Q}_b/\dot{Q}_t$ varies from 0.01 to 0.1[1,2]. In the model the bottom gas injection rates are varied from 1.04 NL min^{-1} to 6.2 NL min^{-1}.

CHAPTER-3

EXPERIMENTAL

The experimental programme of the present investigation consists of two parts: photographic and quantitative measurement.

3.1 EXPERIMENTAL SET-UP

Figure 1 shows the schematic representation of the experimental set-up. Bottom plate of the vessel has been made interchangeable to use separate plates for top blowing and combined blowing experiments. For top blowing experiments the plate does not contain any tuyere where as for combined blown experiments a plate with four tuyeres, for injection of gas from bottom, has been used. The same set-up has been used for quantitative measurements and photographic investigation.

Compressed air has been used to stirr the bath. Air flow rate has been measured by a calibrated capillary and flow meter and rotameter as shown in the figure.

In top blowing experiments air is injected from the top through a vertical lance having multi nozzle at the lance tip. Throat diameter of each nozzle is 1.2 mm, number of nozzles is 3 and their axis is inclined 15° with the vertical axis.

In case of simultaneous top and bottom blowing, besides gas injection from top lance air is also injected through the bottom of the vessel. For this purpose four holes of dimension 0.8 mmϕx 12 mm length have been drilled at a pitch circle diameter 10 cm. Number of holes and the pitch circle diameter has not been changed throughout the study. The pitch circle diameter and number of holes selected from the results available are in a previous work[14].

3.2 CALIBRATION OF FLOW MEASURING DEVICES

3.2.1 Calibration of Capillary Flow Meter

This has been done by means of a wet-test flow meter. Two capillary flow meters has been used for the present study. One is for lower range of flow rate - 1 NL/min to 2.5 NL/min, another is for higher range of flow rate - 3NL/min to 10 NL/min. Their calibration curves have been given in Fig.2(a) and (b).

3.2.2 Calibration of Rotameter

It has been done by using an orifice meter. The procedure for the calculation of flow rates has been given in Appendix I. The calibration curve has been shown in Fig. 3.

3.3 SELECTION OF LIQUIDS

The present study is based on, mass transfer between two immiscible liquid phases. For both photographic investigation

and quantitative measurements, two immiscible liquids used were water (Phase I) and a 1:1 mixture of heavy paraffin oil and toluene (Phase II).

3.3.1 Photographic Investigations

For photographic investigation heavy paraffin oil phase has been coloured by Iodine. No mass transfer onlv the behaviour of two immiscible phases due to the action of gas injection has been studied here. Iodine has been added in phase II simply because of its colouring behaviour.

3.3.2 Quantitative Measurements

For quantitative measurements benzoic acid is used as the transferring species from phase I to phase II. Here phase I is a saturated solution of benzoic acid. This solution has been prepared by dissolving 4.01 gm/litre benzoic acid in distilled water and then filtering it. The strength of benzoic acid solution is determined by titrating against standard KOH solution. For the present study strength of the benzoic acid solution is 0.033 N, and this has been maintained constant for all experiments. Phase II is a mixture of equal volumes (2.50 c.c. each) of heavy paraffin oil and toluene.

3.3.3 Preparation of Solutions for Titration

One main part of the experiment is to determine concentration of benzoic acid time to time, which is done by titration

against standard solution of KOH. A standard solution of KOH cannot be prepared by direct weighting because of its hygroscopic nature. An approximately N/10 solution of KOH has been prepared by dissolving approximately 5.6 gm of KOH in one litre of distilled water. A standard solution of 0.1N oxalic acid is prepared by dissolving exactly 1.575 gm of oxalic acid ($H_2 C_2 O_4 . 2H_2O$) in 250 ml of distilled water.

$$\text{Strength of oxalic acid solution} = \frac{1.575}{63} \times \frac{1000}{25}$$

$$= 0.1N$$

Now this oxalic acid has been titrated against KOH solution using phenolphthalein as indicator. Thus the strength of KOH solution has been determined as follows:

$$25\text{ml of oxalic acid} \equiv 26\text{ ml of KOH}$$

$$\text{Normality of KOH} = \frac{0.1 \times 25}{26} = 0.9615\ (N)$$

This solution has been diluted 5 times and then used for titrating benzoic acid solution.

3.4 EXPERIMENTAL PROCEDURE

3.4.1 Photographic Investigation

For photographic investigation, the experimental procedure is as follows: 25 litre of water has been taken in the glass vessel, 0.5 litre of oil mixture has been coloured by adding iodine solution; then it has been poured carefully along the side of the vessel, and a stop watch has been simultaneously started. Gas has been injected

from top and top and bottom simultaneously at different flow rates. Photographs of two phase solutions has been taken after different time interval of gas blow.

3.4.2 Quantitative Measurements

For all top blown experiments procedure is as follows:

2.5 litre of benzoic acid solution has been taken in the vessel; then 0.5 litre of paraffin oil and toluene mixture has been poured carefully along the side of the vessel, and a stop watch has been simultaneously started (time of pouring oil is 10 sec). Gas injection from top lance starts just after finishing pouring oil. Temperature of the liquid has been measured 25^{o}C. Gas is injected from top lance at a predetermined lance distance and upstream pressure for about 20 to 25 minutes. At a definite time interval 25 ml of phase I is pipetted out and titrated against standard KOH solution using phenolphthaline as indicator. The first appearance of permanent pink colour shows the end point of titration. The particular amount of KOH solution required for titration has been converted to equivalent amount of benzoic acid (1 ml of KOH $\equiv$ 0.00234 gm of benzoic acid) which is nothing but the concentration of benzoic acid at that particular time interval. The location of sampling has been kept fixed through out the experiment. Following the above way titration has been done after 2, 4, 6, 8, 10, 15, 20, 25 minutes of blow and corresponding concentration of benzoic acid has been calculated.

For simultaneous top and bottom blown experiments, both aqueous phase and oil phase are poured in vessel after starting gas injection from bottom. The rest of the procedure is same as that in case of only top blowing.

3.5 EXPERIMENTAL VARIABLES

List of experimental variables is as follows:

(1) Lance distance ranging from 7 cm to 18 cm.

(2) Upstream pressure ranging from 160 KPa to 248.5 KPa.

(3) Top gas flow rate ranging from 25.8 NL/min to 41.4 NL/min.

(4) Bottom gas flow rate ranging from 1.04 NL/min to 6.2 NL/min.

CHAPTER - 4

EXPERIMENTAL RESULTS

In this chapter the experimental results, both photographic investigation and quantitative measurements are presented.

4.1 PHOTOGRAPHIC OBSERVATIONS

Photographic investigation helped to identify the behaviour of two immiscible phases due to action of gas when it is injected from top lance only or injected from both top lance and bottom tuyeres.

Figure 4(a), (b) and (c) show the state of two phases - paraffin oil and aqueous solution when gas is injected from top lance for a definite time. In photograph 4-(a) the upstream pressure is 140 KPa gas flow rate 22.2 NL/min and lance distance is 10 cm and this photograph has been taken after 5 minutes of gas blow. In photograph 4(b) and 4(c) the upstream pressure is 200 KPa gas flow rate 29.3 NL/min at same lance distance and time of gas blow are 2 minutes and 5 minutes respectively. From this three photographs it is observed that in figure 4(b) a light purple coloured layer, which is an oil water imulsion has advanced in water phase.

This layer has advanced further in water phase with increasing time of blow as is observed in Fig.(c). Such a layer is not present for the experimental conditions reported in photograph 1(a When gas is injected simultaneously from top lance and bottom tuyeres the state of two phases is different than presented in Fig. (4) as shown in Figure 5(a), (b) and (c). in All these three cases the top blowing conditions have been kept constant lance distance 10 cm, upstream pressure 180 KPa, and top gas flow rate 29.3 NL/min. Bottom gas flow rates are 7% (2.04 NL/min), 13% (3.8 NL/min) and 21% (6.2 NL/min) of that of top gas flow rate 29.3 NL/min. in Figure 5(a), (b)& 5(c) respectively. The general observation from these three photographs is dispersion of two phases in the form of entrainment of purple coloured oil droplets in water phase just started at lower bottom gas flow rate (Fig.5(a)) and oil droplet formation and entrainment in water increases as % bottom gas injection rate increases (Fig. 5(b) and (c)). Though gas has been injected simultaneously from top lance and bottom tuyeres but no oil water emulsion formation has been observed in the figures.

Both the photographs i.e. 4a-c and 5a-c show that dispersion is the principle mechanism of mass transfer for the gas induced stirring conditions of the present investigation.

4.2 QUANTITATIVE MEASUREMENTS

All the experimental results of measurement of the change in concentration of benzoic acid with respect to time have been reported in Table-3. Table 3.1 contains results for top blowing experiments and Table 3.2 is for simultaneous top and bottom blown experiments.

Experimental results show that the transfer of benzoic acid from phase I to phase II is being affected by the following variables.

4.2.1 Influence of Upstream Pressure

4.2.1.1 Top Injection alone

Figure 6-9 show the fractional change in concentration (C_t/C_o) of benzoic acid in water as a function of time for various upstream pressures or top gas flow rates. In these figures dimensionless lance distance ($X/d_n\sqrt{n}$) has been kept constant and bottom gas flow rate ($\dot{Q}_b$) is zero. The horizontal dotted line in the figures represents the equilibrium ratio C_e/C_o.

In these figures it is observed that starting from unity the ratio C_t/C_o decreases upto some time then it levels off. At any fixed time the decrease is more with increasing upstream pressure. For higher upstream pressure the ratio C_t/C_o decreases faster in the initial period and levels off early.

For example consider Fig. 8, which shows fractional change in (C_t/C_o) vs. time at different upstream pressures and constant dimensionless lance distance 48.11. It is observed that in 20 minutes of transfer the ratio C_t/C_o decreases from unity to 0.66, 0.58, 0.56 and 0.54 for upstream pressures 160 KPa, 180 KPa, 200 KPa and 250 KPa respectively. Levelling off starts after 6 minutes of transfer when pressure level-off is 200 KPa whereas at 160 KPa it does not start to level off within 20 minutes. Similar trend can be observed in Figure 6-9.

4.2.1.2 Simultaneous top and bottom Injection

Figure 10 shows the fractional change in concentration (C_t/C_o) of benzoic acid in water as a function of time for different upstream pressures. In this figure the dimensionless lance distance (X/d_n) is 48.11 and bottom gas flow rate $\dot{Q}_b$ is 2.04 NL/min. It has been observed from the figure that the variation of C_t/C_o with time follows the same trend as that in case of top blown experiments. The important observation is obtained when one compares these results of combined blown experiments with that of top blown experiments. As observed from Fig. 8 after 10 minutes of transfer C_t/C_o decreases from unity to 0.75 and 0.6 for upstream pressure 160 KPa and 200 KPa respectively and at dimensionless lance distance 48.11. But under the same top blowing condition

and after same time C_t/C_o decreases to 0.67 and 0.56 respectively when gas is injected simultaneously from top and bottom.

4.2.2 Influence of Lance Distance

4.2.2.1 Top Injection alone

Figures 11-12 describe the influence of dimensionless lance distance ($X/d_n\sqrt{n}$) on mass transfer process in terms of (C_t/C_o) vs. time plots, at constant upstream pressure. Let us consider Figure 11 which shows variation of C_t/C_o with respect to time at constant upstream pressure 160 KPa and varying dimensionless lance distances. One can observe that starting from unity C_t/C_o decreases for all time intervals at a fixed lance distance. But the decrease is more pronounced with decreasing lance distance. Aftef 15 minutes of transfer C_t/C_o decreases to 0.774 and 0.599 at dimensionless distances 86.6 and 33.7 respectively. Figure 12 also follows the same trend.

4.2.2.2 Simultaneous Top and Bottom Injection

Figure 13 is a typical plot showing the influence of dimensionless lance distance on variation of C_t/C_o with respect to time when gas is injected from top and bottom simultaneously, at a constant rate. Here upstream pressure is 160 KPa and $\dot{Q}_b$ is 2.04 NL/min. Comparing Figure 13 and Figure 11 it is observed that the influence of lance distance is more pronounced when gas is injected from bottom also.

In both the figures the top conditions has been kept constant.

4.2.3 Influence of Bottom Gas Flow Rate

Figures 14-20 shows the variation of fractional concentration (C_t/C_o) change with respect to time for various bottom gas injection rates. In all figures dimensionless lance distance and top gas flow rate have been kept constant. Common observation in these figures are: increasing bottom gas flow rate decreases C_t/C_o for all times in the experiments.

Figure 14 shows the variation of C_t/C_o with respect to time at constant up stream pressure 140 KPa, constant dimensionless distance $X/d_n\sqrt{n}$ = 48.11 and varying bottom gas flow rate. It is observed in the figure that after 10 minutes of transfer of benzoic acid C_t/C_o decreases to 0.8, 0.755, 0.665, 0.575 at gas flow rate 1.08 NL/min, 2.04 NL/min, 3.8 NL/min and 10.0 NL/min respectively. When gas flow rate is 3.8, NL/min change in concentration starts levelling off after 10 minutes of transfer where as at a lower flow rate e.g. 1.08 NL/min , there is a continuous decrease in concentration ratio C_t/C_o till 15 minutes of transfer process, (no levelling off has been observed till 15 minutes of transfer process). Similar trend can be observed in Figs. 14-20.

CHAPTER - 5

ANALYSIS OF RESULTS AND DISCUSSION

In the process of mass transfer between two immiscible liquids followed by mixing of the phases, rate constant of the transfering species is a convenient measure of the intensity of mixing produced by injection of gas into the bath. From the experimental results the rate constant of the transfer of benzoic acid has been evaluated as follows.

5.1 DETERMINATION OF RATE CONSTANT

For a permanent contact mass transfer system (slag is not removed from the system during the process) and for first order reaction kinetics the rate expression is

$$\frac{dc}{dt} = - \frac{\dot{m}_b}{V_w} \qquad (5.1.1)$$

where $\dot{m}_b$ is the mass flow of benzoic acid, V_w is volume of water. Mass flow is related with driving force (concentration gradient) according to the following expression:

$$\dot{m}_b = \beta A (C - C_e) \qquad (5.1.2)$$

where β is mass transfer coefficient of benzoic acid and A is interfacial area between two phases. Substituting Eq. (5.1.2) in eq. (5.1.1) and integrating between the limits at

$t = 0$, $C = C_o$ (initial concentration of benzoic acid) and at $t = t$, $C = C_t$ we get the following expression:

$$\ln \left(\frac{C_t - C_e}{C_o - C_e}\right) = - \frac{\beta A}{V_w} \times t \qquad (5.1.3)$$

$$\Rightarrow \ln \left(\frac{C_t - C_e}{C_o - C_e}\right) = - kt \qquad (5.1.4)$$

In equation 5.1.4 ($k=\beta \times A/V_w$ is the rate constant with dimension min^{-1} and its value signifies the state of mixing in the bath produced by gas injection. Increasing value of k indicates better mixing condition in the bath.

In the present investigation the interfacial area for mass transfer and the amount of liquid dispersed have not been determined, therefore the intensity of mass transfer is determined with reference to the rate constant k according to equation 5.1.4. All the results presented in Fig. (6) - (20) are now plotted according to equation 5.1.4 in figures 21 - 31. Figs. 21 - 24 represents $\ln (C_t-C_e/C_o-C_e)$ vs. time plots when gas is injected from top lance only. In figures 25-31 gas is injected from both top lance and bottom tuyeres. The straight lines in these figures has been drawn by the method of least square analysis. In all these figures the points which has been considered are falling in the range where tha ratio C_t-C_e/C_o-C_e decreases constantly with time. The

experimental results follow closely the eq. (5.1.4) which indicates that diffusion of benzoic acid from water to oil is the rate controlling. All the diffusion processes are accelerated by increasing the intensity of agitation and accordingly the value of k should also indicate the intensity of stirring induced by gas jet in the bath. The value of k is determined by the regression analysis and all these values are listed in Table 4. In the following the variation of k with gas injection parameters is presented.

5.2 RATE CONSTANT AS A FUNCTION OF GAS INJECTION PARAMETERS

5.2.1 Variation of Rate Constant (k_t) with dimensionless lance distance ($X/d_n\sqrt{n}$)

Figure 3.2 shows the variation of rate constant k_t with dimensionless lance distance at different upstream pressures. In the figure we observe that k_t increases with decrease in dimensionless lance distance at all upstream pressures. At lower values of dimensionless lance distance the experimental results suggest a faster increase in k_t in comparison to greater value of distances at all pressures.

5.2.2 Variation of k_t with Upstream Pressure

Figure 3.3 shows the variation of k_t with upstream pressure at different lance distances. It can be seen from the graph that increase in upstream pressure increases k_t at all lance distances.

Both the figures 32 and 33 suggest that a decreasing value of dimensionless lance distance and increasing value of upstream pressure, i.e. making the blow harder increases the value of k_t which indicates improvement in mixing conditions of the bath progressively. The influence of hard blow on improvement in mixing condition has been reported by other investigators in their studies on mixing-time measurements. According to them 'hard' blow decreases mixing - time which is an indicative of better mixing conditions.

5.2.3 Effect of Bottom Gas Injection on Rate Constant in case of Combined Blowing

Figure 34 shows the variation of k_c with the ratio $\dot{Q}_b/\dot{Q}_j$ at different top gas injection conditions. $\dot{Q}_j$ is the bottom gas injection rate at which gas will exit the lance in the form of gas jet. At all values of gas injection rate lower than $\dot{Q}_j$ the gas exits the bottom lance in the form of bubbles. The value of $\dot{Q}_j$ is calculated in Appendix- 2 for the present experimental conditions, it is 40.96 NL/min^{-1}. In the figure an increase in $\dot{Q}_b/\dot{Q}_j$ means increase in $\dot{Q}_b$ only since $\dot{Q}_j$ is a constant parameter.

A set of exponential curves in the above, figures shows a common trend that starting from initial point at $\dot{Q}_b = 0$ and $k_c = k_t$; k_c increases uniformly with increase in

$\dot{Q}_b$ upto a value of the ratio $\dot{Q}_b/\dot{Q}_j$ = 0.14 then each curve starts to level off

This observation suggests that the mixing condition of the top injected bath is improved further by injecting gas through bottom. The amount of bottom gas is around 0.14 times that required to onset the jetting mode of injection i.e. $\dot{Q}_b/\dot{Q}_j$ = 1 ,(onset of jetting mode of injection is relevant for avoiding penetration of liquid into the lance). Levelling-off indicates that the potential of bottom gas injection to improve the mixing condition has been fully utilised. Further increase in $\dot{Q}_b$ beyond 0.14 $\dot{Q}_j$ does not change the value of k_c.

In the industrial scale combined blown steelmaking processes the amount of gas injected through the bottom of the vessel is around 0.15 to 0.2 times that required to onset the jetting mode[1-4,7,17]. This amount is fixed from the consideration of metallurgical characteristics of the process i.e. stabilization of FeO content of slag for a given turndown C content or the product %C x % Fe[1,4,7,17]. Both the considerations are mass transfer controlled. The results reported in figure - 34 suggests that after a particular value of $\dot{Q}_b$ the value of k_c stabilizes which indicates no further improvement in mixing conditions of the bath.

5.3 CORRELATION BETWEEN k AND GAS INJECTION PARAMETERS

The experimental results suggest that in case of top blowing the rate constant for the mass transfer process depend upon top gas injection rate (or supply pressure) and lance distance. In case of combined blowing the rate consta depends further upon the bottom gas injection rate in additi to the top blowing parameters. In the following the experi- mental results are used to develop the empirical correlation between k and gas injection parameters for top blowing and combined blowing.

In the literature on gas induced stirring, the mixing energy is commonly used to quantify the variation of mixing indicator. When gas is injected from top alone the mixing energy is given by[4]

$$\dot{\varepsilon}_t = \frac{0.632 \times 10^{-6} \cos\theta}{V_l} \cdot \frac{\dot{Q}_t^3 \, M}{n^2 \, d_n^3 \, X} \qquad (5.3.1$$

where V_l is in m^3, $\dot{Q}_t$ is in N m^3/min, d_n is in m, X is in m, M is in kg-mole and $\dot{\varepsilon}_t$ is in watt/m^3. For bottom injection the mixing energy is given by[4]

$$\dot{\varepsilon}_b = \frac{6.18 \times \dot{Q}_b \times T_L}{V_l} \left[\ln\left(1 + \frac{l \, g \, h}{P_2}\right) + \left(1 - T_g/T_L\right)\right. \qquad (5.3.2$$

where $\dot{\varepsilon}_b$ is in watt/m^3, $\dot{Q}_b$ is in N m^3/min, T_L is in ^oK, V_l is in m^3, ρ_l is in kg/m^3, g is in m/sec^2, H is in m, P_2 is in N/m^2, T_g is in ^oK.

For combined blowing mixing energy is given by[4],

$$\dot{\varepsilon}_c = \dot{\varepsilon}_b + \lambda \dot{\varepsilon}_t \qquad (5.3.3)$$

Here λ is the coefficient of utilisation of top blowing energy which is about 1/10th of that of top blown energy.

Equation 5.3.1 suggests that mixing energy due to top injection increases when either $\dot{Q}_t$ increases or X decreases. According to eq. 5.3.2 the mixing energy due to bottom injection is directly proportional to $\dot{Q}_b$. According to the experimental results k_t increases with increase in $\dot{Q}_t$ or decrease in X for top injection and k_c increases with increase in $\dot{Q}_b$ for any given combination of top injection parameters. Therefore, the rate constant must bear the following relationship:

$$K \alpha \dot{\varepsilon}^N \qquad (5.3.3)$$

In the eq. 5.3.3, $k = k_t$ and $\dot{\varepsilon} = \dot{\varepsilon}_t$ for top injection and $k = k_c$ and $\dot{\varepsilon} = \dot{\varepsilon}_c$ for simultaneous top and bottom injection. The exponent N characterises the intensity of mixing in bath produced by gas injection. In relation to mass transfer followed by mixing, beside other factors N

would depend mainly upon the mechanism of mass transfer i.e. where mixing of the phases create dispersion or not[14].

In figure 35 k_t has been plotted against the top mixing energy $\dot{\varepsilon}_t$. $\dot{\varepsilon}_t$ has been calculated by using equation 5.3.1 and all values of $\dot{\varepsilon}_t$ has been presented in Table 4.1. Sample calculation of $\dot{\varepsilon}_t$ is in appendix A.3.

Following regression function has been obtained

$$k_t = 2.90 \times 10^{-4} \quad \dot{\varepsilon}_t^{1.06} \tag{5.3.4}$$

The 95% confidence limits about the regression line has been obtained by

$$k_t = \left\{ \dot{\varepsilon}_t^{1.06} \times 10^{C} \right\} \tag{5.3.5}$$

where

$$C = -3.5376 \pm 0.169 \left[1.06 + 0.815 \left(\log \dot{\varepsilon}_t - 2.097 \right)^2 \right]^{1/2}$$

Figure 36 shows variation of k_c and $\dot{\varepsilon}_c$ (i.e. $\dot{\varepsilon}_b + 0.1\ \dot{\varepsilon}_t$). Regression analysis has been given the following relationship:

$$k_c = 2.88 \times 10^{-3} \quad \dot{\varepsilon}_c^{1.05} \tag{5.3.6}$$

The 95% confidence limits about the regression line are obtained by

$$k_c = \dot{\varepsilon}_c^{1.05} \times 10^{C} \tag{5.3.7}$$

where

$$C = -2.54 \pm 0.221\,[\,1.03 + 0.554\,(\log \dot{}_{c} - 1.4489)^2\,]^{1/2} .$$

Combining equation 5.3.1 and equation 5.3.4 we get the following expression

$$k_t = 2.88 \times 10^2 \quad \frac{\dot{Q}_t^{\,3.18}}{X^{1.06}} \qquad (5.3.8)$$

It is interesting to note that the exponent of mixing energy in eqs. 5.3.4 and 5.3.6 is approximately same which indicates that the state of mixing of the phases due to gas injection is approximately same. This observation is supported by the photographic study (See Figs. (4) and (5) in which it is shown that dispersion is the principle mechanism of mass transfer for the present experimental conditions. The difference in the value of pre-exponents in eqs. 5.3.4 and 5.3.6 is probably due to the distribution of the available mixing energy; better distribution of energy e.g. in bottom injection should result in higher value of pre-exponent as compared to top injection. The experimental results, support the above view but further experiments are needed to clarify the above hypothesis.

In the available literature a complete equation is not given but only functional dependence of the type as given in reference[18]

$$k \propto \dot{Q}^{m} \qquad (5.3.9)$$

is given. In some literature complete equation (with reference to values of pre-exponent and exponent) is given [5,11]. An

examination of these equations (See literature survey) suggests that these equations are not general but simply depicts the trend in the variation of rate constant with the gas injection parameters. A complete general equation should include the influence of amount of slag, bath depth, mode of injection etc. on the rate constant for mass transfer process.

In view of the above a quantitative comparison between the k-values of the present investigation with those available in the literature is not being made. However, it may be noted that the value of the exponent (3.12) of the present investigation lay within the range of values reported by other investigation in their studies on mass transfer followed due to dispersion of the phases: these values are 2-3[18]. However a qualitative comparison can be made to show the validity of the results.

5.4 REPRESENTATION OF MIXING CONDITIONS

The experimental results suggests that mixing condition in the bath, either by injecting gas from top above or simultaneously from top and bottom depends upon nozzle distance and top and bottom gas injection rate. The top injection parameters produce two types of blow, "soft" and "hard". "Soft" blow is produced when gas is injected from higher nozzle distance at low flow rate. Decreasing value of nozzle distance or increasing value of gas flow rate makes the blow "harder". The influence of bottom

gas injection is to improve further the mixing conditions in the bath generated by "soft" or "hard" blow.

Both types of blow have strong relevance to the steel-making practice employing top injection of oxygen. For example "soft blow" is needed to produce FeO-rich slag for lime dissolution in order to remove phosphorous whereas hard blow is needed to promote decarburization reaction and to avoid slopping during the progress of refining reactions. The process of slag formation and refining reaction depend to a larger extent on the intensity of stirring generated in the bath by gas injection.

The terms soft and hard blow are relative terms. The definition of these terms requires a reference level. In the following mixing condition in the bath has been presented separately for top injection and simultaneous top and bottom injection in terms of soft and hard blow. The proposed equations 5.3.4 and 5.3.6 can also be used but in the following the experimental values of k are employed.

5.4.1 Top Injection

In Figure - 37 log k_t/k_m has been plotted against $\frac{1}{d_n\sqrt{n}}(X_m - X)$ and $(\dot{Q}_t - \dot{Q}_m)$. X_m and $\dot{Q}_m$ are the arithmetic mean of dimensionless distance and top gas injection rate and these are the reference values.

K_m is the mean value of k_t and depends upon a combination of top gas injection rate and dimensionless lance distance. Height of the bar I_1 shows the variation in k_t/k_m brought by changing the dimensionless lance distance

from 33.7 to 86.6. Similarly I_2 shows the variation of k_t/k_m by changing the top gas injection rate from 25.8 NL/min to 41.4 NL/min. Corresponding to the value of $\frac{1}{d\sqrt{n}}(X_m - X) =$ or $(\dot{Q}_t - \dot{Q}_m) = 0$ on the X-axis the value of $k_t/k_m = 1$ (i.e. log $k_t/k_m = 0$) on the y-axis. Negative values on the X-axis represent soft blow and the positive values "hard"blow, produced by changing either lance distance or gas injection rate.

It can be seen in the graph that a wide range of mixing conditions in the bath (as indicated by the value of k_t/k_m) can be generated either by changing the dimensionless distance or by top gas injection rate. These results indicate that top injection of gas is highly flexible in regulating and controlling the mixing of the phases as required during steel making.

During a steel making cycle top gas injection rate is normally kept constant but the lance distance is varied to control the progress of the refining reactions. In Figure - 38 the ratio $k_t/(k_t)_{min}$ is shown for various lance distances and different gas injection rates on the bar chart. $(k_t)_{min}$ is the minimum value of rate constant obtained in the present investigation at greatest lance distance i.e. 18 cm. Height of the bar indicates the increase in the value of the ratio $k_t/(k_t)_{min}$ brought by decreasing the lance distance at constant gas injection rate.

It can be seen that at lower gas injection rate the ratio $k_t/(k_t)_{min}$ increases from 1 to 3.3 for bath upstream pressure 160 KPa and 180 KPa. But at 200-250 KPa, $k_t/(k_t)_{min}$ increases from 1 to 2.5 at 200 KPa to 1-2 at 250 KPa which suggests that at higher gas rate the lance distance as a parameter to control the stirring potential becomes less effective in comparison to the soft blow.

5.4.2 Bottom Gas Injection Rate for Combined Blowing

In a simultaneous top and bottom injection the amount of bottom gas injection is important for a given top blowing condition. The experimental results are used to determine the optimum amount of bottom gas injection rate with reference to mixing condition in the bath.

In Figure - 39 k_c/k_t has been plotted against $\dot{Q}_c/\dot{Q}_t$ for various top blowing conditions. Dotted lines refer to top injection pressure 200 KPa and solid lines refer to top injection pressure 160 KPa. In the figure at $k_c/k_t = 1$, $\dot{Q}_c/\dot{Q}_t = 1$ which means $1 + \dot{Q}_b/\dot{Q}_t = 1$, so $\dot{Q}_b/\dot{Q}_t = 0$, i.e. $\dot{Q}_b = 0$. So at constant value of $\dot{Q}_t$ increase in the ratio $\dot{Q}_c/\dot{Q}_t$ means increase in $\dot{Q}_b$ only. It is observed from the graph that as $\dot{Q}_c/\dot{Q}_t$ increases k_c/k_t increases at all top blowing parameters. It means that bottom injection improves further the mixing condition in a top injected bath. Second observation is that each curve starts to level-off beyond $\dot{Q}_c/\dot{Q}_t$ _ 1.14 or $\dot{Q}_b/\dot{Q}_t$ _ 0.14. Levelling-off

indicates that the potential of bottom gas injection to improve mixing condition of a top injected bath has been fully utilised.

It can be seen from the graph that at a fixed upstream pressure increase in k_c/k_t with increasing $\dot{Q}_c/\dot{Q}_t$ is more pronounced at higher lance distance (18 cm) than that in case of 15 cm and 10 cm.

For example; At upstream pressure 160 KPa, lance distance 18 cm, $\dot{Q}_t$ = 25.8 NL/min and $\dot{Q}_b$ = 6.2 NL/min the values of rate constants are $(k_t)_1$ = 0.01531, $(k_c)_1$ = 0.1115 and the ratio $\dot{Q}_c/\dot{Q}_t$ = 1.24. Changing lance distance from 18 cm to 10 cm and keeping all other gas injection conditions same, the values of rate constants are $(k_t)_2$ = 0.0272, $(k_c)_2$ = 0.1519; Now $(k_t)_2/(k_t)_1$ = 1.77 where as $(k_c)_2/(k_c)_1$ = 1.36, $(k_c/k_t)_1$ = 7.28, $(k_c/k_t)_2$ = 5.58.

So,

$$\left(\frac{k_c}{k_t}\right)_1 > \left(\frac{k_c}{k_t}\right)_2 .$$

This result indicates that bottom gas injection has greater advantages under "soft blow" conditions than hard blow conditions. The effect of bottom gas injection rate can be further illustrated in the form of bar chart.

In Figure - 40, the influence of bottom gas injection rate $\dot{Q}_b$ on k_c/k_t at constant upstream pressure and lance

lance distance is shown on the bar chart. $k_c/k_t = 1$ is the condition when gas is injected only from top. Increase in k_c/k_t above 1 is due to bottom gas injection. Height of the bar indicates the improvement at different $\dot{Q}_b$ from the base line, i.e. $k_c/k_t = 1$. It can be seen that at lower upstream pressure and higher lance distance, e.g. 160 KPa and 18 cm (which creates a soft blow in the bath) injection of bottom gas improve the ratio (k_c/k_t) from 1 to 7.5. Where as at higher upstream pressure and lower lance distance, e.g. 200 KPa and 10 cm, (which creates a hard blow in the bath) injection of gas from bottom improves the ratio (k_c/k_t) from 1 to 3.0. This suggests that bottom gas injection is much more effective parameter to control the mixing condition in a soft blown bath in comparison to a hard blown bath.

CHAPTER 6

CONCLUSION

Following conclusions can be drawn from the results of the present investigation:

i) Top injection parameters produce two types of blow in a steel making bath 'soft' blow and ' hard' blow. Soft blow is produced when gas is injected from higher nozzle distance at lower gas flow rate resulting low value of k_t. Decreasing value of nozzle distance or increasing value of gas flow rate makes the blow 'harder' which means improvement in k_t value.

ii) In hard blow region, the lance distance or upstream pressure as parameters to improve stirring potential of the bath becomes less effective in comparison to that in 'soft' blow region. By decreasing lance distance from 18 cm to 7 cm, $k_t/(k_t)_{min}$ increases from 1 to 3.5 at an upstream pressure 160 KPa ($\dot{Q}_t$ - 25.8 NL/min), and it increases from 1 to 2 at an upstream pressure 250 KPa (41.3 NL/min).

iii) Top gas injection parameters defines the type of blow produced in the bath. In case of simultaneous top and bottom blowing, influence of bottom gas injection is simply to improve the mixing condition further. Bottom gas injection is much effective - parameter to control mixing condition in a soft blown bath than in care of a hard blown bath. k_c/k_t increases

from 1 to 7.5 by increasing $\dot{Q}_b$ from 1.08 to 6.2 NL/min at top injection condition pressure - 160 KPa and lance distance 18 cm. whereas k_c/k_t increases from 1 to 3.0 by varying $\dot{Q}_b$ in the same range at top injection condition upstream pressure 200 KPa and lance distance 10 cm. The amount $\dot{Q}_b$ is equal to around 0.14 $\dot{Q}_t$ gives maximum improvement in mixing condition in a bath; increasing $\dot{Q}_b$ beyond this range does not increase k_c.

iv) Correlations between rate constant and mixing energy which has been developed in this present investigation are as follows:

For top injection $k_t = 2.90 \times 10^{-4} \dot{\varepsilon}_t^{1.06}$

For simultaneous top and bottom injection, it is $k_c = 2.88 \times 10^{-3} \dot{\varepsilon}_c^{1.05}$

The exponents in both the expressions are approximatelv same - 1.06 and 1.05 respectively. This suggests that the mechanism of mass transfer in both the cases are same which is dispersion formation between slag-metal.

v) The difference in the value of pre-exponents in above correlations is probably due to the distribution of the available mixing energy; better distribution of energy, e.g. by bottom injection should result in higher value of pre-exponent as compared to top injection. The experimental results support the above view but further experiments are needed to clarify the above hypothesis.

SUGGESTION FOR FUTURE WORK

Future work can be done along following lines:

(1) The present study has been done keeping the bottom-tuyere configuration fixed. Influence of other configuration (e.g. semicircular, quarter circular etc.) on the mass transfer rate between slag and metal can be studied.

(2) Influence of volume of slag and initial concentration of the transferring entity on the mass exchange reaction can be studied.

Table-1 : Similarity between the industrial scale converters and the cold model experiments

Dimensionless Number	Numerical definition	Industrial scale, converter	Cold model experiments
1. Distribution number	$\frac{d_n \sqrt{n}}{d_b}$	0.0119 - 0.0196	0.0104
2. Aspect ratio	h_b/d_b	0.25 - 0.37	0.375
3. Nozzle inclination for a multi nozzle	α	9 - 20°	14°
4. Type of nozzle design		Non-coalescing	Non-coalescing
5. Intensity of jet at the bath surface		Sonic subsonic	Subsonic
6. Froude No. (hr)	$\frac{2 q_m}{\rho_l g h_b}$	0.4 - 3.5	0.37 - 5.18
7. Dimensionless momentum flow	$\frac{\dot{m}}{n \rho_l g X^3}$	0.8×10^{-3} to 0.1	2.019×10^{-3} to 0.0726

Table-2 : Froude number and dimensionless momentum flow rate as a function of gas injection parameters

Experimental conditions		$\dot{m}$ (Newton)	$\dot{M}=\dot{m}/\rho_L gX^3$	$r_{1/2}= X \tan\alpha/2$ at $\alpha/2 = 7.5^o$	q_m (N/m^2)	$(N_{Fr})_h = 2q_m/\rho_l gh_b$	$N_{Fr(d)} = 2q_m/\rho_l gd_b$
X (m)	P_o(bar)						
0.18	1.6	0.3466	6.058×10^{-3}	0.0236	137.34	0.373	23.35
	1.8	0.432	7.55×10^{-3}		171.184	0.465	29.10
	2.0	0.5180	9.05×10^{-3}		205.26	0.557	34.908
	2.48	0.733	12.8×10^{-3}		290.46	0.7896	49.397
0.15	1.6	0.3466	10.46×10^{-3}	0.0197	197.107	0.5358	33.52
	1.8	0.432	13.04×10^{-3}		245.67	0.667	41.78
	2.0	0.5180	15.64×10^{-3}		294.58	0.8008	50.098
	2.48	0.733	22.1×10^{-3}		416.84	1.133	70.89
0.1	1.6	0.3466	35.33×10^{-3}	0.013	452.63	1.33	76.97
	1.8	0.432	44.0×10^{-3}		564.16	1.533	95.94
	2.0	0.5180	52.8×10^{-3}		676.5	1.839	115.05
	2.48	0.733	74.7×10^{-3}		957.2	2.60	162.789
0.07	1.6	0.3466	10.3×10^{-2}	0.00921	901.8	2.45	153.36
	1.8	0.432	12.8×10^{-2}		1124.0	3.055	191.15
	2.0	0.5180	15.39×10^{-2}		1347.7	3.66	229.21
	2.48	3.733	21.78×10^{-2}		1907.1	5.184	324.40

Table-3 : Influence of gas injection parameters on change in concentration of benzoic acid with time in water bath

Initial volume of aqueous phase	=	2.5 lit.
Volume of oil phase	=	0.5 lit.
Volume of aqueous phase used for each titration	=	25 ml
Initial concentration of benzoic acid	=	4.012 gm/litre
Equilibrium concentration of benzoic acid	=	2.006
Strength of KOH solution	=	0.0192 (N)
1 ml of KOH	=	0.0023447 gm of bentoic acid

3.1 : Top injection - Number of nozzle, n(3) and diameter of nozzles d_n (1.2 mm) are fixed

Experimental conditions	time (min)	Volume of KOH required (ml)	wt. of acid (W) in 25 ml of bath (gm)	wt. of acid/lit. $C_t = \frac{W \times 1000}{25}$
Lance distance - 18 cm	0	42.8	0.1003	4.012
	2	41.05	0.0962	3.849
	5	38.4	0.0899	3.598
Pressure-180 KPa	10	34.0	0.0795	3.183
$\dot{Q}_t$ = 29.3 NL min^{-1}	15	31.5	0.073	2.946
	20	29.9	0.0699	2.798
	25	29.7	0.0696	2.784
Lance distance-18 cm	0	42.8	0.1003	4.012
	3	40.7	0.0955	3.819
Pressure - 160 KPa	6	39.5	0.0927	3.7102
	10	35.9	0.0840	3.363
$\dot{Q}_t$ = 25.8 NL min^{-1}	15	33.2	0.0776	3.106
	20	32.5	0.076	3.049

Continued....

Table 3.1 (Continued):

Experimental conditions	time (min)	Volume of KOH required (ml)	wt.of acid (W) in 25 ml of bath (gm)	wt% of acid in 1 litre $C_t = \frac{Wx1000}{25}$
Lance distance- 18 cm	0	42.8	0.1003	4.012
	2	40.5	0.0948	3.7937
	5	37.3	0.087	3.494
Pressure - 200 KPa	10	31.2	0.073	2.931
$\dot{Q}_t$ = 32.8 NL min^{-1}	15	29.6	0.069	2.7688
Lance distance- 18 cm	0	42.8	0.1003	4.012
	2	34.2	0.0799	3.199
	4	31.5	0.073	2.949
Pressure - 248 KPa	6	29.6	0.069	2.774
$\dot{Q}_t$ = 41.4 NL min^{-1}	10	29.0	0.0678	2.71
	15	27.5	0.0643	2.573
	20	27.1	0.0635	2.538
Lance distance- 15 cm	0	42.8	0.1003	4.012
	2	40.5	0.095	3.791
	5	40.1	0.0938	3.753
Pressure - 160 KPa	8	36.2	0.0847	3.39
$\dot{Q}_t$ - 25.8 NL min^{-1}	12	33.2	0.0777	3.108
	15	32.23	0.0754	3.0169
	20	31.00	0.0727	2.908
Lance distance- 15 cm	0	42.8	0.1003	4.012
	3	39.01	0.0914	3.658
	5	36.3	0.0850	3.402
Pressure - 180 KPa	8	33.0	0.0772	3.088
$\dot{Q}_t$ = 29.3 NL min^{-1}	12	31.7	0.0741	2.966
	15	29.3	0.0686	2.747
	20	28.0	0.0656	2.625

Contd.....

Table 3.1 (Continued):

Experimental conditions	time (min)	Volume of KOH required (ml)	wt. of acid (W) in 25 ml of bath (gm)	wt% of acid litre $C_t = \frac{Wx100}{25}$
Lance distance-15 cm	0	42.8	0.1003	4.012
	3	37.1	0.08826	3.5306
Pressure - 200 KPa	6	31.43	0.0735	2.942
	10	28.0	0.0656	2.627
$\dot{Q}_t$ = 32.8 NL min^{-1}	15	26.0	0.06096	2.4387
	20	25.9	0.0605	2.422
Lance distance-15 cm	0	42.8	0.1003	4.012
	2	33.8	0.079	3.161
Pressure - 248 KPa	4	28.2	0.066	2.643
	7	25.2	0.059	2.360
$\dot{Q}_t$ = 41.4 NL min^{-1}	10	24.4	0.0570	2.288
	15	23.7	0.055	2.218
Lance distance-10 cm	0	42.8	0.1003	4.012
	2	40.5	0.09477	3.79
Pressure - 160 KPa	5	38.4	0.0899	3.596
	8	33.6	0.0786	3.147
$\dot{Q}_t$ = 25.8 NL min^{-1}	12	30.5	0.07135	2.854
	15	29.6	0.0692	2.767
	20	28.3	0.0661	2.646
Lance distance-10 cm	0	42.8	0.1003	4.012
	2	38.8	0.0907	3.6308
	4	36.9	0.0862	3.452
Pressure - 180 KPa	6	34.6	0.08104	3.2416
	10	30.5	0.0713	2.8523
$\dot{Q}_t$ = 29.3 NL min^{-1}	15	25.3	0.0591	2.365
	20	24.9	0.05826	2.3305
	25	24.7	0.0578	2.3128
Lance distance-10cm	0	42.8	0.1003	4.012
	2	35.8	0.084	3.3546
Pressure - 200 KPa	4	31.2	0.073	2.9247
	6	27.5	0.06448	2.579
$\dot{Q}_t$ = 32.8 NL min^{-1}	10	26.1	0.0611	2.444
	15	24.6	0.0575	2.30186
	20	23.6	0.055	2.208

Continued.....

Table 3.1 (Continued):

Experimental conditions	time (min)	Volume of KOH required (ml)	wt.of acid (W) in 25 ml of bath (gm)	Wt% of acid/litre $C_t = \frac{W \times 1000}{25}$
Lance distance-10cm	0	42.8	0.1003	4.012
	2	32.1	0.0752	3.009
Pressure - 248 KPa	4	24.1	0.0564	2.256
	9	23.4	0.0547	2.1899
$\dot{Q}_t$ = 41.4 NL min^{-1}	15	23.0	0.0539	2.156
	20	23.0	0.0539	2.156
Lance distance-7 cm	0	42.8	0.1003	4.012
	2	38.7	0.0906	3.627
Pressure - 160 KPa	4	34.6	0.0810	3.243
	7	31.3	0.07334	2.9336
$\dot{Q}_t$ = 25.8 NL min^{-1}	10	28.3	0.0662	2.649
	15	25.7	0.0601	2.407
	20	25.2	0.0590	2.360
Lance distance-7 cm	0	42.8	0.1003	4.012
	2	37.3	0.0873	3.494
Pressure - 180 KPa	4	32.3	0.0756	3.0268
	8	26.5	0.06201	2.4807
$\dot{Q}_t$ = 29.3 NL min^{-1}	10	15.2	0.05889	2.355
	12	24.3	0.0569	2.2773
	15	24.0	0.05615	2.246
	20	23.6	0.05517	2.207
Lance distance - 7 cm	0	42.8	0.1003	4.012
	2	36.7	0.0858	3.432
Pressure - 200,KPa	4	31.3	0.0733	2.9325
	7	27.1	0.0635	2.5402
$\dot{Q}_t$ = 32.8 NL min^{-1}	10	25.0	0.0585	2.3403
	12	24.2	0.0565	2.2623
	15	24.0	0.0561	2.246
Lance distance - 7 cm	0	42.8	0.1003	4.012
	2	30.2	0.0707	2.8284
Pressure - 248 KPa	4	25.4	0.0595	2.382
	7	24.0	0.0561	2.244
$\dot{Q}_t$ - 41.4 NL min^{-1}	10	23.6	0.0553	2.213
	12	23.5	0.0549	2.198

Table 3.2 : Simultaneous Top and bottom injection

Fixed top conditions - 3 hole nozzles with nozzle dia 1.2 mm

Fixed bottom conditions - 4 injection elements in circular arrangements

Experimental conditions	time (min)	Volume of KOH required (ml)	wt% of acid (W) in 25 ml of bath (gm)	wt% of acid/litre $C_t = \frac{W \times 1000}{25}$
1	2	3	4	5
Top blowing conditions:	0	42.8	0.1003	4.012
Lance distance-10 cm	2	40.6	0.09493	3.797
Pressure - 140 KPa	4	37.90	0.08876	3.5507
$\dot{Q}_t$ - 22.2 NL min^{-1}	7	36.2	0.08474	3.3897
Bottom blowing conditions	10	34.1	0.0799	3.1966
$\dot{Q}_b$ - 1.08 NLmin^{-1}	13	33.0	0.0772	3.0894
	15	32.3	0.0756	3.025
Lance distance-10cm	0	42.8	0.1003	4.012
Pressure - 140 KPa	2	39.9	0.0933	3.7356
$\dot{Q}_t$ - 22.2 NL min^{-1}	4	37.5	0.0878	3.5121
$\dot{Q}_b$ - 2.04 NL min^{-1}	7	34.7	0.08115	3.246
	10	32.2	0.07528	3.011
	15	30.8	0.07209	2.884
Lance distance-10cm	0	42.8	0.1003	4.012
Pressure - 140 KPa	2	39.2	0.0917	3.6702
$\dot{Q}_t$ - 22.2 NL min min^{-1}	4	34.4	0.0805	3.222
$\dot{Q}_b$ - 3.8 NL min^{-1}	6	32.4	0.07576	3.0307
	8	29.87	0.06989	2.7959
	10	28.7	0.0672	2.6893

Continued....

Table 3.2 (Continued):

1	2	3	4	5
Lance distance -10 cm Pressure - 140 KPa $\dot{Q}_t$ - 22.2 NL min^{-1} $\dot{Q}_b$ -10 NL min^{-1}	0 2 3.5 6 8 10	42.8 31.6 27.2 25.2 24.8 24.6	0.1003 0.0739 0.0636 0.0591 0.0580 0.0575	4.012 2.956 2.5448 2.3648 2.3229 2.3018
Lance distance -10 cm Pressure-160 KPa $\dot{Q}_t$ = 25.8 NL min^{-1} $\dot{Q}_b$ = 1.08 NL min^{-1}	0 2 5 7 10 13 16	42.8 39.6 35.9 33.7 31.8 30.6 29.5	0.1003 0.09258 0.08396 0.07886 0.07442 0.0717 0.06898	4.012 3.7033 3.3589 3.1545 2.977 2.868 2.7593
Lance distance -10 cm Pressure - 160 KPa $\dot{Q}_t$ - 25.8 $NLmin^{-1}$ $\dot{Q}_b$ - 2.04 $NLmin^{-1}$	0 2 4 6 8 10 15	42.8 37.1 34.6 31.6 30.0 28.7 25.6	0.1003 0.0869 0.0809 0.074 0.07009 0.06724 0.0598	4.012 3.4762 3.236 2.963 2.8036 2.689 2.3935
Lance distance-10 cm Pressure-160 KPa $\dot{Q}_t$ - 25.8 $NLmin^{-1}$ $\dot{Q}_b$ - 3.2 $NLmin^{-1}$	0 2 4 6 8 10 15	42.8 33.1 28.2 26.4 25.0 24.9 23.9	0.1003 0.0773 0.0659 0.06185 0.0585 0.0582 0.0559	4.012 3.0955 2.6378 2.4741 2.3415 2.3315 2.2398

Continued.....

Table 3.2 (Continued):

1	2	3	4	5
Lance distance-10 cm	0	42.8	0.1003	4.012
	2	32.8	0.0768	3.0752
Pressure - 160 KPa	4	27.5	0.0643	2.5729
$\dot{Q}_t$ - 25.8 NL min^{-1}	6	24.8	0.0587	2.3274
	8	23.8	0.0558	2.2329
$\dot{Q}_b$ - 3.8 NL min^{-1}	10	23.8	0.0558	2.2329
	15	23.4	0.0548	2.194
Lance distance-10 cm	0	42.8	0.1003	4.012
	2	29.7	0.0696	2.7856
Pressure - 160 KPa	4	26.5	0.06213	2.4852
$\dot{Q}_t$ - 25.8 NL min^{-1}	6	24.9	0.05825	2.330
	8	24.5	0.0573	2.29415
$\dot{Q}_b$ - 6.2 NL min^{-1}	10	24.5	0.0573	2.29415
Lance distance-10 cm	0	42.8	0.1003	4.012
	2	29.5	0.0691	2.765
Pressure - 160 KPa	3	26.6	0 0623	2.4923
$\dot{Q}_t$ - 25.8 NL min^{-1}	4	24.8	0.0579	2.3192
	6	24.5	0.0572	2.2897
$\dot{Q}_b$ - 10 NL min^{-1}	8	24.2	0.0567	2.2691
Lance distance-10 cm	0	42.8	0.1003	4.012
	1	34.9	0.08175	3.2702
Pressure - 160 KPa	2	28.3	0.06615	2.646
$\dot{Q}_t$ - 25.8 NL min^{-1}	4	25.3	0.05916	2.3666
	6	24.6	0.0575	2.302
$\dot{Q}_b$ - 13 NL min^{-1}	8	24.6	0.0575	2.302
Lance distance-10 cm	0	42.8	0.1003	4.012
	2	36.4	0.08525	3.4101
Pressure - 200 KPa	5	30.8	0.0722	2.8893
$\dot{Q}_t$ - 32.8 NL min^{-1}	8	28.3	0.066	2.6479
	10	26.6	0.06225	2.4903
$\dot{Q}_b$ - 1.08 NL min^{-1}	15	26.6	0.06225	2.4903

Continued.....

Table 3.2 (Continued):

1	2	3	4	5
Lance distance -10 cm Pressure - 200 KPa $\dot{Q}_t$ - 32.8 NL min^{-1} $\dot{Q}_b$ - 2.04 NL min^{-1}	0 2 4 6 88 10	42.8 33.3 28.4 25.7 24.3 24.2	0.1003 0.0778 0.06655 0.0603 0.0568 0.0566	4.012 3.1153 2.662 2.4127 2.274 2.2648
Lance distance - 10 cm Top pressure - 200 KPa $\dot{Q}_t$ - 32.8 NL min^{-1} $\dot{Q}_b$ - 6.2 NL min^{-1}	0 2 4 6 8 10	42.8 28.8 26.7 24.9 24.4 24.2	0.1003 0.0673 0.0624 0.0583 0.057 0.0566	4.012 2.6959 2.498 2.334 2.286 2.266
Lance distance - 10 cm Top pressure - 200 KPa $\dot{Q}_t$ - 32.8 NL min^{-1} $\dot{Q}_b$ - 10 NL min^{-1}	0 2 3 4 6 8	42.8 27.8 25.5 24.2 23.9 23.9	0.1003 0.06503 0.0597 0.0565 0.05603 0.05603	4.012 2.6015 2.3915 2.2615 2.2412 2.2412
Lance distance - 15 cm Top pressure - 160 KPa $\dot{Q}_t$ - 25.8 NL min^{-1} $\dot{Q}_b$ - 1.08 NL min^{-1}	0 2 5 7 10 15 20	42.8 39.7 36.8 35.2 33.3 30.6 29.7	0.1003 0.0929 0.0861 0.0823 0.0778 0.07167 0.0694	4.012 3.716 3.444 3.294 3.115 2.867 2.779
Lance distance - 15 cm Pressure - 160 KPa $\dot{Q}_t$ - 25.8 NL min^{-1} $\dot{Q}_b$ = 2.04 NL min^{-1}	0 2 5 7 10 15	42.8 39.8 34.3 33.2 30.1 26.0	0.1003 0.0932 0.0802 0.0777 0.0704 0.0608	4.012 3.730 3.209 3.111 2.818 2.435

Continued....

Table 3.2 (Continued):

1	2	3	4	5
Lance distance - 15 cm	0	42.8	0.1003	4.012
	2	36.4	0.0852	3.411
Pressure - 160 KPa	4.5	31.7	0.07423	2.969
$\dot{Q}_t$ - 25.8 NL min^{-1}	6	28.0	0.0656	2.626
	8	25.10	0.0587	2.3506
$\dot{Q}_b$ - 3.8 NL min^{-1}	10	23.6	0.0552	2.211
	15	23.2	0.05434	2.173
Lance distance - 15 cm	0	42.8	0.1003	4.012
	2	33.5	0.07848	3.139
Top pressure - 160 KPa	4	28.3	0.06613	2.645
$\dot{Q}_t$ - 25.8 NL min^{-1}	6	23.8	0.05576	2.2307
	8	23.1	0.05411	2.1646
$\dot{Q}_b$ - 6.2 NL min^{-1}	10	23.1	0.05411	2.1646
Lance distance - 15 cm	0	42.8	0.1003	4.012
	2	36.3	0.0849	3.398
Top pressure - 200 KPa	4	31.6	0.0740	2.9611
$\dot{Q}_t$ - 32.8 NL min^{-1}	6	28.1	0.0658	2.6322
	8	26.3	0.06152	2.4608
$\dot{Q}_b$ - 1.08 NL min^{-1}	10.5	25.7	0.06115	2.4046
Lance distance - 15 cm	0	42.8	0.1003	4.012
	2	34.6	0.08104	3.2417
Top pressure - 200 KPa	4	30.0	0.0704	2.8164
$\dot{Q}_t$ - 32.8 NL min^{-1}	6	27.2	0.0638	2.552
	8	25.7	0 0.0602	2.4106
$\dot{Q}_b$ - 2.04 NL min^{-1}	10	25.2	0.0589	2.3589
Lance distance - 15 cm	0	42.8	0.1003	4.012
	2	32.2	0.0753	3.0146
Top pressure - 200 KPa	4	26.5	0.06205	2.482
$\dot{Q}_t$ - 32.8 NL min^{-1}	6	24.3	0.05683	2.273
	8	22.7	0.05326	2.1306
$\dot{Q}_b$ - 3.8 NL min^{-1}	11	22.7	0.05326	2.1306

Continued....

Table 3.2 (Continued):

1	2	3	4	5
Lance distance-15 cm	0	42.8	0.1003	4.012
Top pressure-200 KPa	2	31.3	0.0732	2.930
	4	24.5	0.05725	2.2901
$\dot{Q}_t$ - 32.8 NL min^{-1}	6	22.8	0.0533	2.135
	8	22.3	0.0522	2.088
$\dot{Q}_b$- 6.2 NL min^{-1}	10	22.3	0.0522	2.088
Lance distance-15 cm	0	42.8	0.1003	4.012
Top pressure-160 KPa	3	39.1	0.09149	3.659
	5	37.4	0.08749	3.499
$\dot{Q}_t$ - 25.8 NL min^{-1}	7	35.5	0.0832	3.329
	10	33.5	0.0784	3.137
$\dot{Q}_b$ - 1.08 NL min^{-1}				
Lance distance-18 cm	0	42.8	0.1003	4.012
Pressure - 160 KPa	2	39.1	0.0917	3.668
	5	34.4	0.0804	3.218
$\dot{Q}_t$ - 25.8 NL min^{-1}	7	32.5	0.0761	3.046
	10	30.0	0.07026	2.8105
$\dot{Q}_b$ - 2.04 NL min^{-1}	15	28.6	0.0670	2.681
	20	28.2	0.065	2.638
Lance distance-18 cm	0	42.8	0.1003	4.012
Pressure - 160 KPa	2	34.1	0.0798	3.192
	4	28.3	0.0663	2.653
$\dot{Q}_t$ - 25.8 NL min^{-1}	6	25.8	0.06039	2.415
	9	24.4	0.0571	2.286
$\dot{Q}_b$ - 3.8 NL min^{-1}	12	23.4	0.0547	2.189
Lance distance-18 cm	0	42.8	0.1003	4.012
Pressure-160 KPa	2	32.4	0.0759	3.036
	4	27.5	0.0644	2.577
$\dot{Q}_t$ - 25.8 NL min^{-1}	6	25.6	0.0599	2.398
	9	24.8	0.0581	2.325
$\dot{Q}_b$ - 6.2 NL min^{-1}	12	24.8	0.0581	2.325

Continued...

Table 3.2 (Continued):

1	2	3	4	5
Lance distance-18 cm	0	42.8	0.1003	4.012
Pressure - 160 KPa	2	29.8	0.0698	2.793
$\dot{Q}_t$ - 25.8 NL min^{-1}	4	25.6	0.0598	2.3939
$\dot{Q}_b$ - 10.0 NL min^{-1}	6	24.2	0.0567	2.268
	8	24.0	0.0560	2.2435
Lance distance-18 cm	0	48.2	0.1003	4.012
Pressure - 200 KPa	3	36.3	0.0850	3.401
$\dot{Q}_t$ - 32.8 NL min^{-1}	5	33.1	0.07739	3.095
$\dot{Q}_b$ - 1.08 NL min^{-1}	7	30.5	0.07134	2.8536
	10	28.9	0.0676	2.706
	15	28.3	0.0663	2.653
	20	28.2	0.0660	2.643
Lance distance-18 cm	0	48.2	0.1003	4.012
Pressure - 200 KPa	2	36.7	0.0859	3.438
$\dot{Q}_t$ - 32.8 NL min^{-1}	5	30.8	0.0721	2.886
$\dot{Q}_b$ - 2.04 NL min^{-1}	7	28.0	0.0655	2.621
	10	26.4	0.0618	2.473
	15	26.0	0.0610	2.441
Lance distance-18 cm	0	48.2	0.1003	4.012
Pressure - 200 KPa	2	30.8	0.07205	2.882
$\dot{Q}_t$ - 32.8 NL min^{-1}	4	25.9	0.0607	2.428
$\dot{Q}_b$ - 3.8 NL min^{-1}	6	24.1	0.0564	2.259
	8	23.2	0.0543	2.174
	10	22.9	0.0535	2.143
Lance distance-18 cm	0	8.2	0.1003	4.012
Pressure - 200 KPa	2	29.1	0.06878	2.727
$\dot{Q}_t$ - 32.8 NL min^{-1}	4.5	23.9	0.0560	2.242
$\dot{Q}_b$ - 6.2 NL min^{-1}	6	23.6	0.0552	2.208
	8	23.5	0.0549	2.197
	10	23.5	0.0549	2.197

Continued.....

Table 4 : Rate constant and mixing energy as a function of gas injection parameters

4.1 Top blown experiments

Experimental conditions			$k_t (min^{-1})$	$\dot{\varepsilon}_t$ watt/m^3
Lance distance (cm)	Top pressure (KPa)	Flow rate NL min^{-1}		
18	160	25.8	0.01531	43.41
	180	29.3	0.021	63.58
	200	32.8	0.03158	89.2
	248	41.4	0.0808	179.36
15	160	25.8	0.01896	52.1
	180	29.3	0.0281	76.3
	200	32.8	0.04779	107.03
	248	41.4	0.10238	215.24
10	160	25.8	0.0272	78.14
	180	29.3	0.0423	114.4
	200	32.8	0.07575	160.56
	248	41.4	0.1386	322.85
7	160	25.8	0.04815	111.6
	180	29.3	0.0702	163.5
	200	32.8	0.0779	229.37
	248	41.4	0.1568	461.22

4.2: Combined Blown Experiments

Experimental conditions for top blowing	Bottom flow rate $NLmin^{-1}$	Combined rate constant k_c min^{-1}	Bottom mixing energy $\dot{\varepsilon}_b$ Watt/m^3	Top mixing energy $\dot{\varepsilon}_t$ $watt/m^3$
1	2	3	4	5
Lance distance-18cm Pressure - 200 KPa $\dot{Q}_t$ - 32.8 NL min^{-1}	1.08 2.04 3.8 6.2	0.05 0.0687 0.139 0.189	5.75 10.87 20.26 32.05	89.2
Lance distance -18cm Pressure - 160 KPa $\dot{Q}_t$ - 25.8 NL min^{-1}	1.08 2.04 3.8 6.2 10	0.024 0.0369 0.1 0.1115 0.168	5.75 10.87 20.26 32.05 53.3	43.41
Lance distance - 15 cm Pressure - 200 KPa $\dot{Q}_t$ - 32.8 NL min^{-1}	1.08 2.04 3.8 6.2	0.076 0.088 0.150 0.201	5.75 10.87 20.26 33.05	107.03
Lance distance -15cm Pressure - 160 KPa $\dot{Q}_t$ - 25.8 NL min^{-1}	1.08 2.04 3.8 6.2	0.0244 0.04125 0.0941 0.142	5.75 10.87 20.26 33.05	52.1
Lance distance-10 cm Pressure - 200 KPa $\dot{Q}_t$ - 32.8 NL/min	1.08 2.04 6.2 10	0.09176 0.115 0.2245 0.2373	5.75 10.87 33.05 53.3	160.56

Continued.....

Table 4.2 (Continued):

1	2	3	4	5
Lance distance-10cm Pressure - 160 KPa $\dot{Q}_t$ - 25.8 NL/min^{-1}	1.08 2.04 3.2 3.8 6.1 10.0 13.0	0.03 0.0498 0.1087 0.128 0.1519 0.2048 0.2059	5.75 10.87 17.06 20.26 33.05 53.3 68.77	78.14
Lance distance-10cm Pressure-140 KPa $\dot{Q}_t$ - 22.2 NL/min^{-1}	1.08 2.04 3.8 10.0	0.0217 0.0298 0.0522 0.1431	5.75 10.87 20.26 53.3	

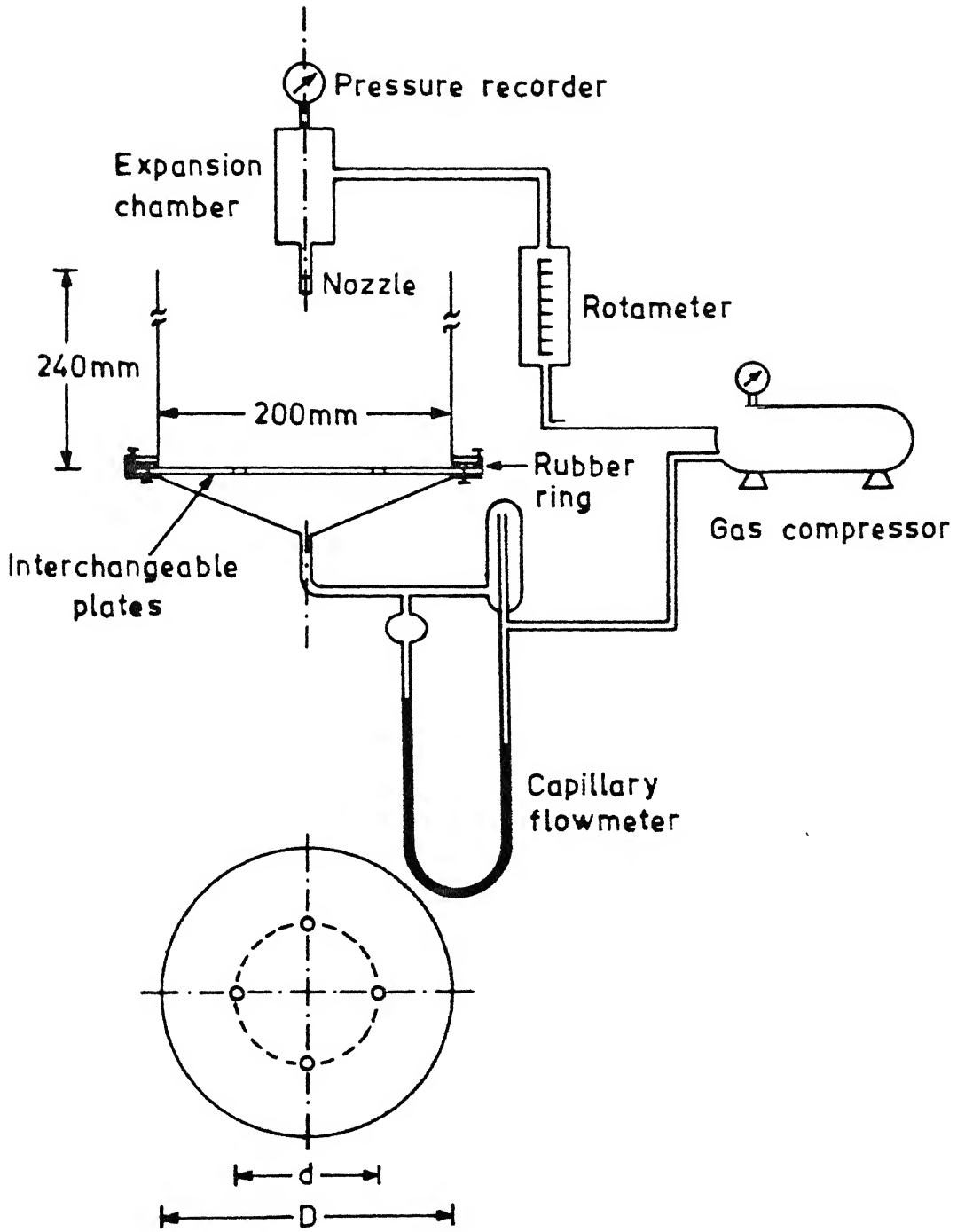

Fig. 1 : Schematic representation of experimental set-up

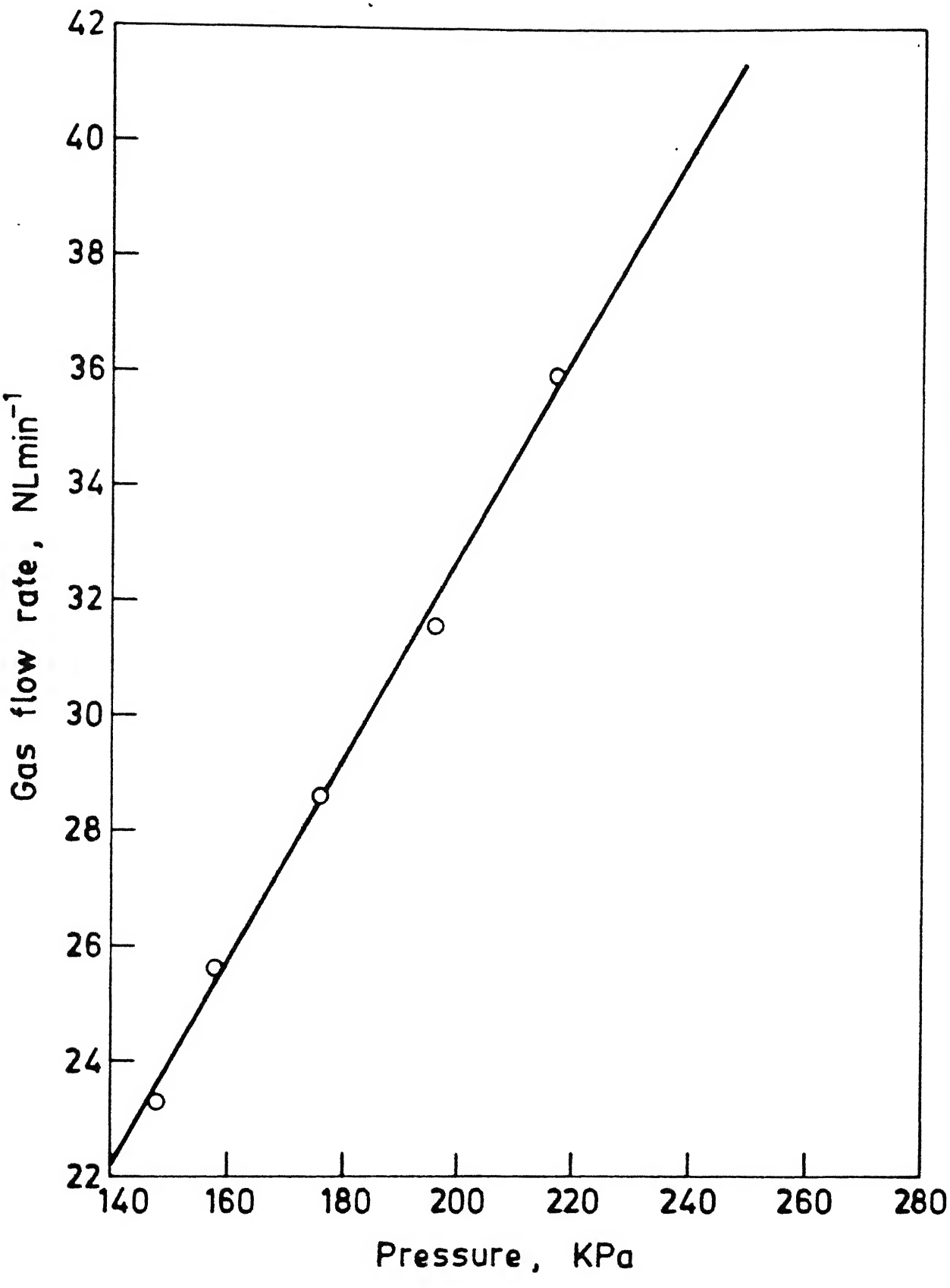

Fig.3 : Calibration curve for rotameter.

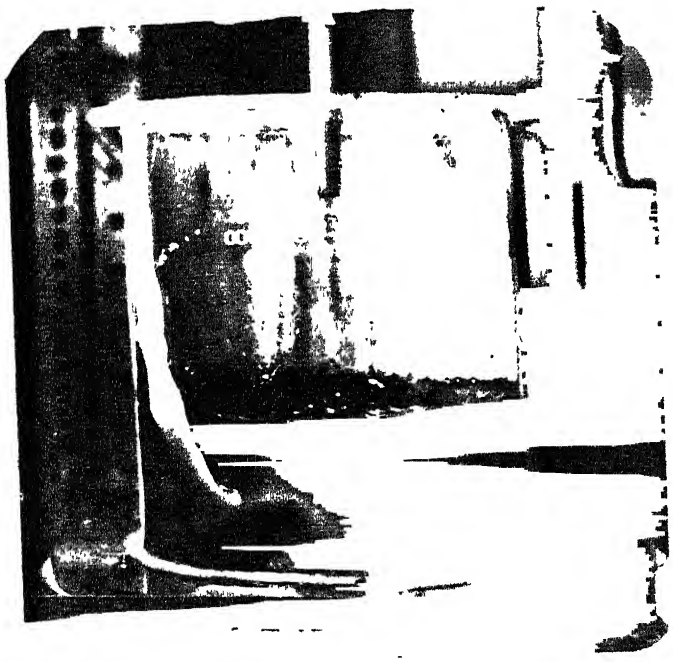

Fig.4(a): Pressure 140 KPa ($\dot{Q}_t$ =22.2 NL/min) lance distance 10 cm.

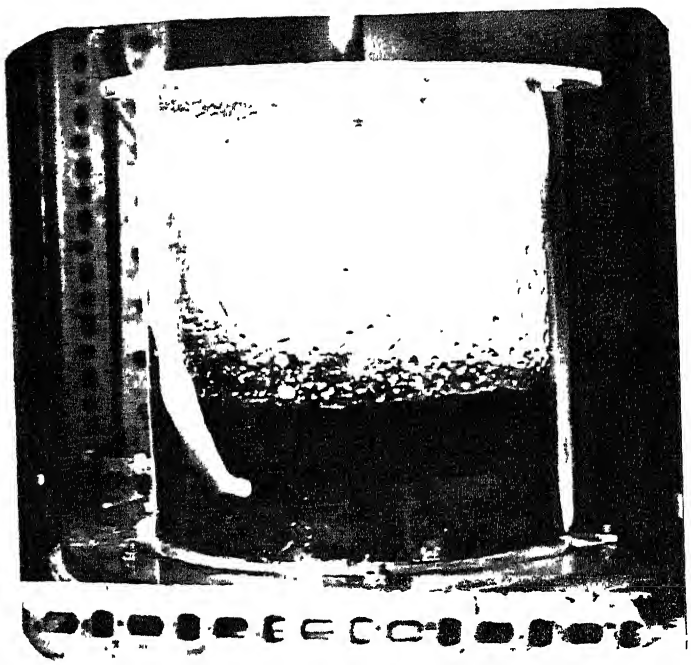

Fig.4(b): Pressure 200 KPa ($\dot{Q}_t$ = 29.3 NL/min) lance distance 10 cm.

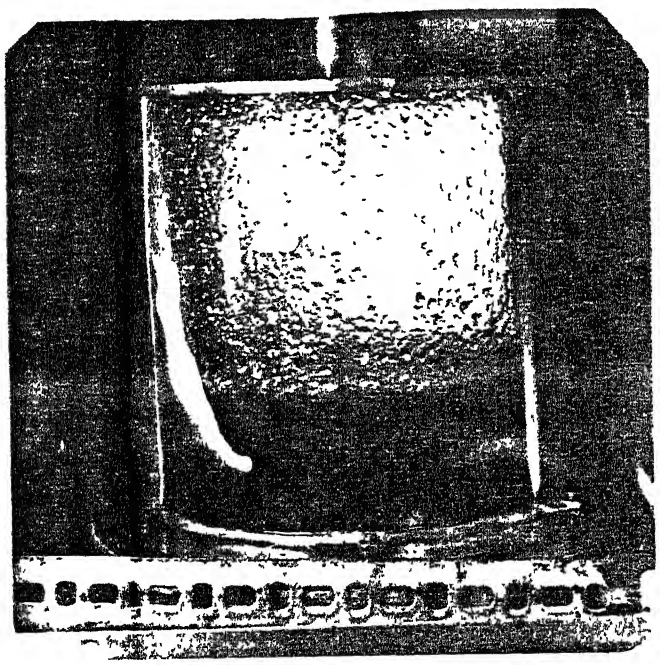

Fig.4(c) : Pressure 200 KPa ($\dot{Q}_t$ = 29.3 NL/min) lance distance 10 cm.

Fig. 4 : Photographs showing the behaviour of two immiscible phases (water and oil phase coloured iodine) under the action of top gas jet.

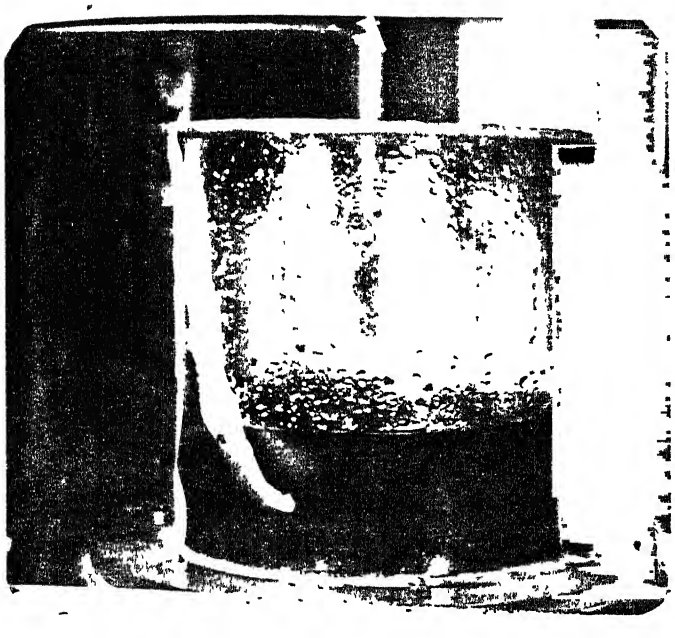

Fig.5(a) : Pressure 180 KPa, lance distance 10 cm. $\dot{Q}_b$ - 2.04 NL/min.

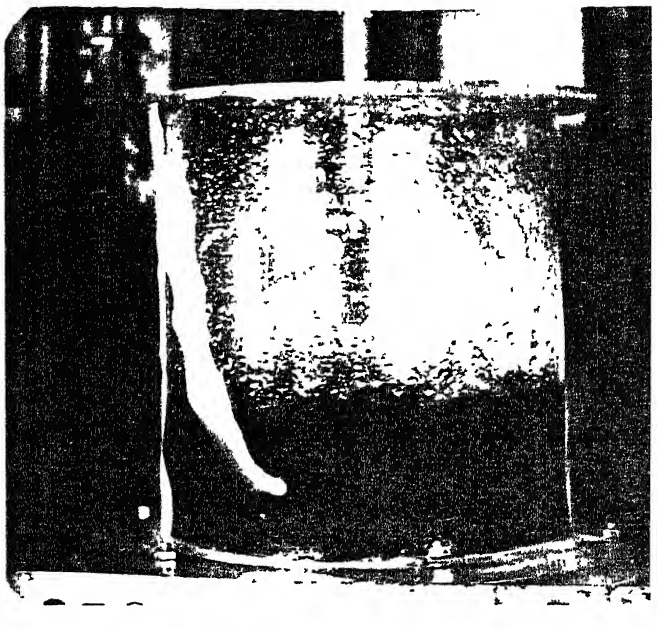

Fig.5(b): Pressure - 180 KPa and lance distance - 10 cm. $\dot{Q}_b$ - 3.8 NL/m

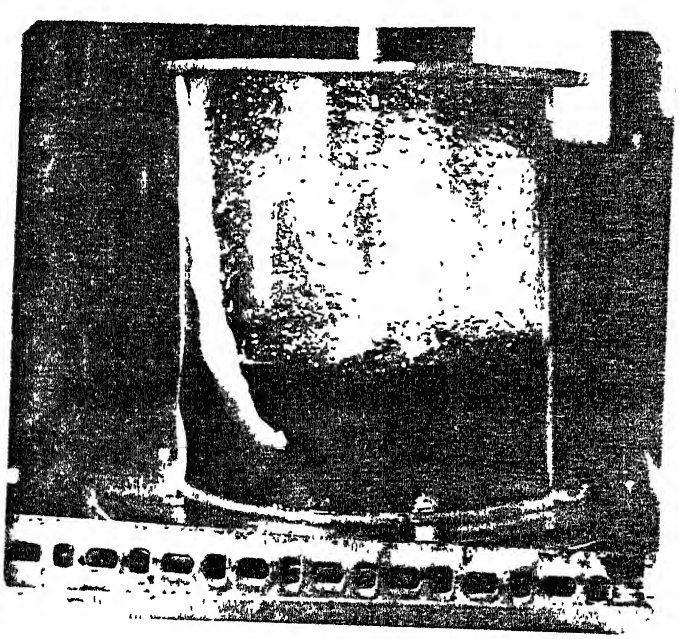

Fig.5(c) : Pressure - 180 KPa and Lance distance - 10 cm $\dot{Q}_b$ - 6.2 NL/min.

Fig. 5 : Photographs showing the behaviour of two immisble phases (water and oil) when gas is injected simultaneously from top and bottom.

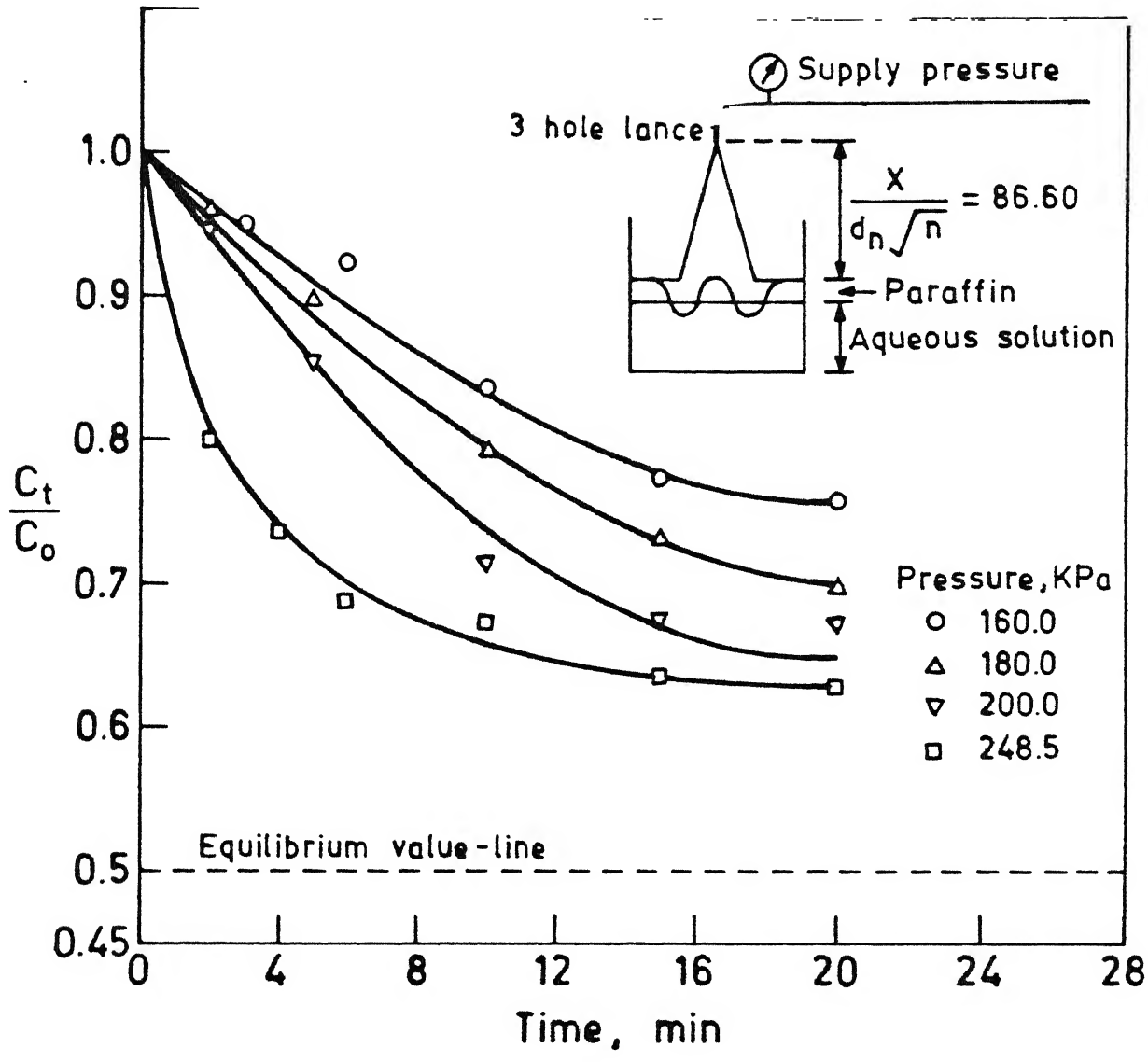

Fig.6 : Fractional change of concentration of benzoic acid in water vs. time during top injection at various upstream pressures and constant dimensionless lance distance ($X/d_n\sqrt{n}$ = 86.6)

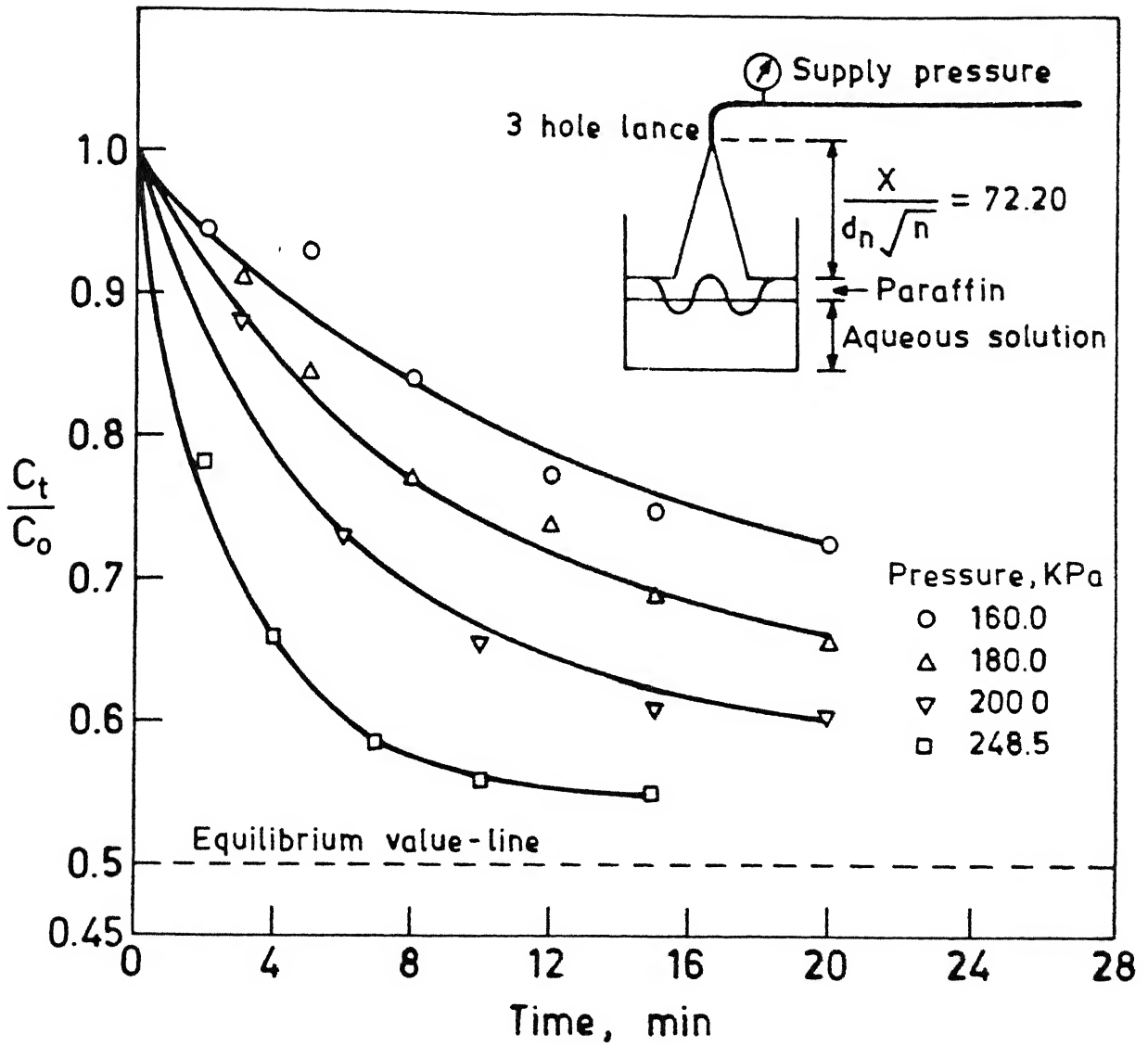

Fig.7 : Fractional change of concentration of benzoic acid in water vs. time, for top injection at various upstream pressures and constant dimensionless lance distance ($X/d_n\sqrt{n} = 72.2$)

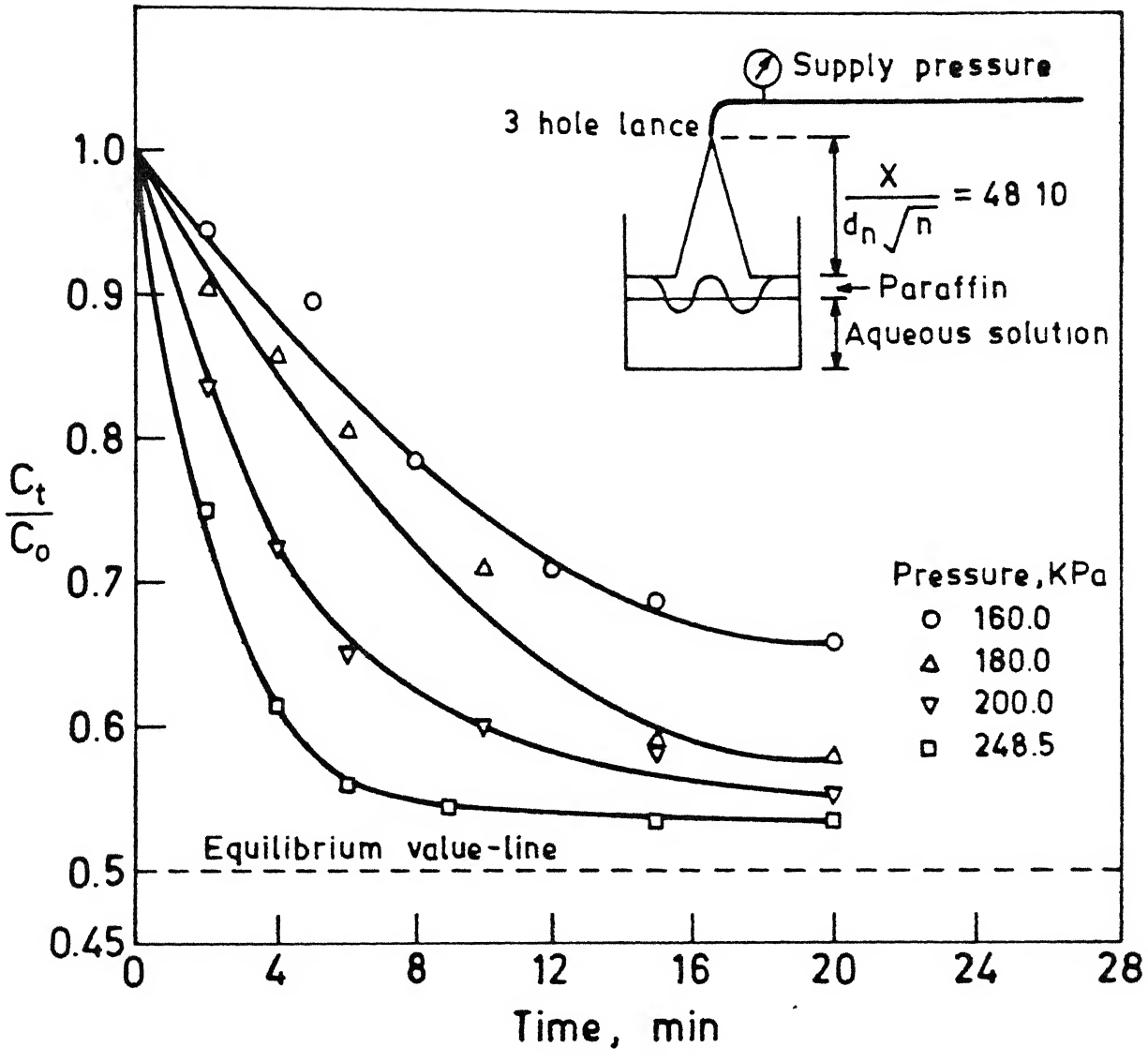

Fig. 8 : Fractional change of concentration of benzoic acid in water vs. time, for top injection at various upstream pressures and constant dimensionless lance distance ($X/d_n\sqrt{n}$ = 48.11)

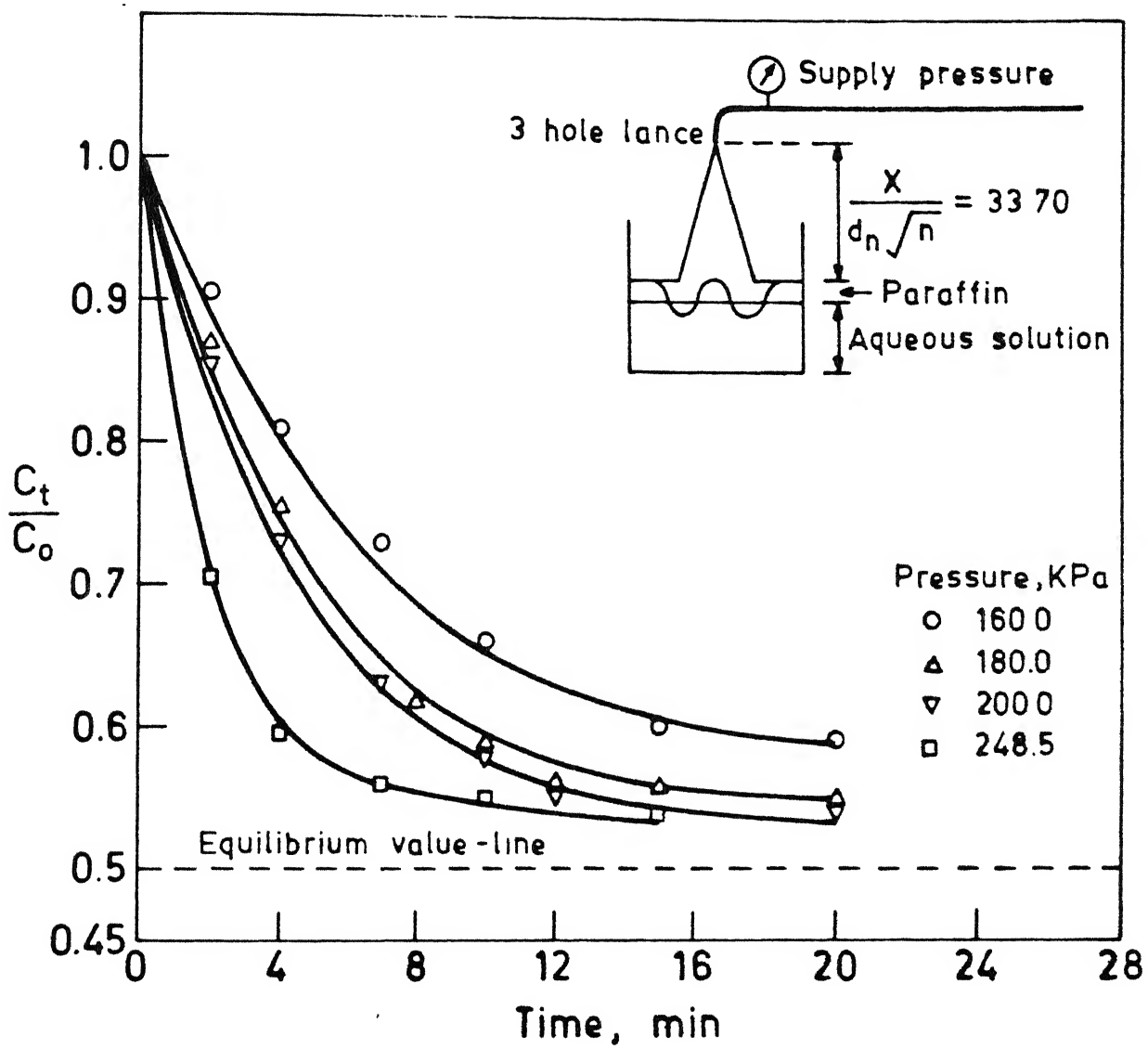

Fig. 9 : Fractional change of concentration of benzoic acid in water vs. time, for top injection at various upstream pressures and constant dimensionless lance distance ($X/d_n\sqrt{n}$ = 33.7).

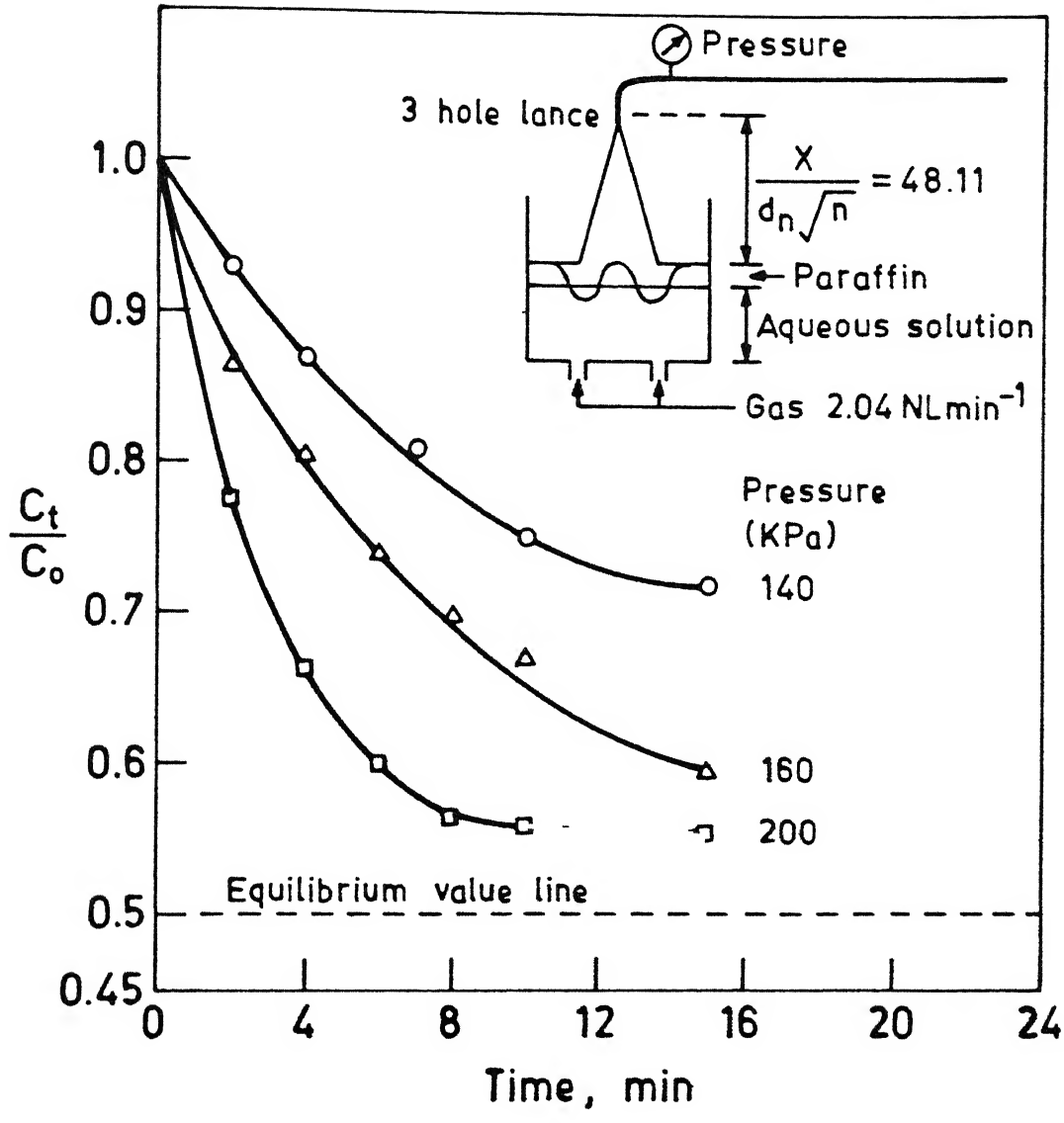

Fig. 10 : Fractional change of concentration of benzoic acid in water vs. time, for simultaneous top and bottom injection, at various upstream pressures, constant dimensionless lance distance ($X/d_n\sqrt{n} = 48.11$), and constant bottom gas injection rate ($\dot{Q}_b$ = 2.04 NL min^{-1}

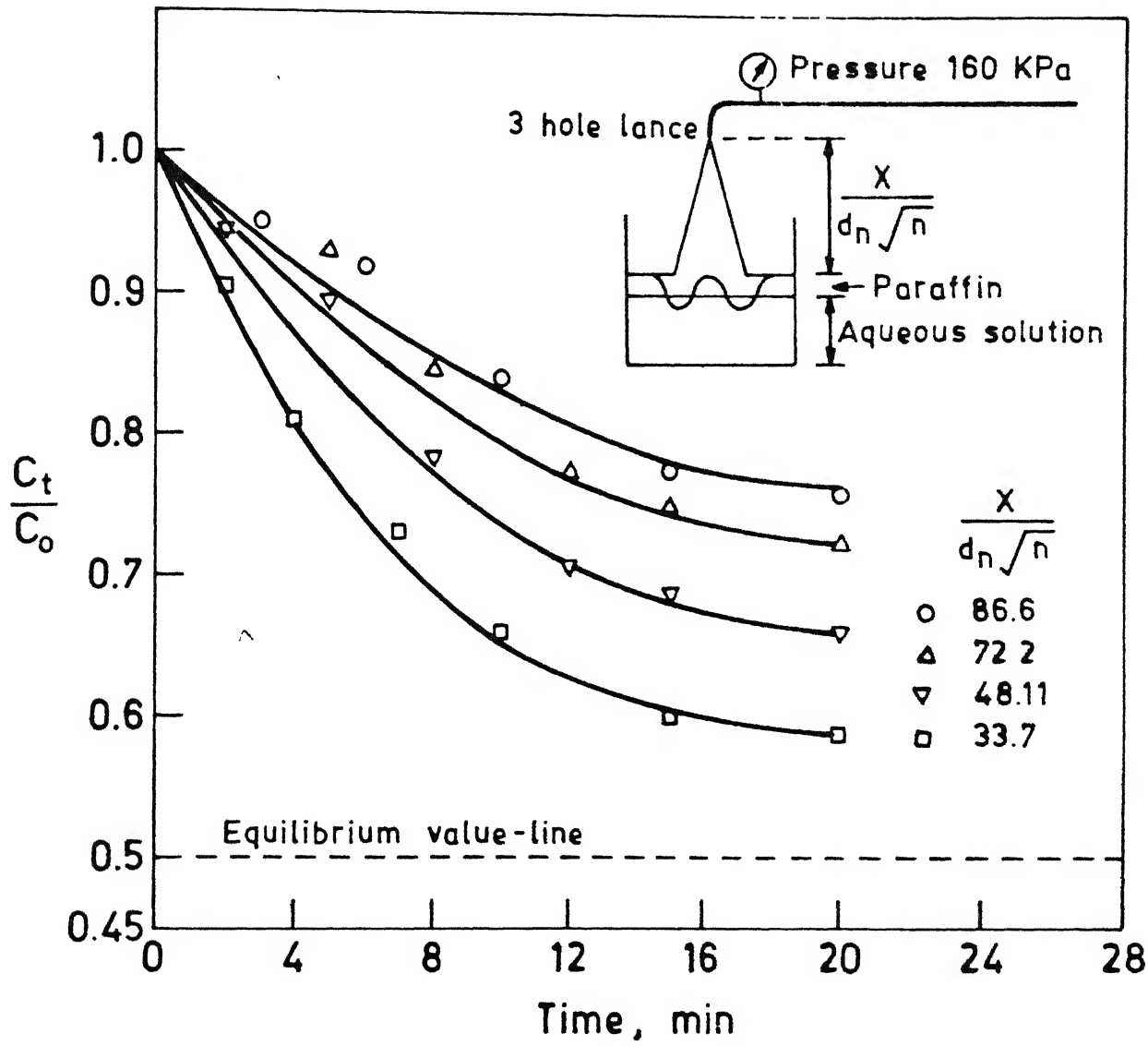

Fig. 11 : Fractional change of concentration of benzoic acid in water vs. time, during top injection, at various dimensionless lance distances ($X/d_n\sqrt{n}$) and at constant upstream pressure (160 KPa)

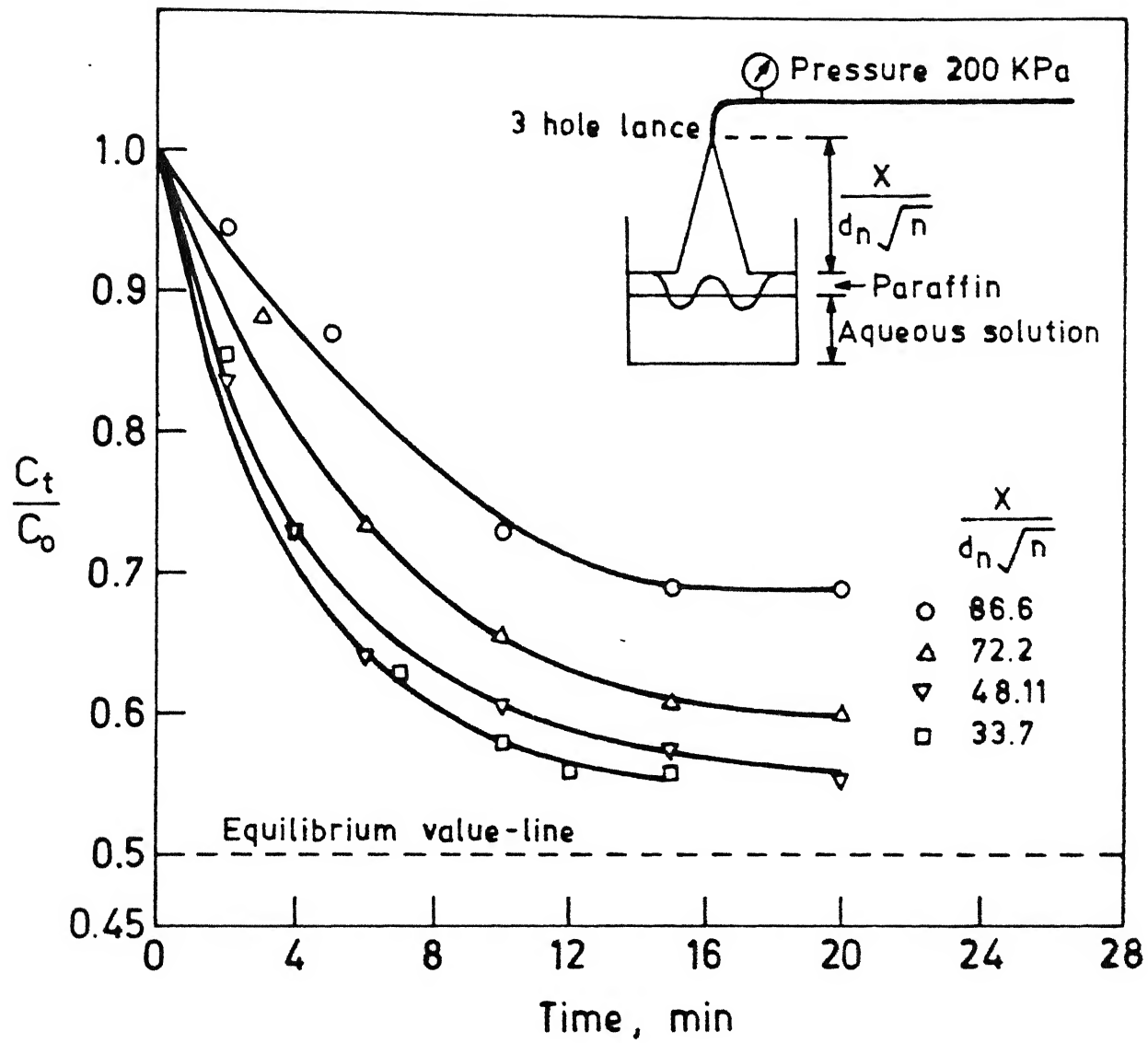

Fig. 12 : Fractional change of concentration of benzoic acid in water vs. time, during top injection, at various dimensionless lance distances ($X/d_n\sqrt{n}$) and at constant upstream pressure (200 KPa)

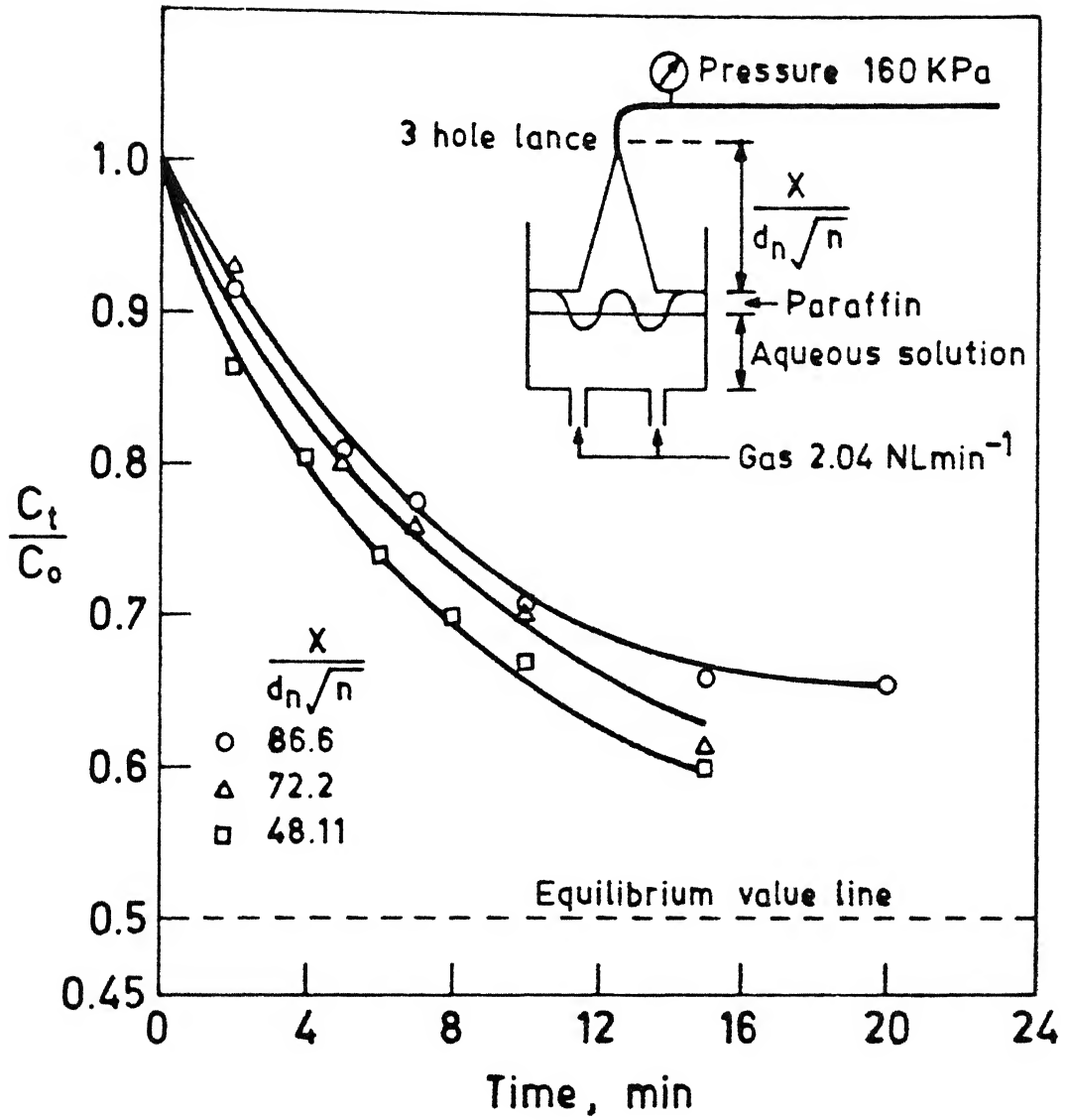

Fig.13 : Fractional change of concentration of benzoic acid in water vs. time, during simultaneous top and bottom injection, at various dimensionless lance distances ($X/d_n\sqrt{n}$), constant upstream pressure 160 KPa, and constant bottom gas injection rate ($\dot{Q}_b$ = 2.04 NL/min)

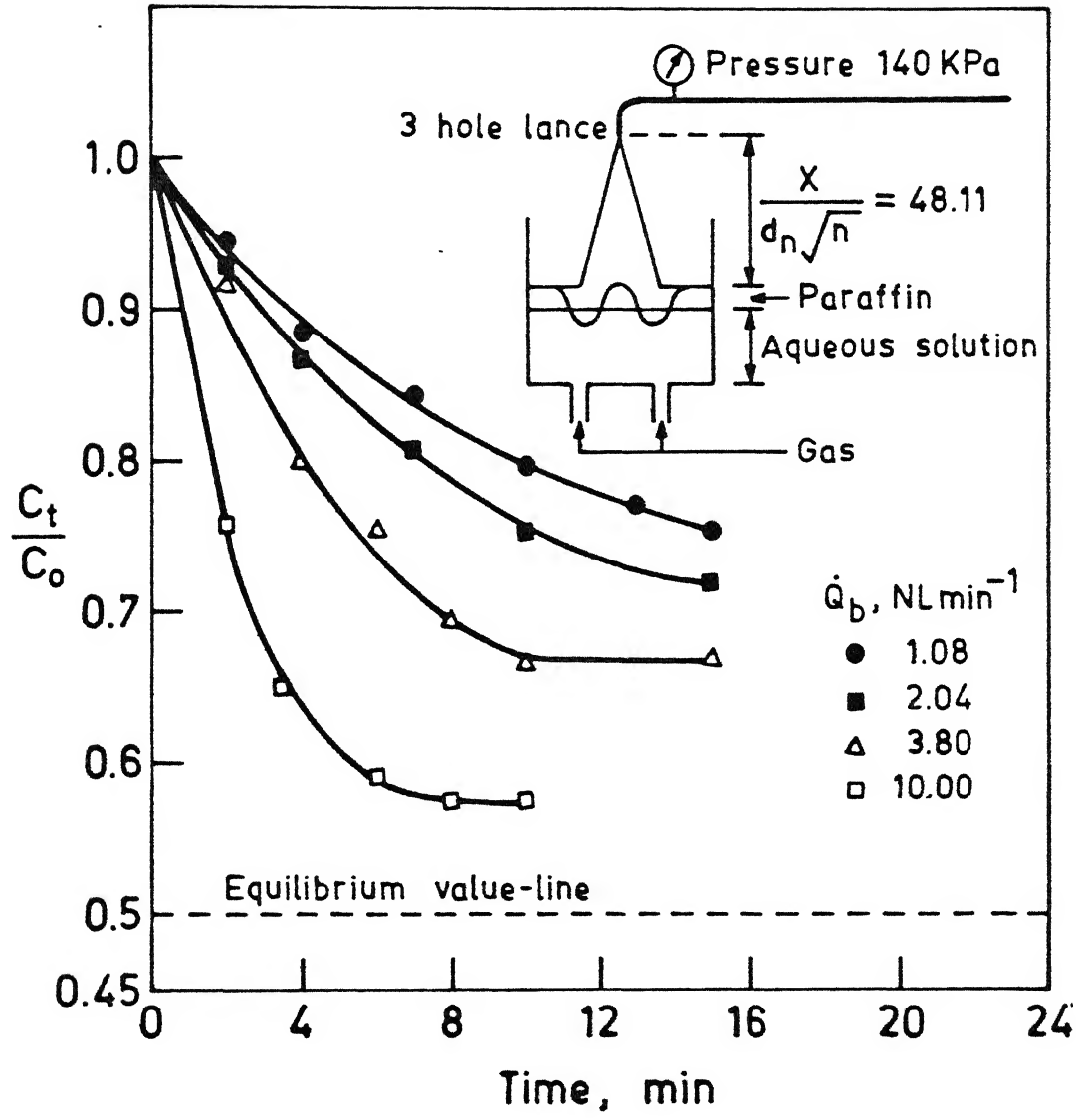

Fig. 14 : Fractional change of concentration of benzoic acid in water vs. time, during simultaneous top and bottom injection, at various bottom gas injection rates ($\dot{Q}_b$ NL/min), constant upstream pressure and dimensionless lance distance, 140 KPa and 48.11 respectively.

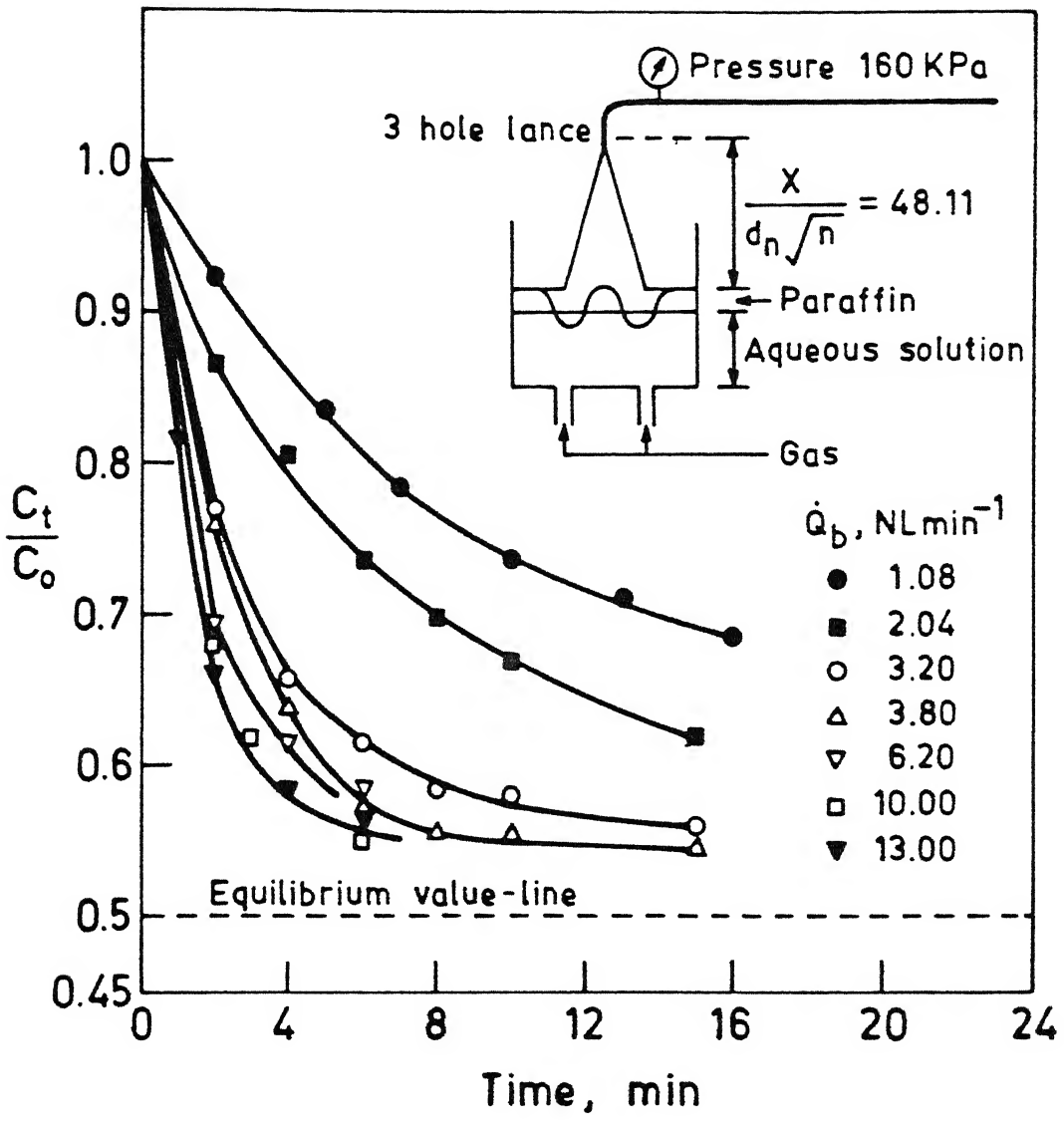

Fig.15 : Fractional change of concentration of benzoic acid in water vs. time, during simultaneous top and bottom injection, at various bottom gas injection rates ($\dot{Q}_b$ NL/min), constant upstream pressure and dimensionless lance distance, 160 KPa and 48.11 respectively.

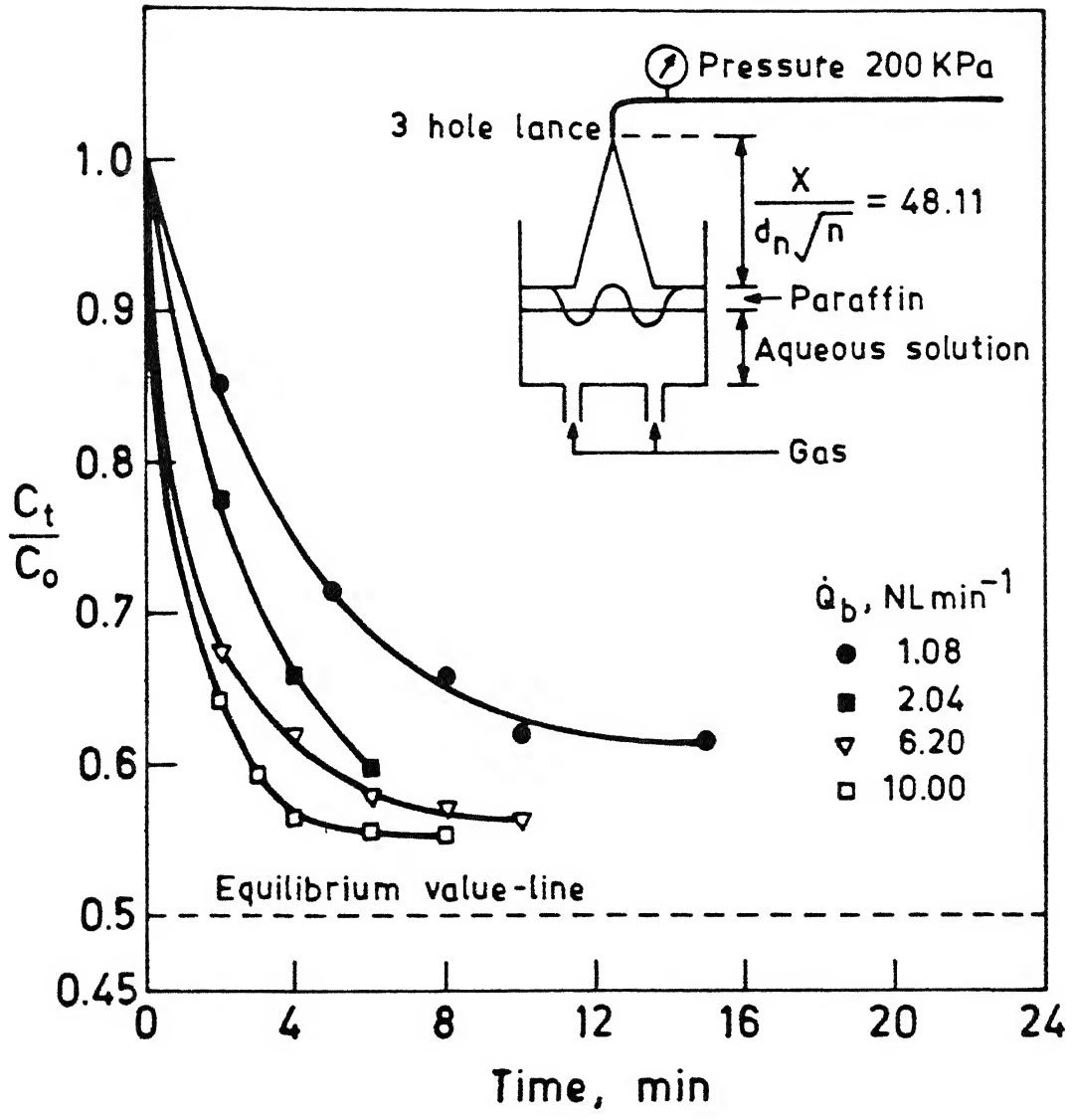

Fig.16 : Fractional change of concentration of benzoic acid in water vs. time, during simultaneous top and bottom injection, at various bottom gas injection rates ($\dot{Q}_b$ NL/min), constant upstream pressure and dimensionless lance distance, 200 KPa and 48.11 respectively.

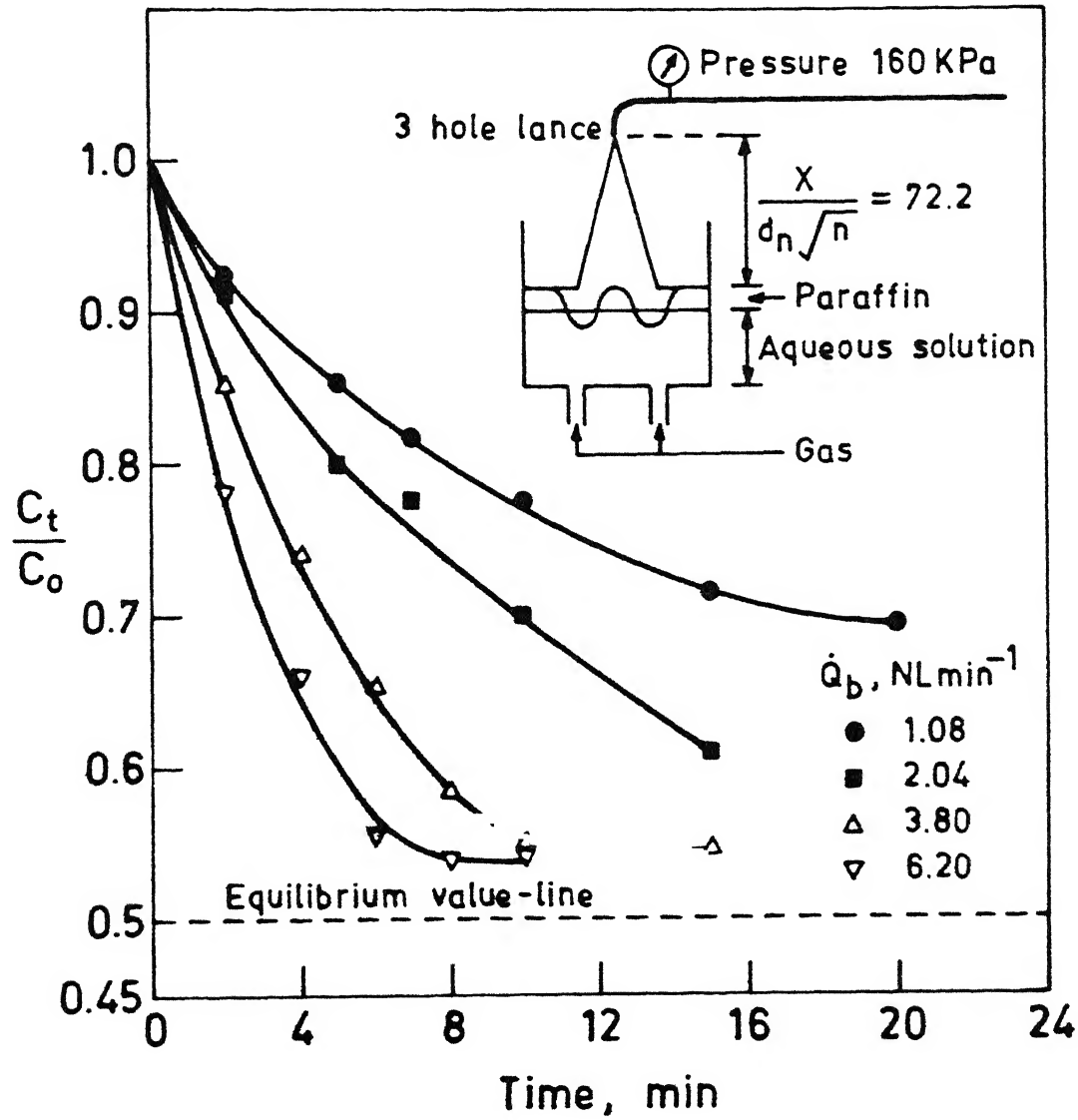

Fig. 17 : Fractional change of concentration of benzoic acid in water vs. time, during simultaneous top and bottom injection, at various bottom gas injection rates ($\dot{Q}_b$ NL/min), constant upstream pressure and dimensionless lance distance, 160 KPa and 72.2 respectively.

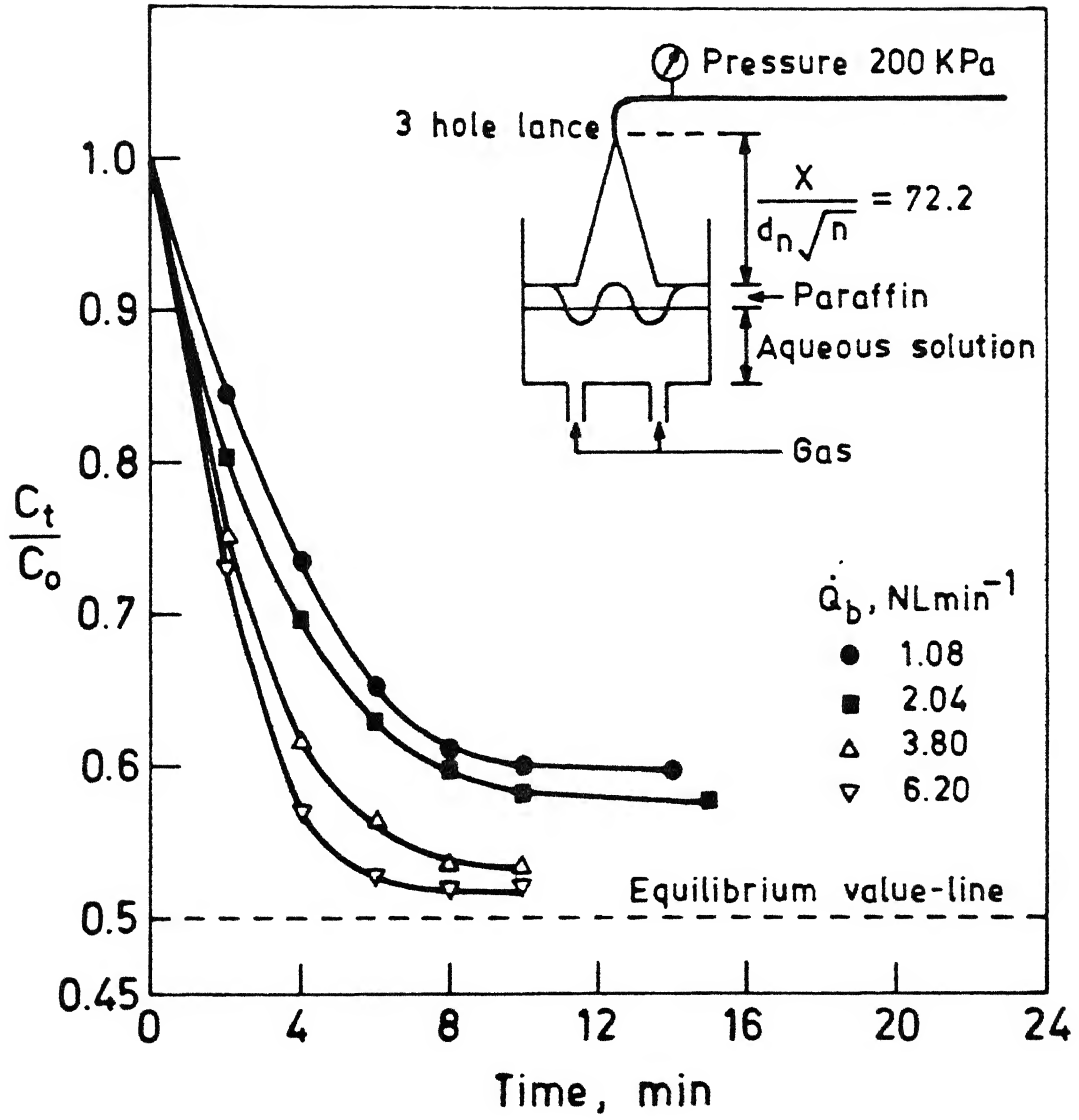

Fig. 18 : Fractional change of concentration of benzoic acid in water vs. time, during simultaneous top and bottom injection, at various bottom gas injection rates ($\dot{Q}_b$ NL/min), constant upstream pressure and dimensionless lance distance, 200 KPa and 72.2 respectively.

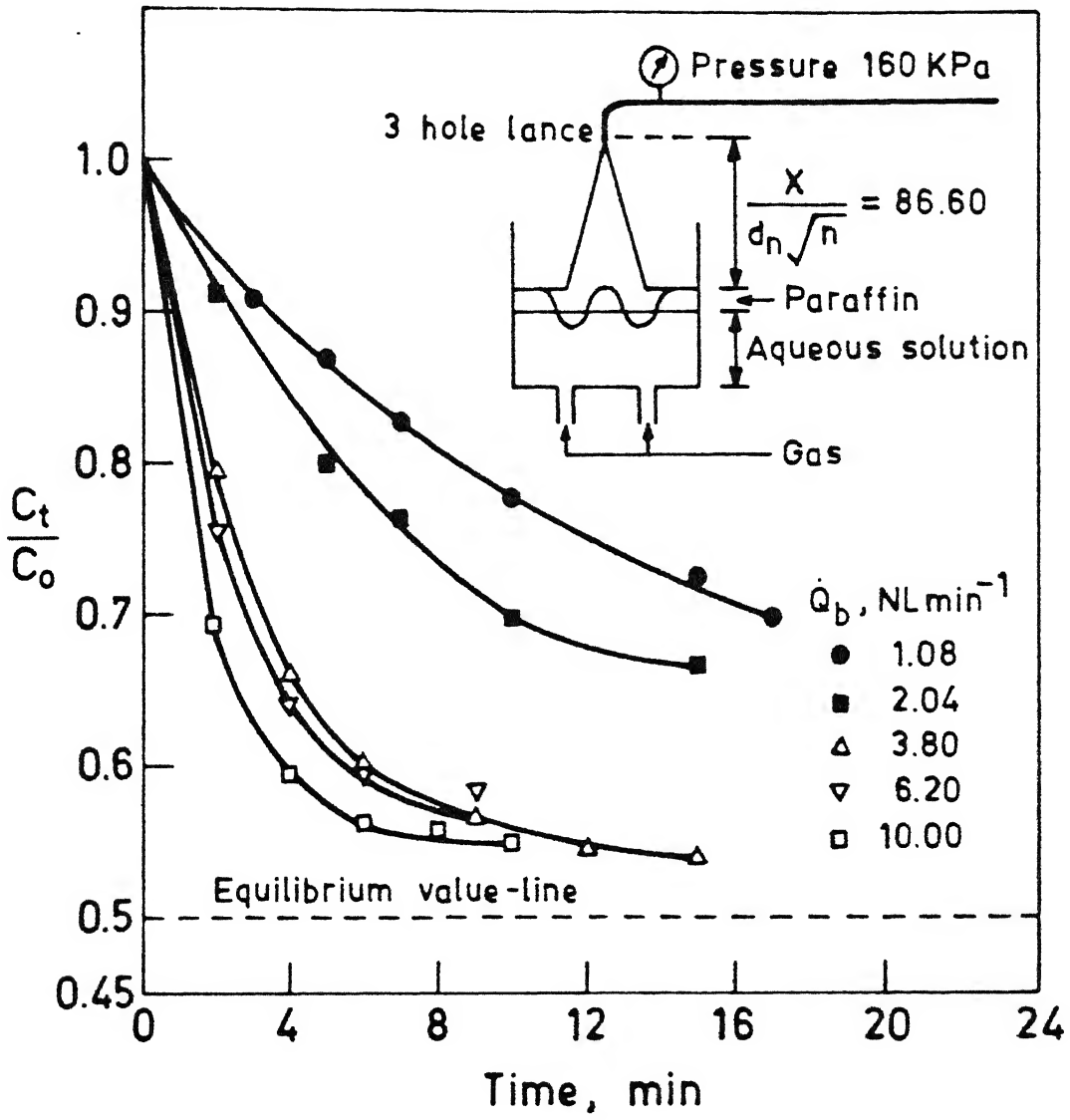

Fig. 19 : Fractional change of concentration of benzoic acid in water vs. time, during simultaneous top and bottom injection, at various bottom gas injection rates ($\dot{Q}_b$ NL/min), constant upstream pressure and dimensionless lance distance, 160 KPa and 86.6 respectively

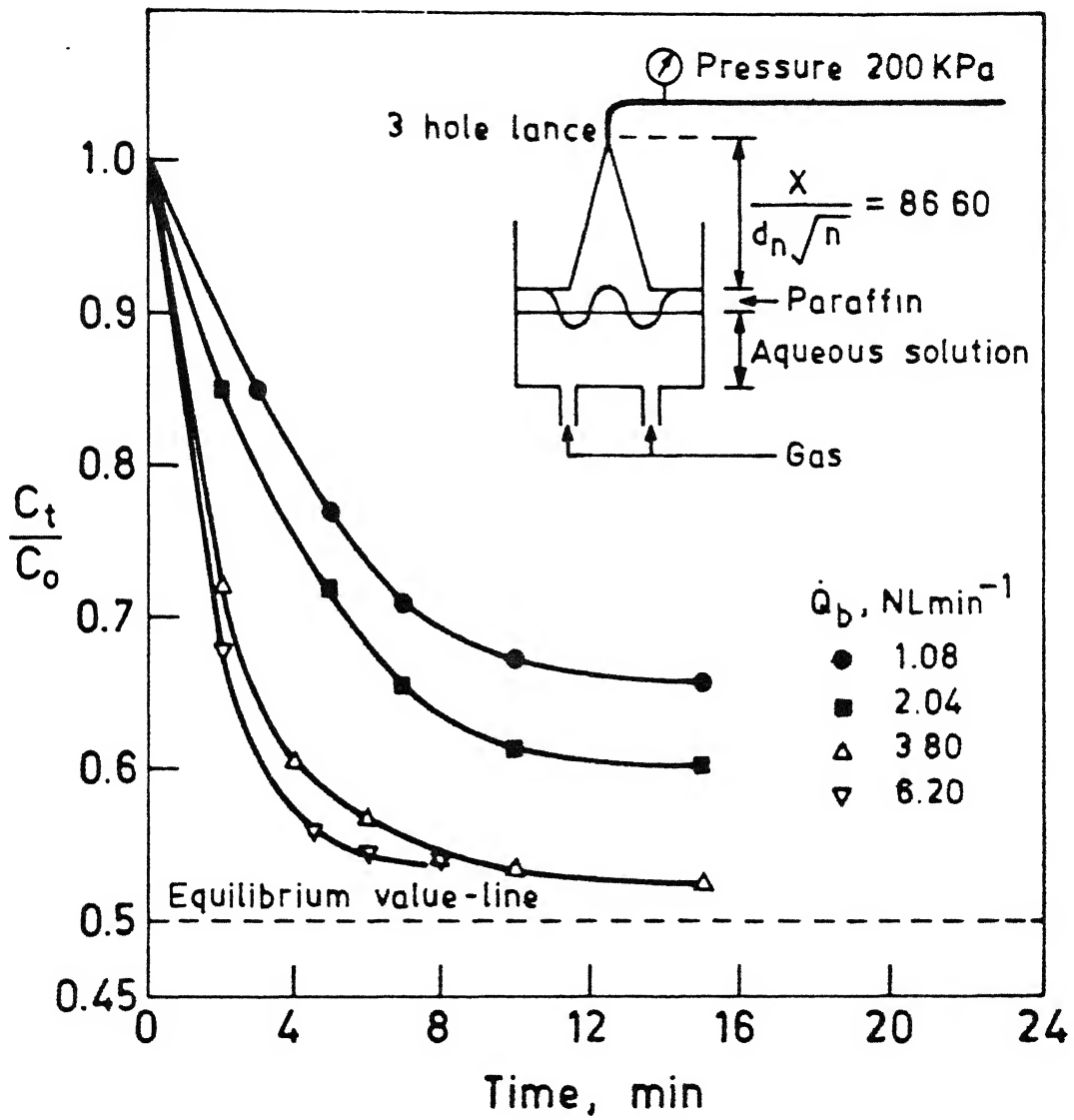

Fig. 20 : Fractional change of concentration of benzoic acid in water vs. time, during simultaneous top and bottom injection, at various bottom gas injection rates ($\dot{Q}_b$ NL/min), constant upstream pressure and dimensionless lance distance, 200 KPa and 86.6 respectively.

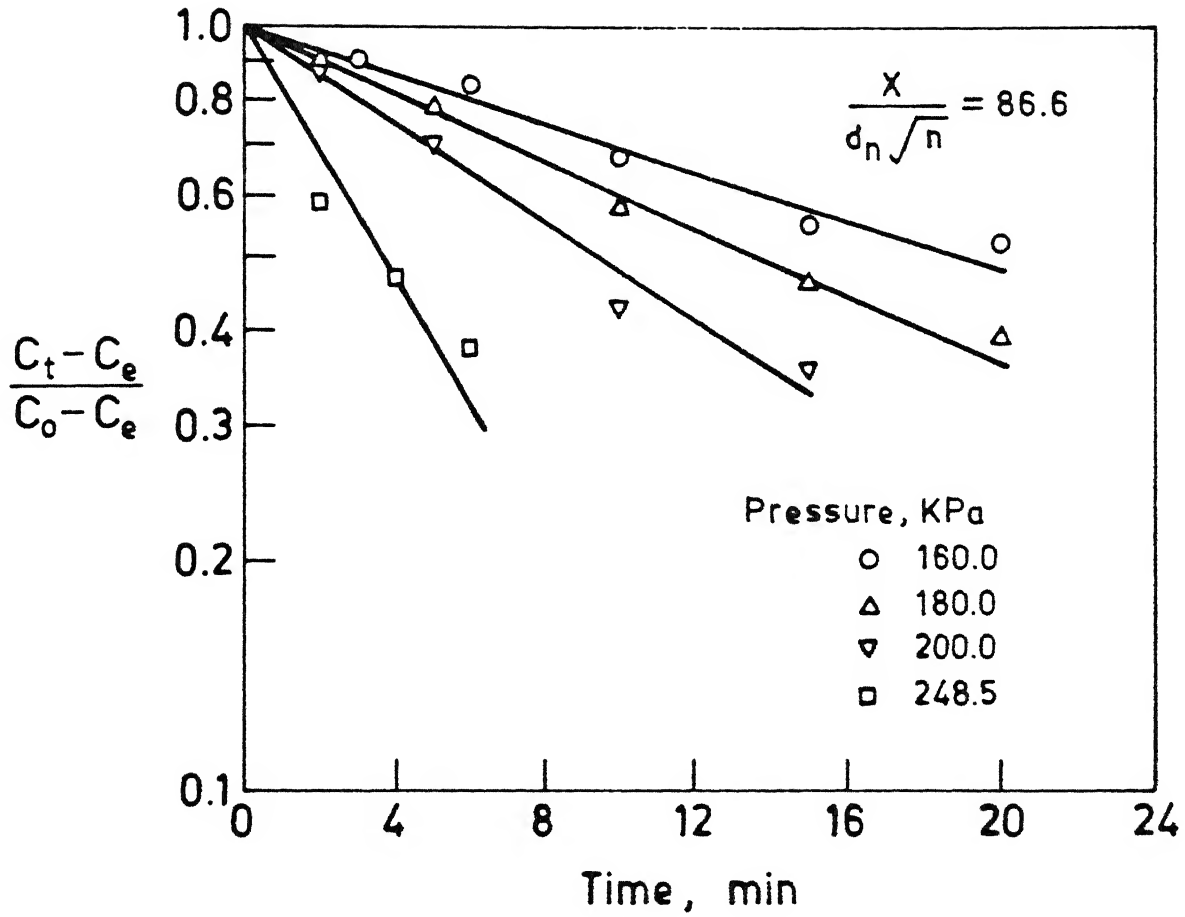

Fig. 21 : Variation of $\ln\left(\frac{C_t - C_o}{C_e - C_o}\right)$ as a function of time, ($X/d_n\sqrt{n} = 86.6$)

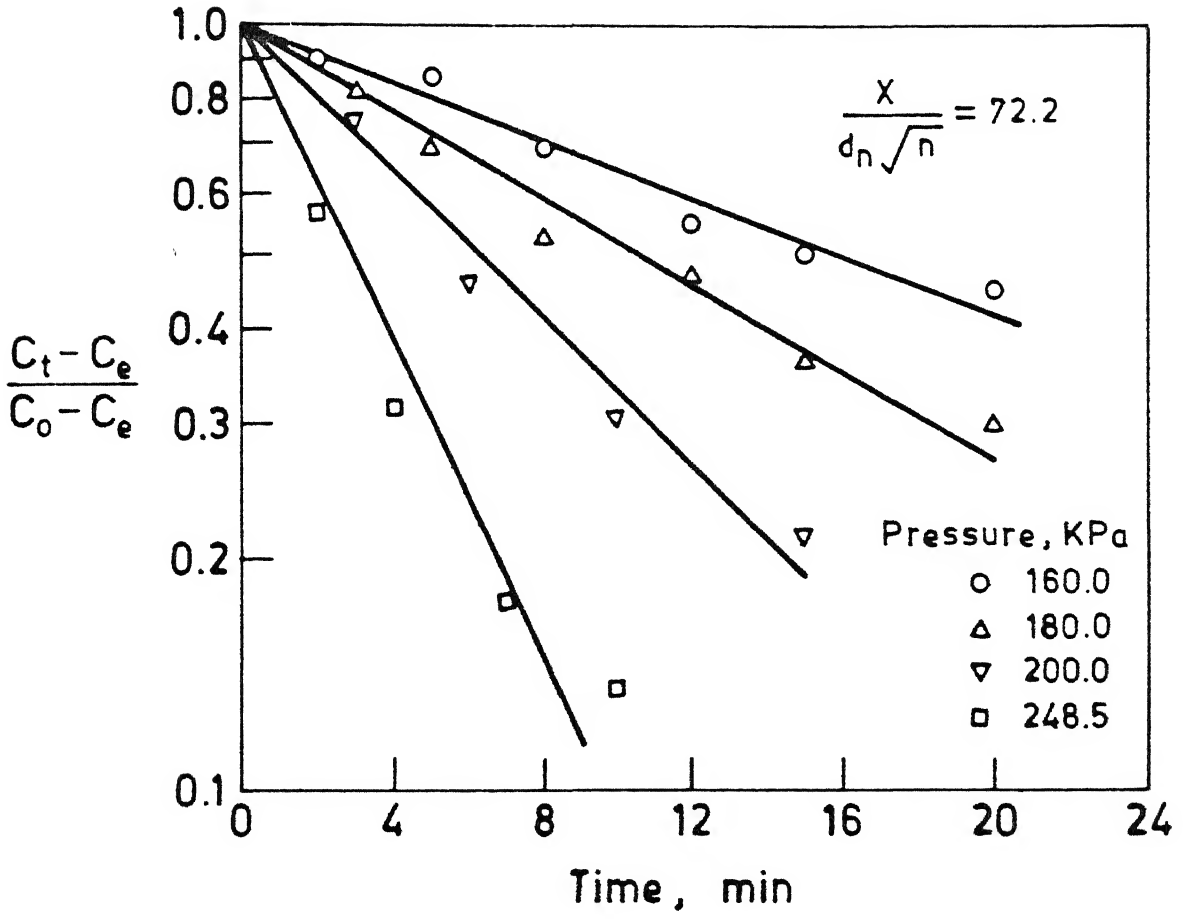

Fig. 22 : Variation of $\ln(\frac{C_t - C_o}{C_e - C_o})$ as a function of time, $(X/d_n\sqrt{n} = 72.2)$

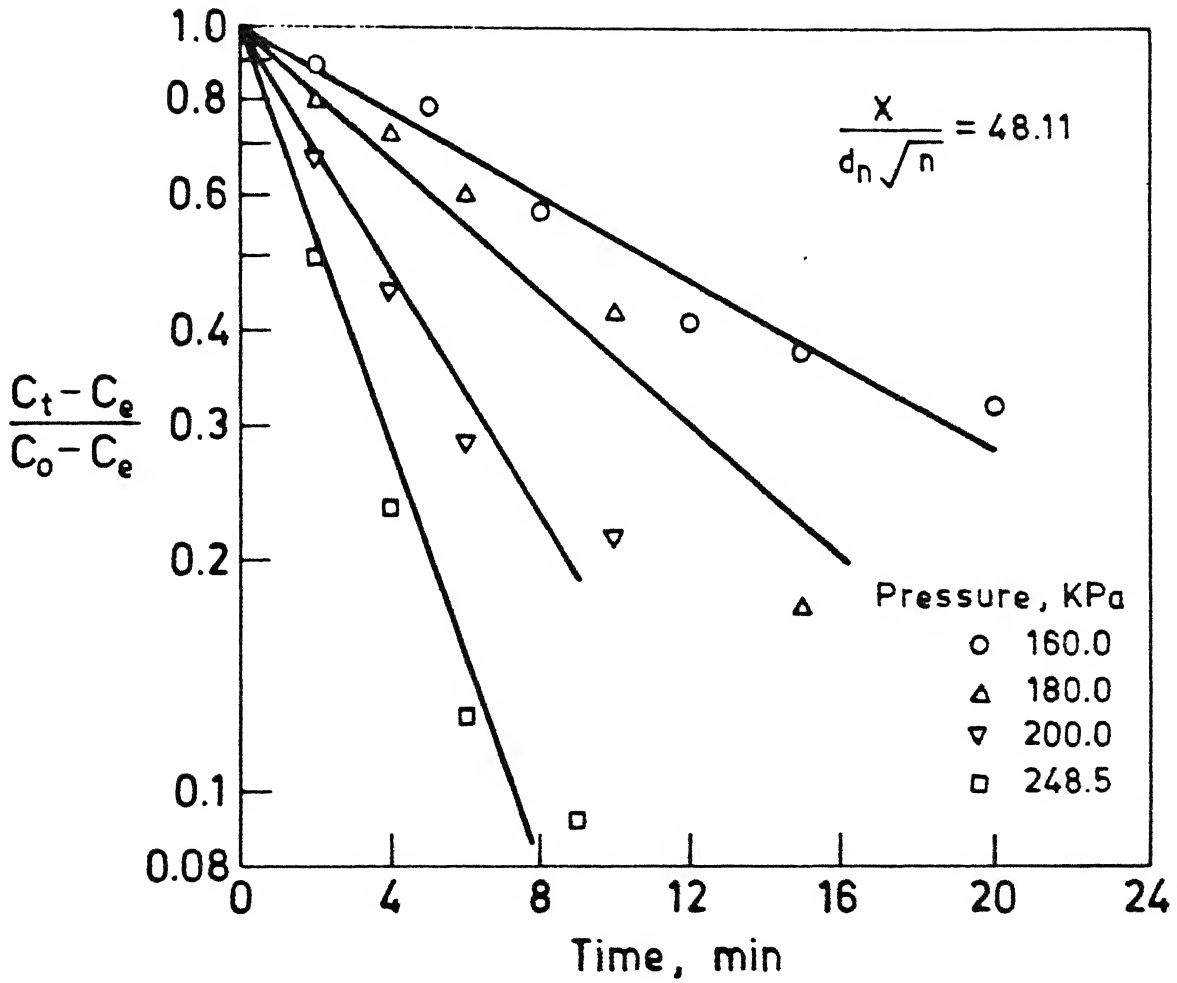

Fig. 23 : Variation of $\ln\left(\frac{C_t - C_o}{C_e - C_o}\right)$ as a function of time. $\left(\frac{X}{d_n\sqrt{n}} = 48.11\right)$

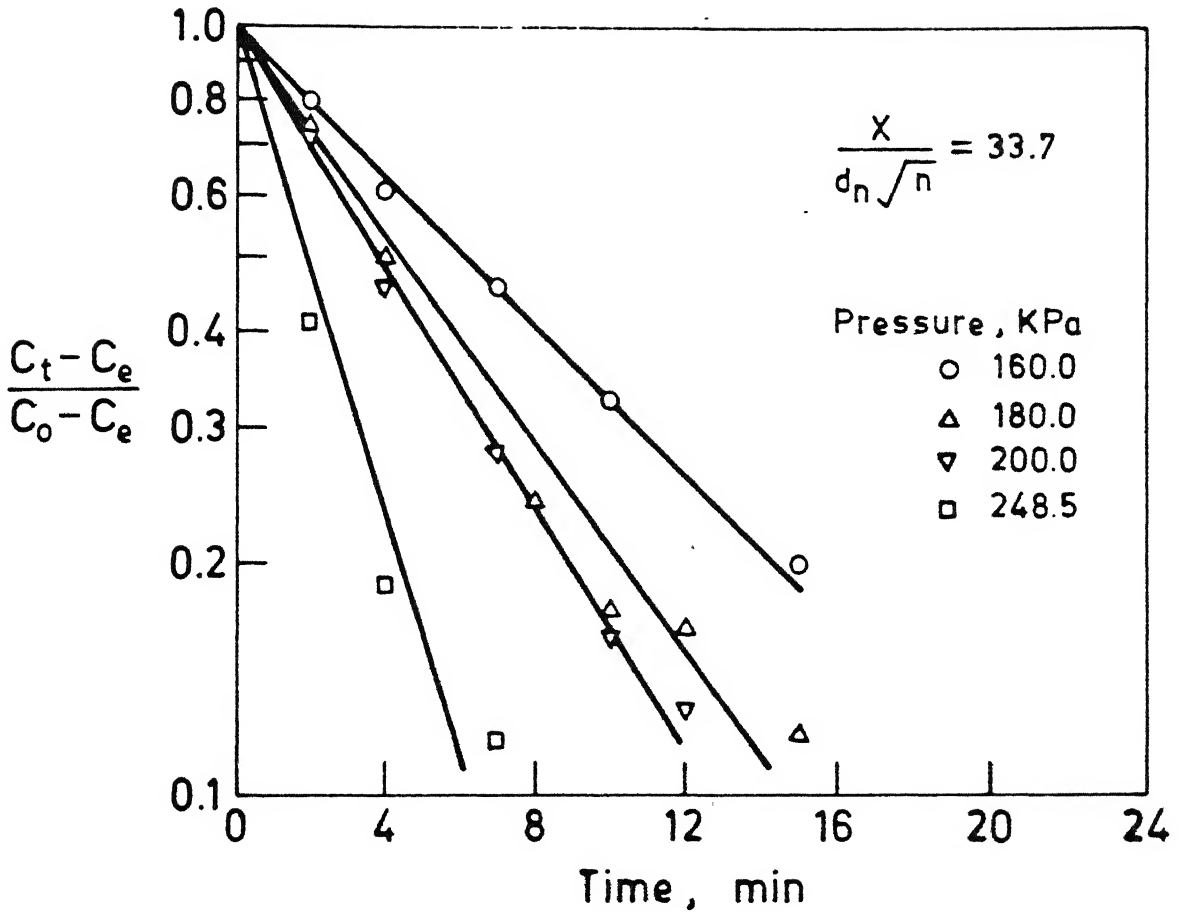

Fig. 24 : Variation of $\ln\left(\frac{C_t - C_o}{C_e - C_o}\right)$ as a function time. $\left(\frac{X}{d_n\sqrt{n}} = 33.7\right)$.

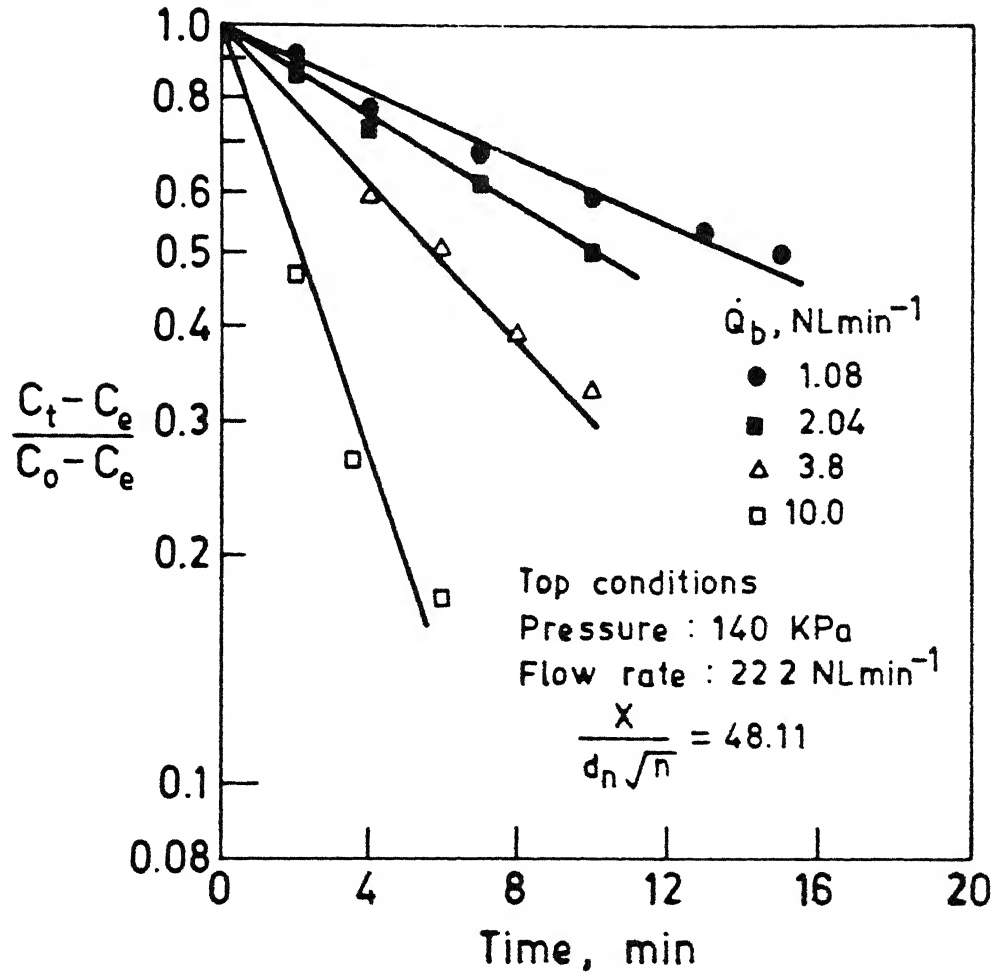

Fig. 25 : Variation of ln $(\frac{C_t - C_o}{C_e - C_o})$ as a function of time. $(\frac{X}{d_n\sqrt{n}} = 48.11$, top pressure - 140 KPa)

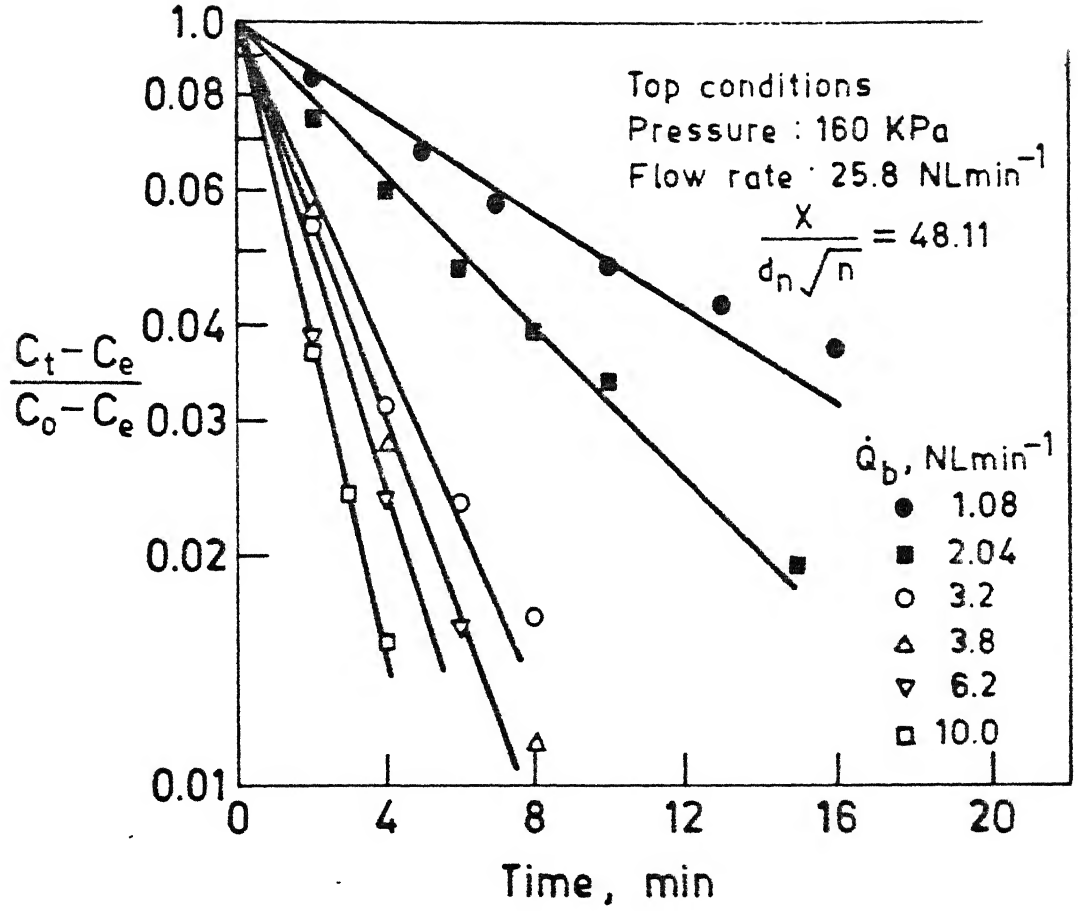

Fig. 26 : Variation of ln $(\frac{C_t - C_e}{C_e - C_o})$ as a function of time. ($X/d_n\sqrt{n}$ = 48.11, upstream pressure - 160 KPa top gas flow rate - 25.8 NL/min)

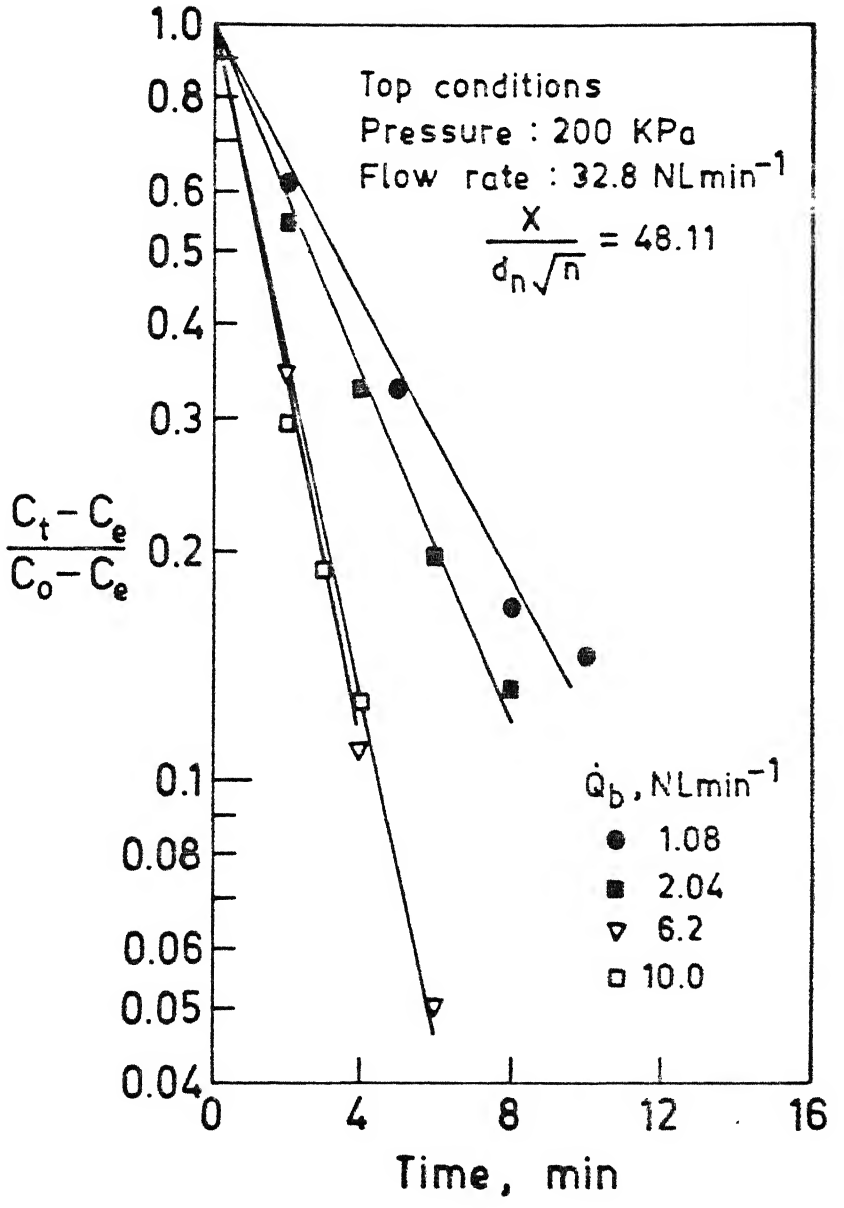

Fig. 27 : Variation of $\ln \left(\frac{C_t - C_o}{C_e - C_o}\right)$ as a function of time. ($X/d_n\sqrt{n}$ = 48.11, Top pressure - 200 KPa, top gas flow rate - 32.8 NL/min).

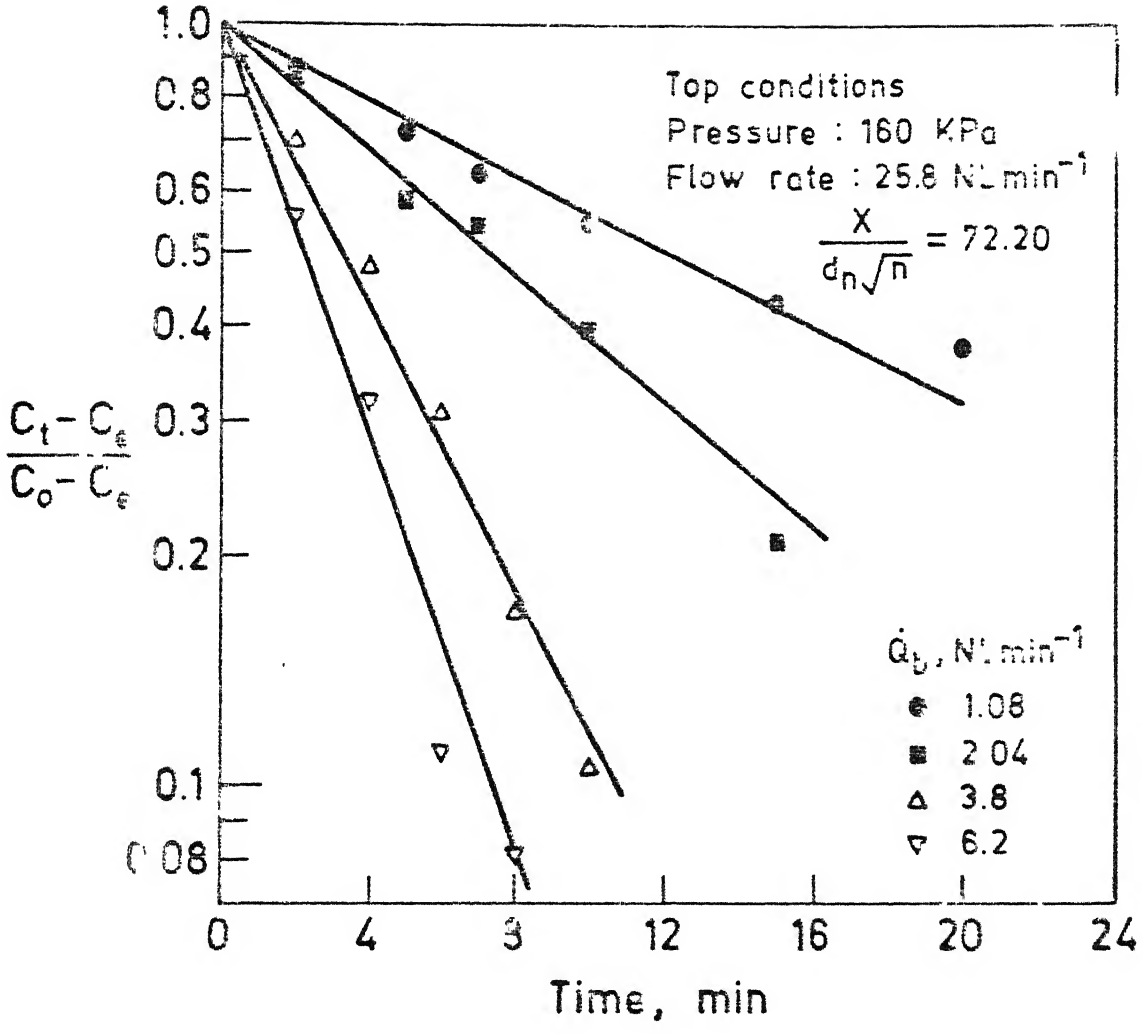

Fig. 28 : Variation of $\ln\left(\frac{C_t - C_o}{C_e - C_o}\right)$ as a function of time. ($X/d_n\sqrt{n}$ = 72.2, top pressure - 160 KPa, top gas flow rate - 25.8 NL/min)

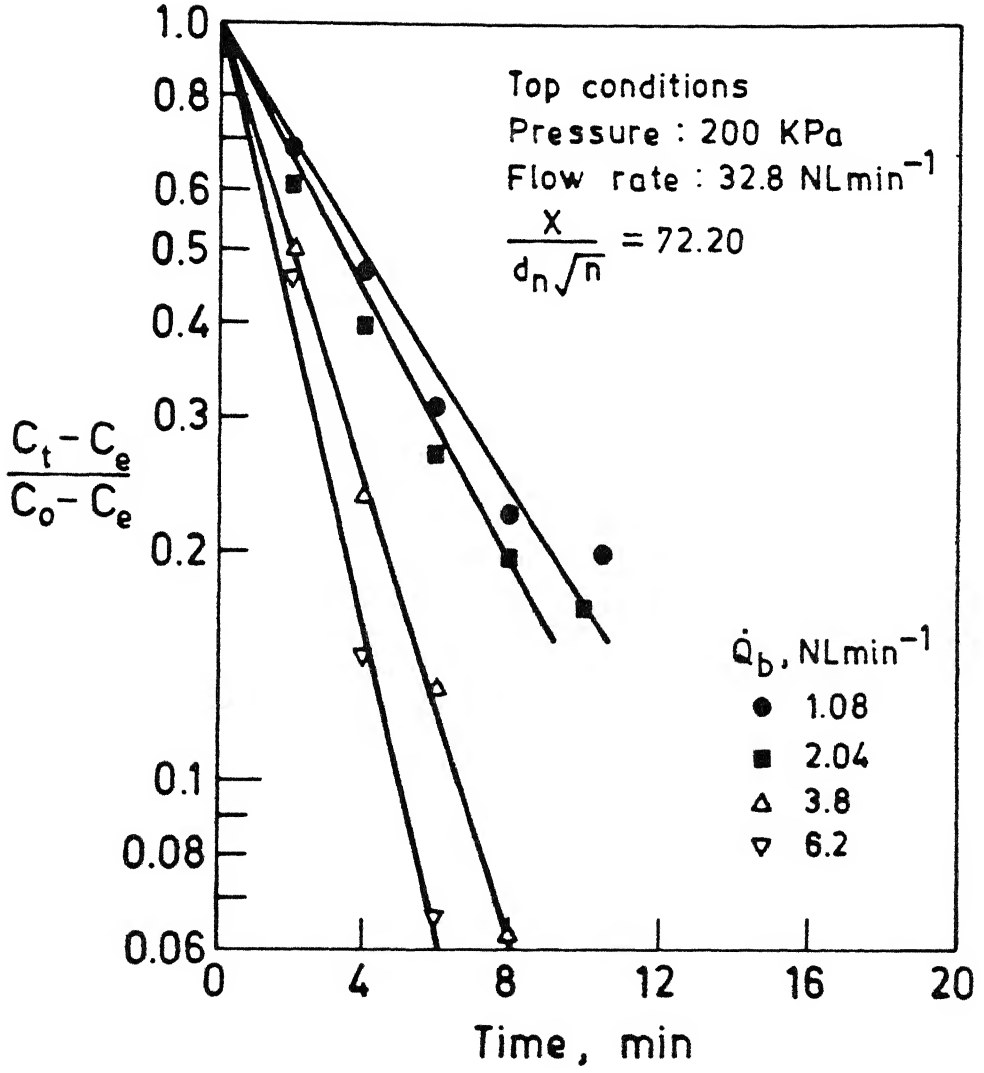

Fig. 29 : Variation of $\ln\left(\frac{C_t - C_o}{C_e - C_o}\right)$ as a function of time. ($X/d_n\sqrt{n}$ = 72.2, top pressure - 200 KPa, top gas flow rate - 32.8 NL/min).

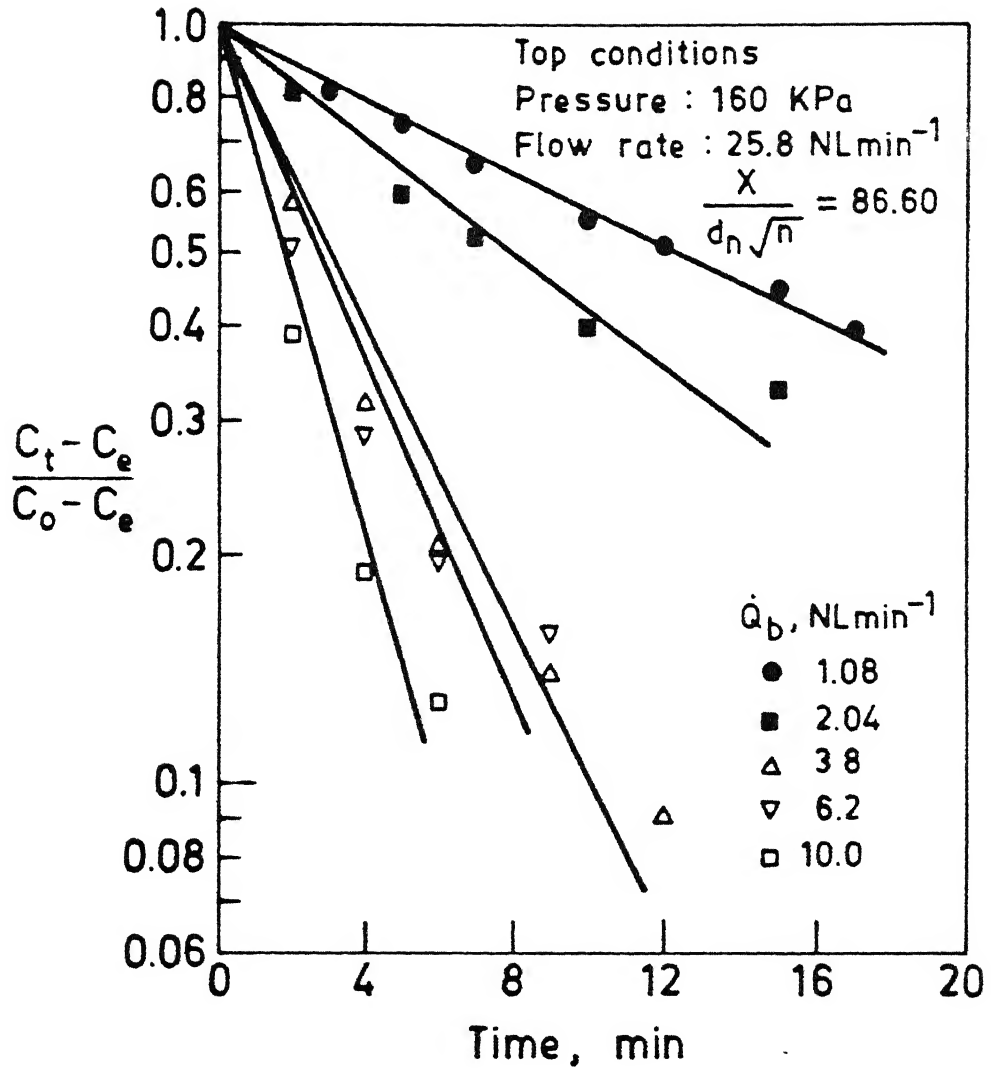

Fig.30 : Variation of $\ln \left(\frac{C_t - C_o}{C_e - C_o}\right)$ as a function of time. ($X/d_n\sqrt{n}$ = 86.6, top pressure - 160 KPa, top gas flow rate - 25.8 NL/min)

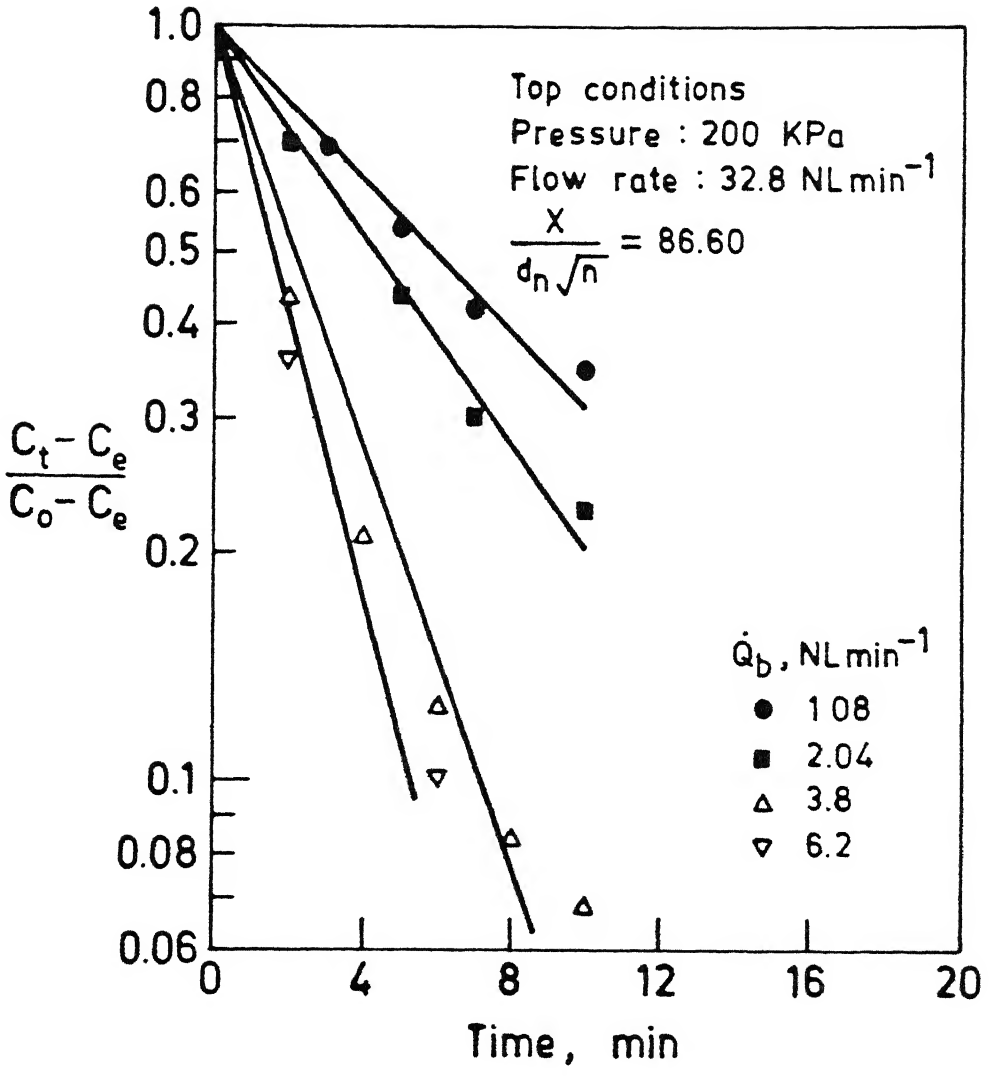

Fig.31 : Variation of $\ln \left(\frac{C_t - C_o}{C_e - C_o}\right)$ as a function of time. ($X/d_n \sqrt{n} = 86.6$, top pressure - 200 KPa, top gas flow rate - 32.8 NL/min).

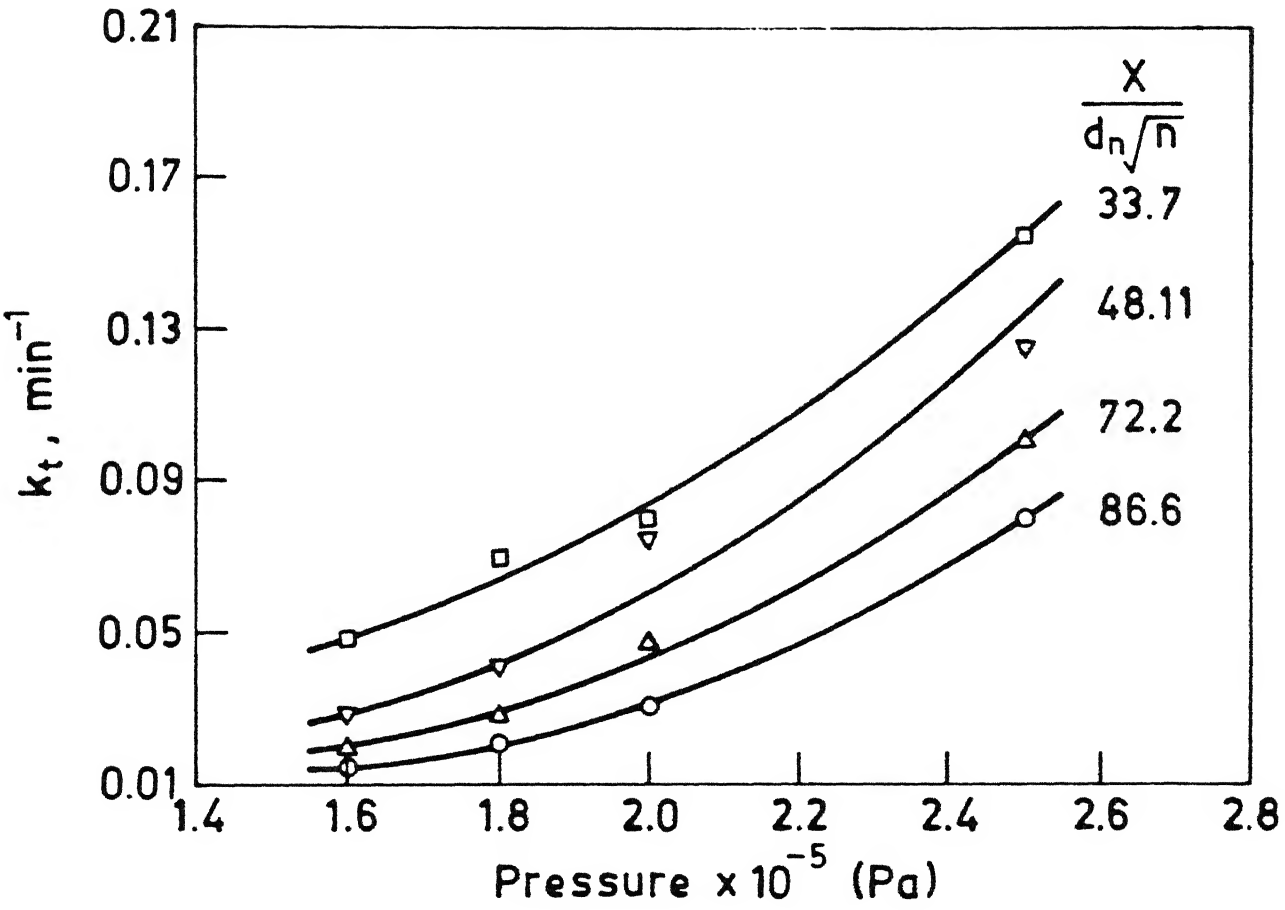

Fig. 32 : Effect of upstream pressure on k_t at various dimensionless lance distances.

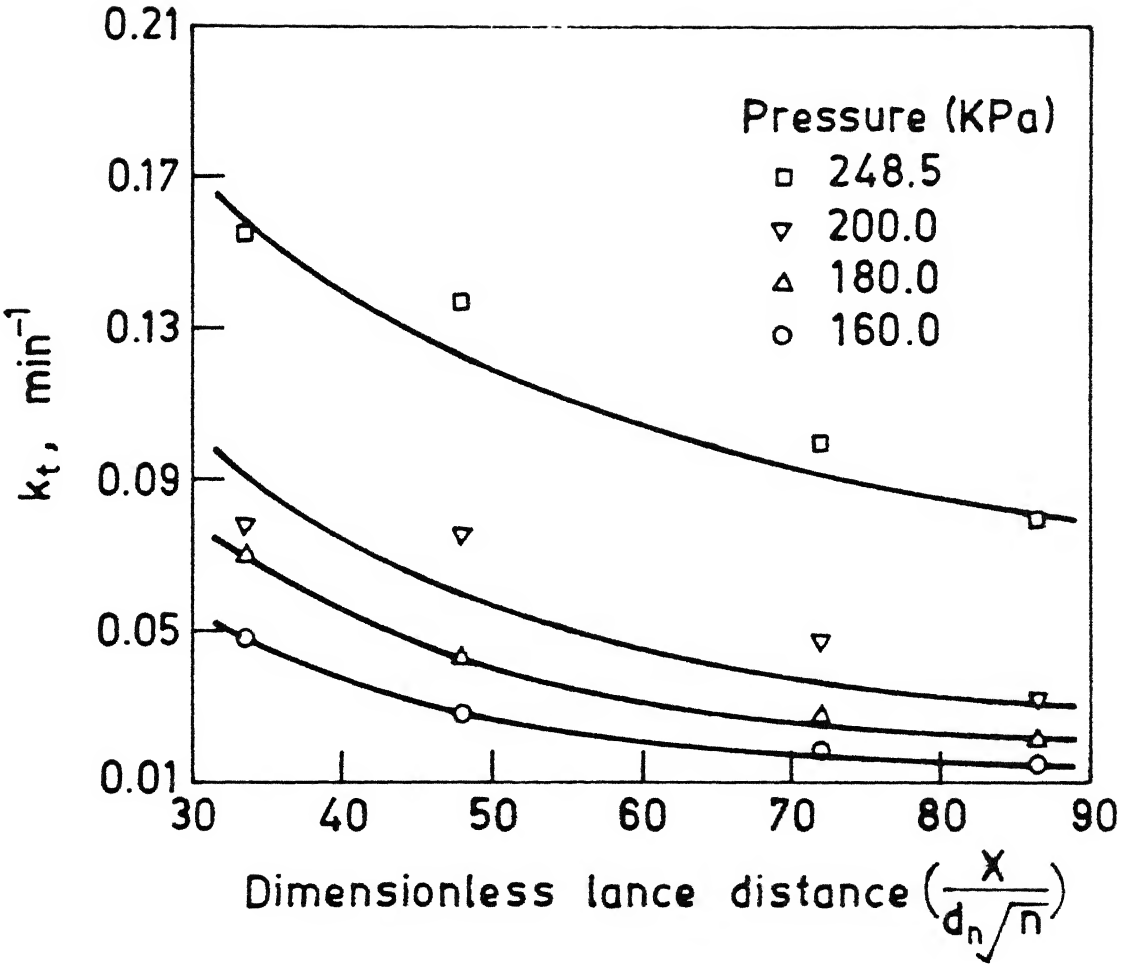

Fig. 33 : Effect of dimensionless lance distance on k_t at various upstream pressures.

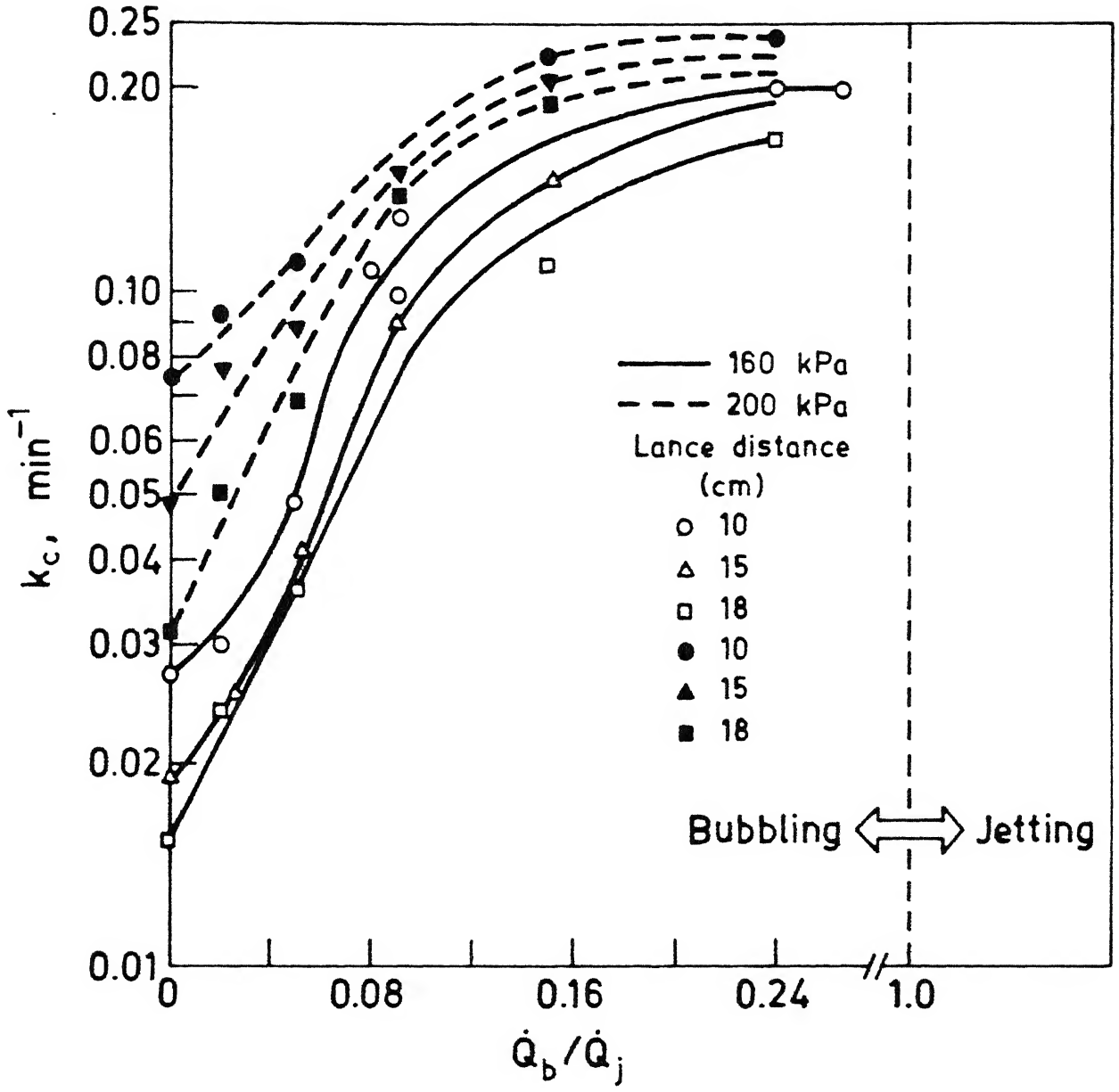

Fig. 34 : Effect of $\dot{Q}_b/\dot{Q}_j$ on k_c at various upstream pressures and lance distances.

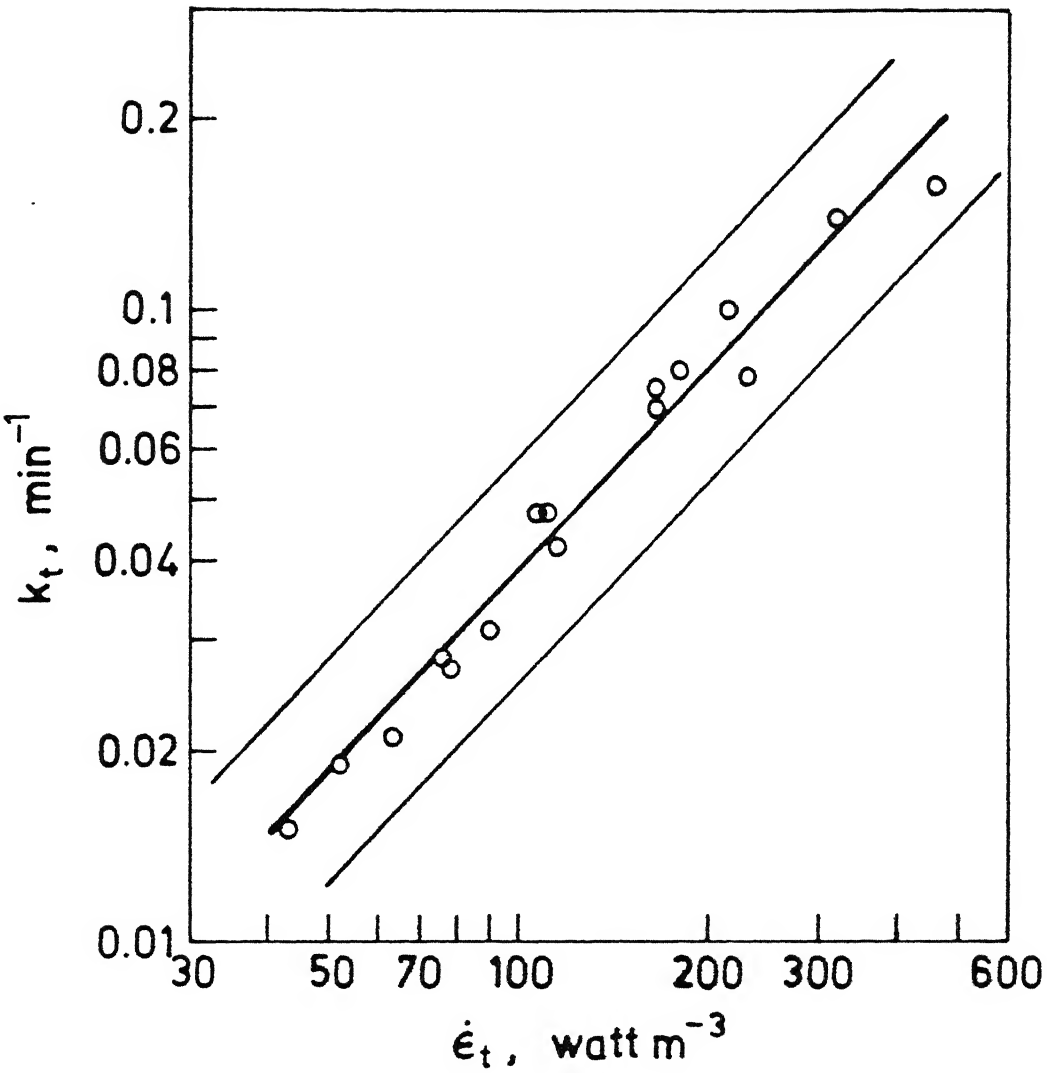

Fig. 35 : Variation of rate constant (k_t) with mixing energy during top injection.

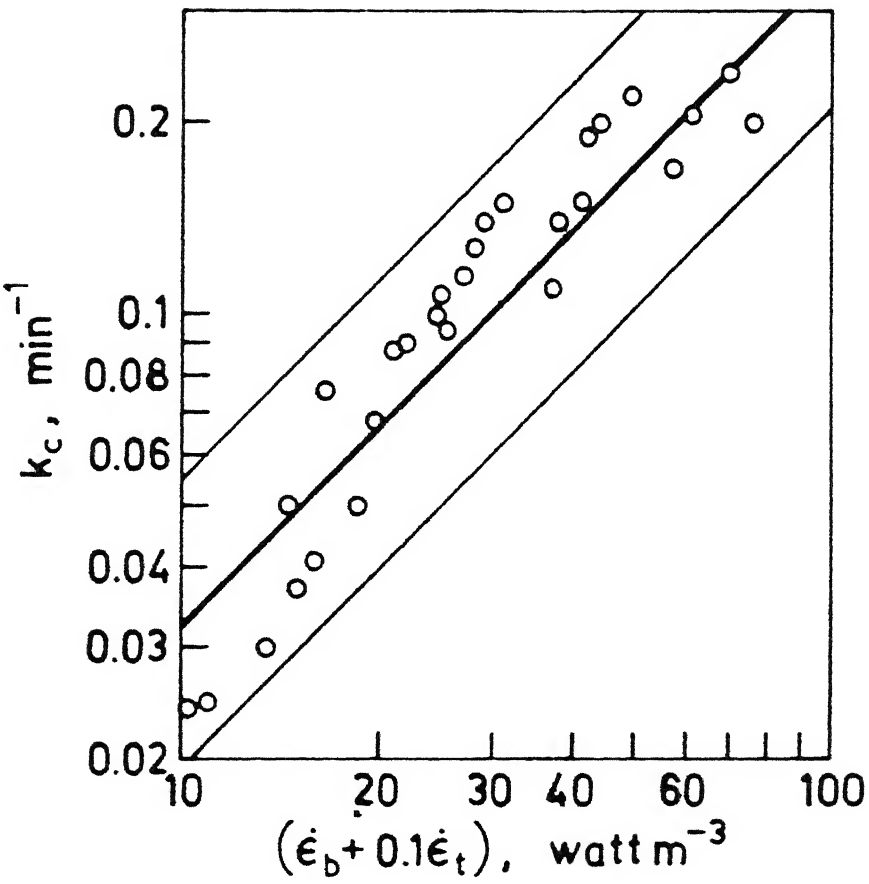

Fig. 36 : Variation of rate constant (k_c) with mixing energy during simultaneous top and bottom injection.

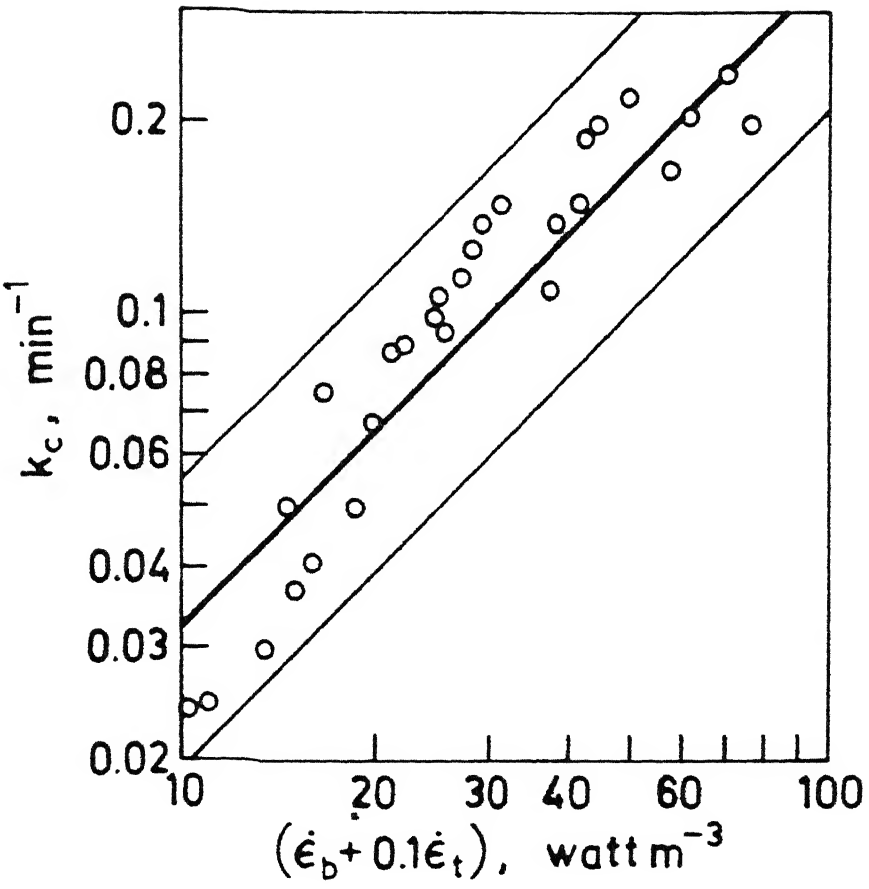

Fig. 36 : Variation of rate constant (k_c) with mixing energy during simultaneous top and bottom injection.

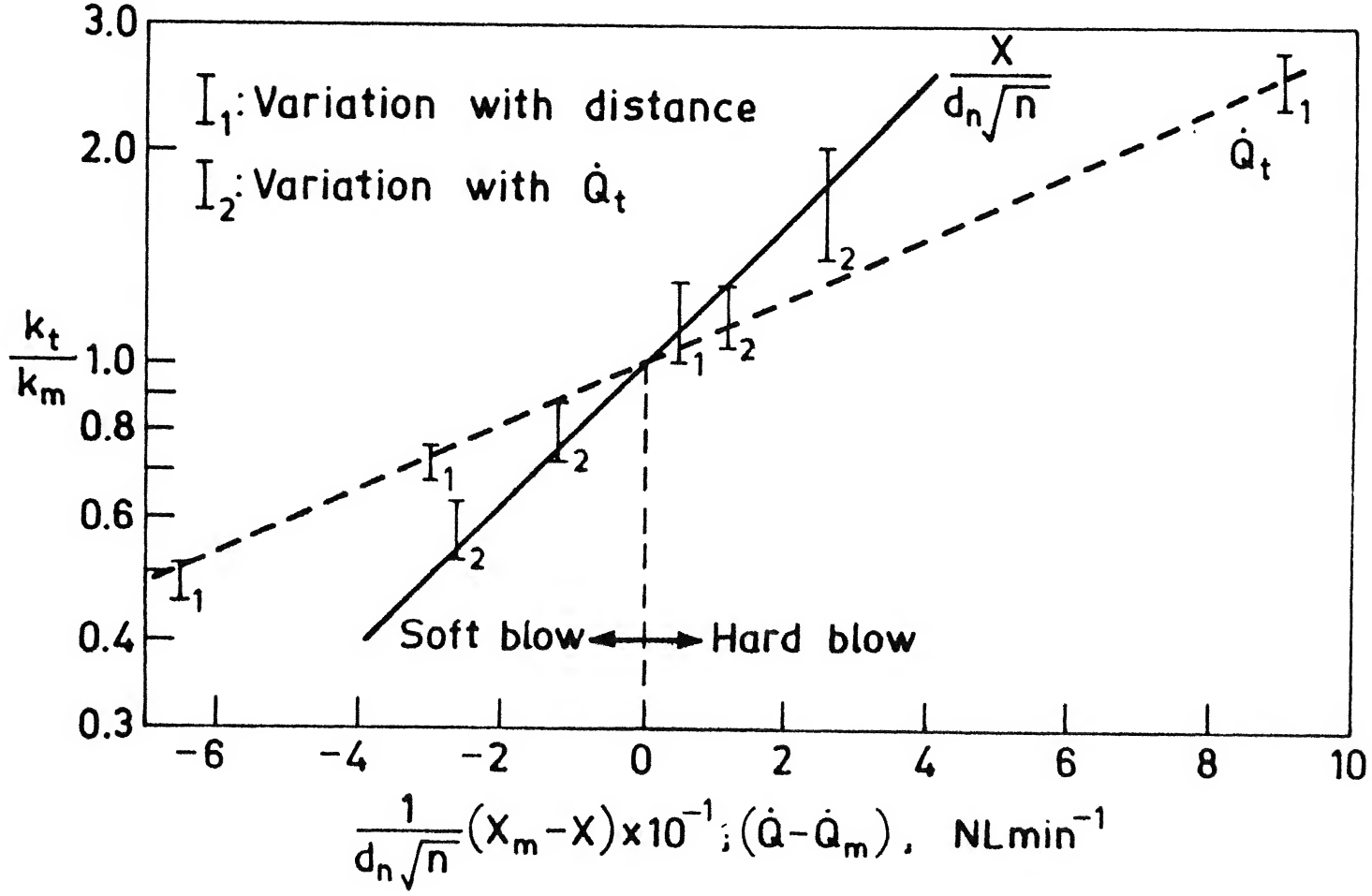

Fig. 37 : Representation of mixing condition in a top injected bath in terms of 'soft' and 'hard' blow .

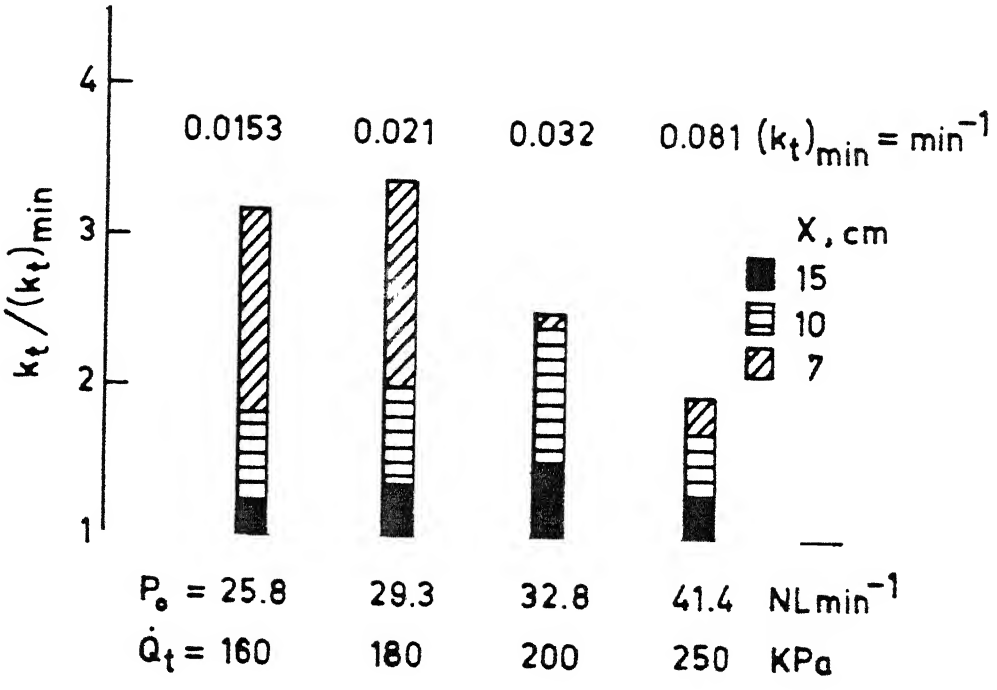

Fig. 38 : Bar-chart illustrating the improvement in mixing condition of a top injected bath. The base represents minimum value of k_t.

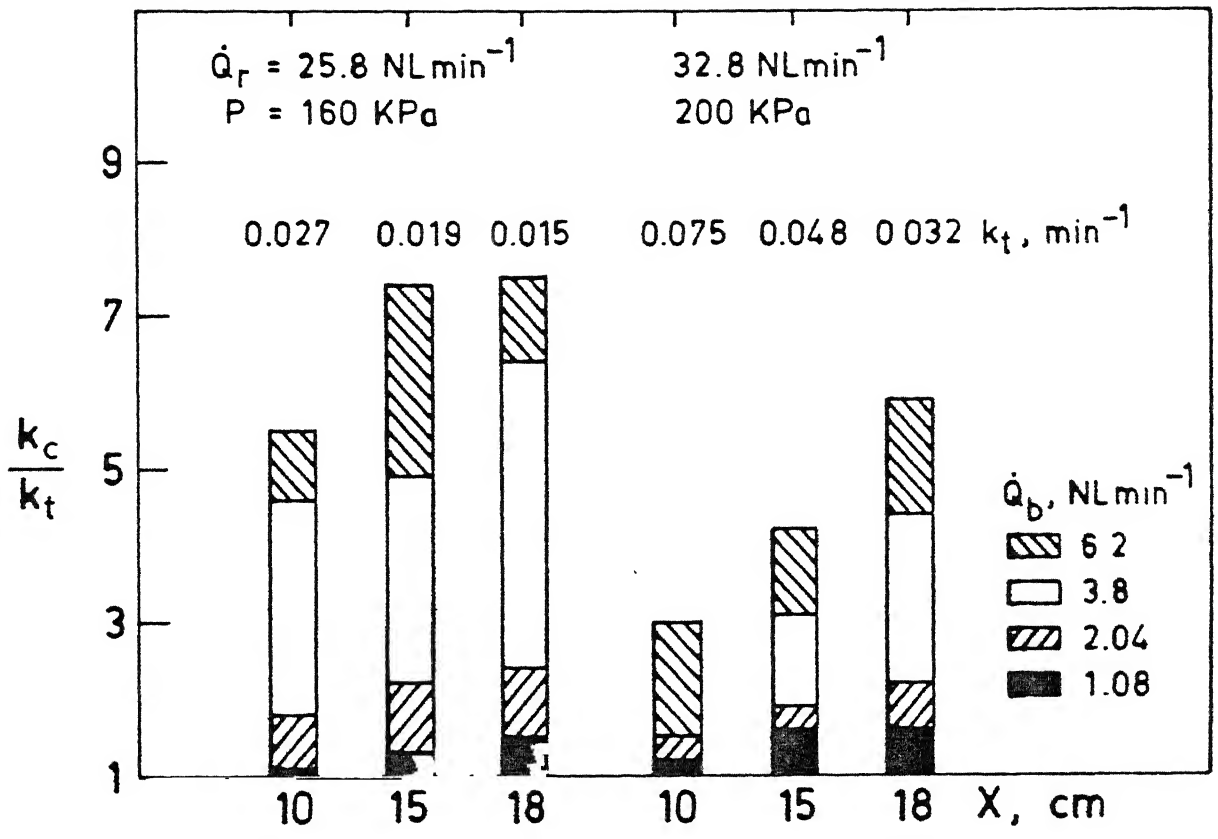

Fig. 40 : Illustration of further improvement in mixing condition of a top injected bath on the bar-chart. The base refers top injection only.

APPENDIX

CALCULATION PROCEDURES

A.1 CALCULATION OF FLOW RATE OF AIR

The flow rate of air was measured by using an orifice water. Following equation has been used to calculate the air flow rate:

$$W = 34.77 \; D_2^2 F_k Y_1 \sqrt{\rho_1 \; h_w} \qquad \text{(A.1.1)}$$

where

W = mass flow rate of air, gm/sec,

D_2 = diameter of the orifice, cm,

F_k = Flow coefficient, dimensionless,

Y_1 = Expansion factor, dimensionless,

ρ_1 = Density of air at upstream pressure tap conditions , gm/c.c.

h_w = differential pressure across the orifice, cm of water

Following are the steps involved in the calculation[19]

1. Calculate $\beta = \frac{D_2}{D_1}$ (A.1.2)

   where D_1 = diameter of the pipe of the orifice meter.

2. Calculate the expansion factor Y_1 using the following empirical expression

$$Y_1 = 1 - (0.41 - 0.35\beta^4) \frac{\Delta P}{P_1 \gamma} \qquad \text{(A.1.3)}$$

where γ = ratio of specific heat of air at constant pressure to the specific heat at constant volume

= 1.4

and ΔP = differential pressure across the orifice

= $h_w \cdot \rho_l / \rho_{Hg}$

where

ρ_l = density of Di - bulyle phthalate coloured with methyl orange

= 1.0465 gms/c.c.

ρ_{Hg} = density of mercury = 13.6 gms/c.c.

3. Calculate ρ_1 at temperature T and pressure P_1.
4. Calculate W using equation A.1.1 in terms of F_k.
5. Calculate the Reynolds number N^o_{Re} (referred to the diameter of the orifice) in terms of F_k using the following expression

$$N^o_{Re} = \frac{1.273\ W}{D_2\ \mu_{air}} \qquad (A.1.4)$$

where μ_{air} = viscosity of air at room temperature, poise. Determine the approximate value N^o_{Re}, by substituting F_∞ for F_k. F_∞ is flow coefficient at infinite N^o_{Re}. The value of F_∞ as a function of D_1 and β is available in the literature.

6. Determine the value of F_k using the following empirical equation:

$$F_k = F_\infty \left(1 + \frac{A}{N_{Re}^{o}}\right) \qquad (A.1.5)$$

The value of A as a function of D_1 and β is available in the literature.[19]

7. Determine W by substituting K in the results of step 4.

8. Calculate the volumetric flow rate of air from W and ρ_2.

Example:

Given h_w = 0.8 cm of di-bulyle.

P_1 = 118.7 cm of Hg

T = 20°C

D_2 = 0.8 cm, D_1 = 3.8 cm

ρ_1 = 1.0465 gms/c.c.

1. β = 0.8/3.8 = 0.2105

2. $\Delta P = \frac{0.8 \times 1.0465}{13.6}$ = 0.0615 cm Hg

Therefore, $Y_1 = 1 - (0.41 + 0.35 \times 0.2105^4) \times \frac{0.0615}{1.4 \times 118.7}$

3. ρ_1 at $P_1 = \frac{P_1}{RT_1} = \frac{118.7 \times 10^{-2} \times 13.6 \times 10^{-3} \times 9.8 \times 29}{8314 \times 293}$ kg/m^3

$= 1.88 \times 10^{-3}$ gm/c.c.

4. $W = 34.71 \times 0.8^2 \times F_k \times 0.9998 \sqrt{1.88\times10^{-3} \times 0.84}$

$= 0.884\ F_k$

5. At room temperature, viscosity of air is about 1.85×10^{-4} poise[2]. Therefore

$$N_{Re}^{o} = \frac{1.273 \times 0.884\ F_k}{0.8 \times 1.85\times10^{-4}}$$

$$= 7.603\times10^{3}\ F_k$$

For $\beta = 0.21$ and $D_1 = 3.8$ cm, $K = 0.5973$.[19]

Therefore, $N_{Re}^{o} = 7.603\times10^{3} \times 0.5973$

$= 4.542\times10^{3}$

6. For $\beta = 0.21$ and $D_1 = 3.80$ cm $A = 200$.

Therefore,

$$K = 0.5973\ (1 + \frac{200}{4542.007}) = 0.6236$$

7. $W = 0.6236 \times 0.884$

$= 0.5513$ gms/sec.

8. Density of air at N.T.P. $= 1.294\times10^{-3}$ gms/c.c.[20]

So volumetric flow rate of air at N.T.P.

$$= \frac{0.5513}{1.294 \times 10^{-3}} \text{ c.c./sec.}$$

$$= 0.426\times10^{3} \text{ c.c./sec.}$$

i.e. $\dot{Q}_{air} = 25.6$ NL/min.

A.2 CALCULATION OF $\dot{Q}_j$

The gas injection rate required to onset the jetting mode of injection is calculated by the following equation [21]

$$\dot{m} = P_b \; A_1 \sqrt{\frac{W \cdot X_1}{R_k \, T_t}} \sqrt{\frac{1 + X_1}{2}} \qquad (A.2.1)$$

where

$$P_b = P_a + {}_w \dot{g} \, h_n + {}_o g \, h_{air}$$

X_1 = 1.4

W = weight of air/mole = 29 kg/mole

T_t = Temperature of liquid = $298^{\circ}k$

R_k = Universal gas constant = 8314 J/kg mole$^{\circ}k$

A_1 = Area of four tuyers = $4 \times \frac{\pi}{4} \left(\frac{0.8}{1000}\right)^2 m^2$

h_w = height of water bath = 7.5 cm

h_{oil} = height of oil layer = 1.3 cm

ρ_w = density of water = 1000 kg/m^3

ρ_o = density of oil = 960 kg/m^3

P_a = atmospheric pressure 1 101.325 KPa

ρ_{air} = density of air = 1.334 kg/m^3 at N.T.P.

Substituting the values we get from equation (A.2.2) $\dot{m}$ = 0.05465 kg/min. Dividing this value by density of air, we get $\dot{Q}_j$ = 40.96 NL/min-

A.3 CALCULATION OF MIXING ENERGIES

A.3.1 In case of top blowing mixing energy is represented by the following equation:

$$\dot{\varepsilon}_t = \frac{0.632\times10^{-6}\cos\theta}{V_L} \times \frac{\dot{Q}_t^{.3} \times M}{N^3 \, d_n^3 \, x} \qquad (A.1.2)$$

where

$\dot{\varepsilon}_t$ = Agitation energy in watt/m^3

θ = inclination angle of nozzles with the axis of lance

V_L = volume of the bath (m^3)

$\dot{Q}_t$ = top flow rate (N m^3/min)

N = number of nozzles

x = Lance distance (m)

d_n = diameter of nozzle (m)

M = molecular weight of gas (air).

Example:

Given $\theta = 15^\circ$, $V_L = 2.5\times10^{-3}$ m^3

$\dot{Q}_t = 25.8\times10^{-3} m^3$, N = 3

x = 0.18m , d_n = 0.0012 m

M = 29

$$\dot{\varepsilon}_t = \frac{0.632 \times 10^{-6} \cos 15^\circ}{2.5\times10^{-3}} \cdot \frac{(25.8)^3 \times 10^{-9} \times 29}{3^2 \times (0.0012)^3 \times 0.18}$$

$\dot{\varepsilon}_t$ = 43.41 watt/m^3.

A.3.2 Bottom blown mixing energy can be represented by the following expression:

$$\dot{\varepsilon}_b \ (\text{watt/m}^3) = \frac{6.18 \times \dot{Q}_b \times T_L}{V_L} \left[\ln\left(1 + \frac{\rho_1 \ g \ H}{P_2}\right) + \left(1 - \frac{T_g}{T_1}\right) \right] \qquad \text{(A.1.3)}$$

where

$\dot{\varepsilon}_b$ = mixing energy watt/m^3

$\dot{Q}_b$ = bottom flow rate N m^3/min

T_L = temperature of liquid (^{o}K)

V_L = volume of bath (m^3)

g = acceleration due to gravity (m/sec^2)

H = Bath height (m)

P_2 = atmospheric pressure

ρ_1 = 1000kg/m^3

T_g = temperature of gas (^{o}K)

Example:

Given $\dot{Q}_b = 1.08 \times 10^{-3}$ N m^3/min

$T_L = 298^oK$, $V_L = 2.5 \times 10^{-3}$ m^3

$g = 9.81$ m/sec^2 $H = 0.075$ m

$P_2 = 1.013 \times 10^5$ N/m^2, $T_g \approx T_1$

So,

$$\dot{\varepsilon}_b = \frac{6.18 \times 1.08 \times 10^{-3} \times 298}{2.5 \times 10^{-3}} \ln\left(1 + \frac{1000 \times 9.81 \times 0.075}{1.013 \times 10^5}\right)$$

$$= 5.75 \text{ watt/m}^3.$$

REFERENCES

1) Lance, K.W., Stahlhersallung durch Kowbinierty Blasen (Production of Steel by Combine Blowing) Dusseldorf, Verlag Stahleisen, Oct. 1985, 116 pages 174 Figures, ISBN-514-00353-X.

2) Emi, T. : Stahl U. Eisen 101 (1980) No. 17, p.998/1011.

3) Ito, S. et.al.: Proc. 65th Steelmaking Conf., AIME (1982) 123/30.

4) Kohtani, T. et.al. : Proc. 65th Steelmaking Conf. AIME 1982, 211/20.

5) Nakanishi, K. et al. : Proc. 65th Steelmaking Conf., AIME 1982, 101/8.

6) Suzuki, K.I. et al. : Trans. Iron & Steel Inst. Japan 22 (1982) B-236.

7) Tanaka, S.; Miyawaki, Y. : Fachber. Huttenpraxis MWV 20 (1982) 786/95.

8) Koria, S.C.; Lange, K.W. : Proc. 6th Japan-Germany Seminar; Tokyo, 1984 91/101.

9) Jun-Ichi Sakare et.al. : Trans. ISI Japan Vol. 24, 1984, page B/204.

10) Qu Ying, Lang Yun, Liu Liu: Proceeding International Conference on Injection Metallurgy, Luka Sweden June 15-17, 1983, p..21 : 1-21:16.

11) Paul, S.; Ghosh, D.N. : Metall. Trans. 13B (1982) 193/211.

12) S.C. Koria: Steel Research, 59 (1988), p. 257/262.

13) S.C. Koria : Steel Research, 59 (1988), p. 104/109.

14) S.C. Koria and A. George: Ironmaking and Steelmaking 1988, Vol. 15 No.3, pp. 127/133.

15) S.C. Koria and K.W. Lange: Arch. Eisenbistteues 55(1984) p. 97/101.

16) G.K. Lee, J.H. Nelson et al. : Iron and Steel International, V-50, 1977, pp. 175/184.

17) L. Feege, V. Schiel, H. Sch Roner, L. Weber H.M. Delhey, Stahl Eisen, 1983, 103(4), 159-163.

18) S.A.Sai, M. Kawachi and I. Muchi : Scan Inject-III held at Luka Sweden, June 15-17, 1983, p. 12:1, 12:29.

19) Stearm, R.F., Johnson, R.R., Jackson, R.M. and Larson, C.A.; 'Flow Measurement with Orifice Meters', D. Van Nostrand Co. Inc., New York (1951).

20) Handbook of Chemistry and Physics, Edited by Hodgman, C.D. et al., Chemical Rubber Pub. Co., Cleveland (1961).

21) S.C. Koria : Modelling of Submerged Gas Injection Lance Design Parameters: To be published in Steel Research, Feb. 1989.